Corso di dottorato di ricerca in:

"Scienze biomediche e biotecnologiche"

XXXVI CICLO

Exploring the protective role of EMILIN-1 in Gastric Cancer: insights into microenvironment modifications and lymphatic function.

Dottorando Maddalena Vescovo

Supervisore Dott.ssa Paola Spessotto

Co-supervisore Dott.ssa Alessandra Capuano

Anno 2024

CONTENTS

LIST OF ABBREVIATIONS

BSA - Bovine Serum Albumin

CAF – Cancer Associated Fibroblast

CAFCA - Centrifugal Assay for Fluorescent based Cell Adhesion

CM – Conditioned Media

ECM – Extracellular Matrix

EDTA - Ethylene Dyamine Tetra-Acetate

EMILIN1 - Elastin Microfibril Interface Located proteIN 1 *(Human and Mouse gene)*

EMILIN-1 - Elastin Microfibril Interface Located proteIN 1 (*Human and Mouse protein*)

FBS - Fetal bovine serum

FN - Fibronectin

GC - gastric cancer

gC1q - Globular C1q domain

GIN – Gastric Intraepithelial Neoplasia

KI - Knock In

KO - Knock Out

LECs - Lymphatic Endothelial Cells

MMP – Matrix Metallo Proteinase

MNU - N-Methyl-N-nitrosourea

NE – Neutrophil Elastase

PAGE - PolyAcrilammide Gel Electrophoresis

PBS - Phosphate Buffer Saline

PCR - Polymerase Chain Reaction

PFA - Paraformaldehyde

SDS - Sodium Dodecyl Sulphate

TGF-β - Transforming Growth Factor Transforming Growth Factor-β

TME – Tumor MicroEnvironment

WT - Wild Type

ABSTRACT

Gastric Cancer (GC) is the fifth most common neoplastic malignancy worldwide, whose aggressiveness is significantly influenced by the tumor microenvironment (TME). GC progression is closely related to profound alterations in lymphatic vessels (LVs), with lymphatic metastasis being a pivotal determinant of clinical outcome. Recent research has revealed the functional relationship between the Extra-Cellular Matrix (ECM) protein EMILIN-1, tumor growth, and lymphangiogenesis. EMILIN-1, an essential structural element for maintaining the integrity of the LVs, exhibits anti-proliferative and oncosuppressive properties through interactions with $\alpha 4 \beta 1$ integrin.

Our study revealed lower EMILIN-1 levels in human malignant and pre-neoplastic gastric samples, which were correlated with the presence of abnormal LVs.

Through *in vivo* experiments with genetically modified EMILIN-1 mouse models (knock-out and E933A knock-in mice), we observed earlier and greater tumor development, and enhanced intratumoral lymphangiogenesis in EMILIN-1 transgenic mice. In a model of peritoneal carcinomatosis and dissemination, mutant animals displayed higher histopathological scores for invasion. Consistent with these results, EMILIN-1 transgenic animals showed higher tumor incidence, larger adenomas and lower survival when the N-Methyl-N-nitrosourea protocol for gastric carcinogenesis was performed.

In vitro studies using fibroblasts and lymphatic endothelial cells (LECs), both primary sources of EMILIN-1 in the gastric microenvironment, further supported our findings. Indeed, the treatment of stromal cells with conditioned media derived from GC cell lines (but not normal gastric cells) dramatically affected EMILIN-1 expression, both at the mRNA and protein levels. In addition, downregulation of EMILIN-1 in LECs impaired their ability to form tubes, indicating an important role of this protein also in maintaining homeostasis of the lymphatic tissue.

Preliminary investigations into the mechanisms involved in this complex regulatory network suggest that a candidate for downregulation of EMILIN-1 in small RNAs secreted by GC cells could be identified.

Overall, our study demonstrates how loss of EMILIN-1 affects microenvironment changes, including proliferative imbalance and lymphatic dysfunction that contribute to tumorigenesis in the stomach. Importantly, we present a novel animal model targeting an ECM component in the gastric TME, that sheds light on the role of EMILIN-1 in the onset, progression, and spread of GC.

INTRODUCTION

Gastric cancer

GC represents a highly prevalent global health concern. As indicated by the Globocan report published in 2020, the annual incidence of GC exceeds one million cases at the global level (**Figure 1**). This makes this malignancy the fifth most common cancer worldwide. Due to its often-advanced stage at diagnosis, GC is characterized by a high mortality rate, making it the fourth leading cause of cancer-related deaths. In 2020, there were 768,793 deaths worldwide, accounting for 8.3% of all cancer-related deaths (Sung et al., 2021; Thrift and El-Serag, 2020).
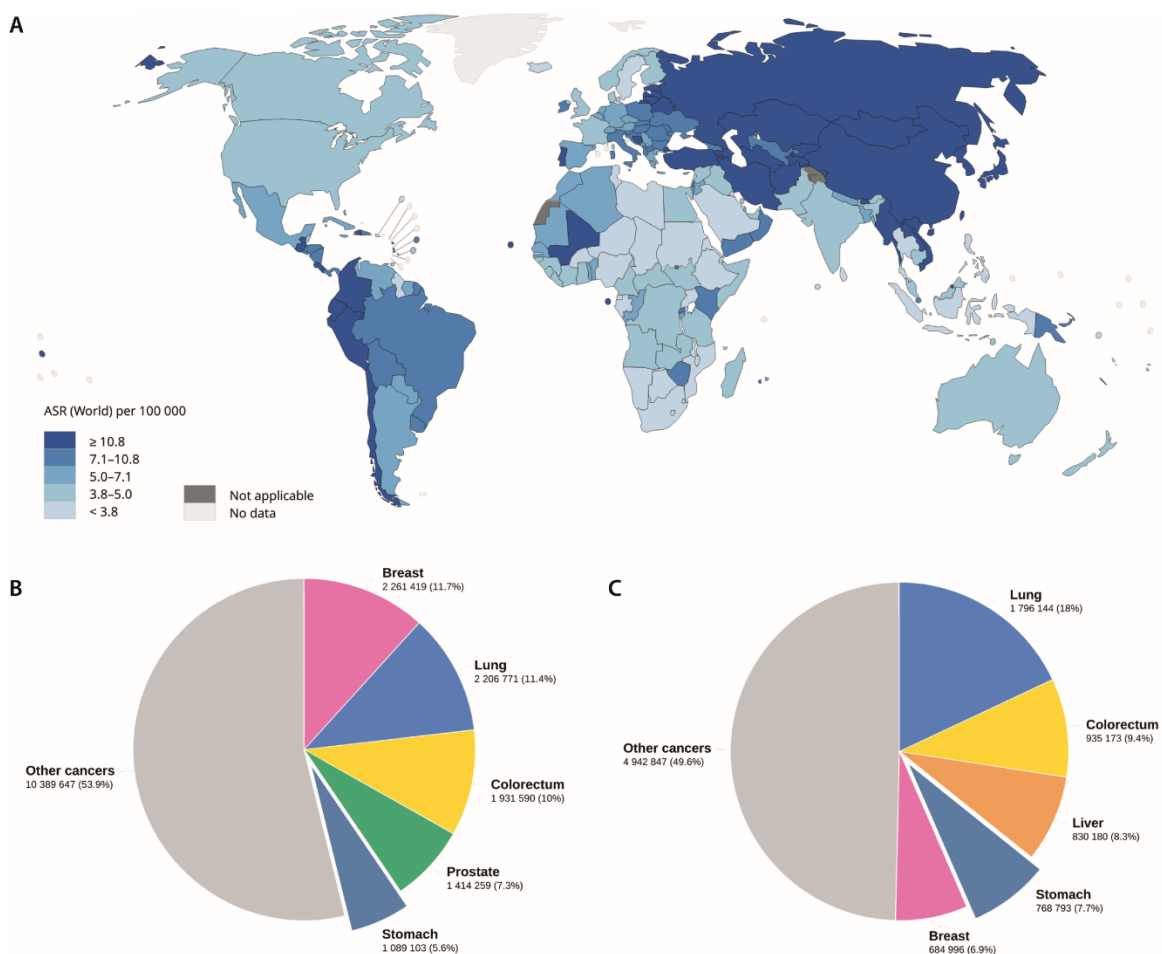
FIGURE 1. **Snapshot of the burden of GC.** A) Global overview. B) Number of new cases in 2020, both sexes, all ages. C) Number of deaths in 2020, both sexes, all ages. Adapted from Globocan, 2020.

Over the past century, a steady decline in both incidence and mortality rates has been observed. However, despite diminishing incidence rates in most regions, clinicians will face an increase in GC cases due to an aging population (Morgan et al., 2022). The improved standard of living that has accompanied economic development has played a critical role in reducing the prevalence of Helicobacter pylori, the principal etiological agent of GC (Smyth et al., 2020). In high-incidence regions, such as Japan and Korea, the implementation of robust screening programs has led to

significant reductions in GC-related mortality (Huang et al., 2020; Suh et al., 2020). Interestingly, an emerging trend in the incidence of GC among younger people in high-income countries suggests an evolving risk profile and epidemiologic shift (Arnold et al., 2020). Close monitoring of ongoing changes in the epidemiology of GC is of important for future cancer control strategies and clinical practice. The complexity of this disease, coupled with its significant global impact, requires ongoing efforts to improve early detection methods, treatment modalities, and prevention strategies (Waldum and Fossmark, 2018). Understanding the molecular mechanisms underlying GC pathogenesis and the interplay of genetic, environmental, and lifestyle factors is of paramount importance.

Diagnosis and staging

Diagnosis and staging of GC are crucial steps in determining appropriate therapeutic strategies for patients affected by this complex malignancy. The development of strategies to improve early detection is an urgent need to improve patient prognosis, as highlighted by recent data demonstrating that the 5-year survival rate for GC increases to 95–99% when diagnosed at an early and resectable stage, in contrast to less than 30% when diagnosed at advanced stages. (Jun et al., 2017; Khanderia et al., 2016; Tanabe et al., 2017). Diagnosis is usually made by endoscopic examination, which determines the localization of the tumor in the stomach and its macroscopic features (Kim and Cho, 2021). Histologic confirmation is achieved by taking biopsies. Clinical staging of GC is a determinant factor in classifying patients into curative or palliative treatment pathways. To ensure accurate and comprehensive evaluation, all patients should be carefully staged according to the latest guidelines established by the Union for International Cancer Control and the American Joint Committee on Cancer (Amin et al., 2017). This process is best performed in the setting of an experienced multidisciplinary tumor board (Lordick et al., 2022). GC can be categorized into two main types based on staging criteria: early-stage and advanced-stage (Smyth et al., 2020). In the context of early-stage GC, the disease remains confined to the mucosal and submucosal layers of the stomach, regardless of tumor size or the presence or absence of lymph node metastases (Hu et al., 2012; Yada et al., 2013). Remarkably, this stage is often referred to as "carcinoma in situ," meaning that the cancer has not yet invaded the inner layer of the stomach (Chiarello et al., 2022). Within this stage, further distinctions are made, notably *Stage 1A*, in which the cancer is limited to growth beneath the surface layer of mucosal cells without invading the primary muscle layer of the stomach wall, and *Stage 1B*, in which the tumor has penetrated the main muscle layer of the stomach wall but has not spread to nearby

lymph nodes, tissues, or organs. In contrast, *Stage 2* GC represents progression beyond the early-stage (Kinami et al., 2022), since the cancer may have reached the inner, supportive, or muscle layers of the stomach or spread through the outermost layer. In some Stage 2 tumors, nearby lymph nodes may be affected, but distant metastases are not present. In *Stage 3*, GC is more advanced and has infiltrated the inner, supportive, muscle, or outer layers of the stomach. This stage is often accompanied by the presence of affected lymph nodes nearby. However, distant or systemic metastases are not seen. Finally, *Stage 4* represents an advanced and critical stage of GC, indicating that the cancer has already spread widely. At this stage, the tumor usually breaks through the outer lining of the stomach and invades surrounding organs or tissues (**Figure 2**). Distant metastases to remote anatomical sites or organs become evident. As our understanding of the disease continues to evolve, precise classification and characterization of GC stages are critical to optimize patient care, in terms of shaping the therapeutic approach and improving clinical outcomes (Chen et al., 2021; Hu et al., 2012).
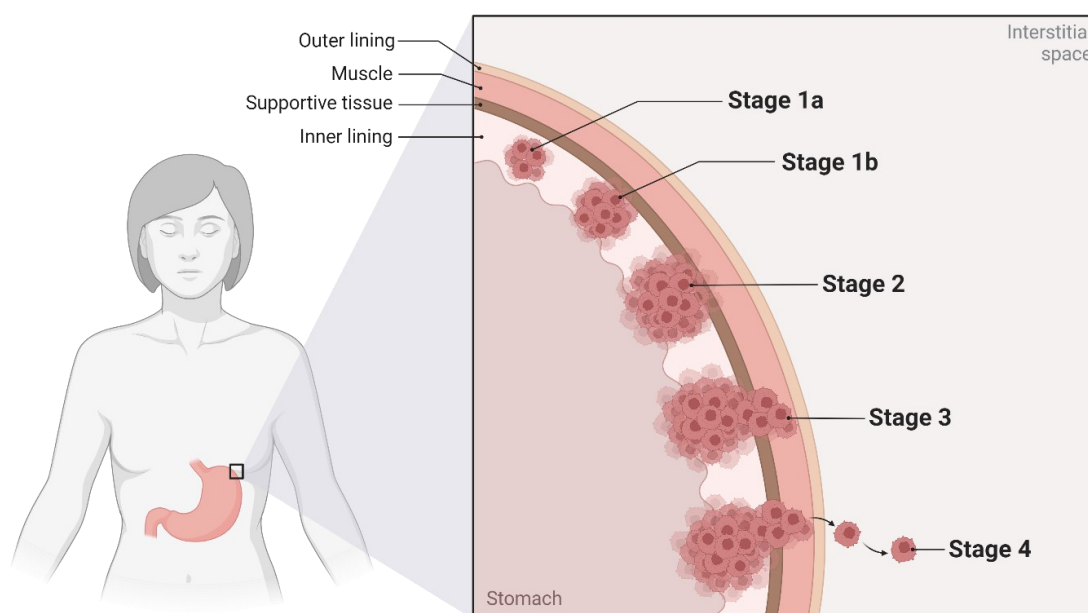
FIGURE 2. **Staging of GC.** *The involvement of different layers of the stomach wall, together with lymph node dissemination, is paramount in defining the advancement of the tumor. Created with BioRender.com.*

The progression of GC in its various stages, from localized early-stage disease to advanced metastatic forms, presents a profound and multifaceted challenge (Smith et al., 2006). Within this intricate process there are fundamental triggers for the transformation of normal gastric cells into malignant counterparts, as well as complex microenvironmental adaptations that support cancer progression. Consequently, there is an urgent need for a comprehensive and meticulous characterization of the underlying molecular and cellular mechanisms to refine treatment strategies.

Classification

GC, as per the Laurén classification, encompasses two primary histological subtypes: intestinal and diffuse (Laurén, 1965). The intestinal type is the most common in terms of incidence and is associated with a more favorable prognosis (Korivi et al., 2019). It is characterized by visible glands and cohesive tumor cell arrangements. Intestinal GC contrasts with diffuse GC, which is characterized by poorly cohesive cells that diffusely infiltrate the gastric wall and form limited glands. Some studies suggest that diffuse GC originates from the normal gastric mucosa. On the other hand, the intestinal subtype is often associated with intestinal metaplasia of the gastric mucosa and Helicobacter pylori infection, underscoring the multistep, multifactorial nature of gastric carcinogenesis (Chen et al., 2016). Environmental factors, including Helicobacter pylori infection, diet, and lifestyle, are primarily associated with the intestinal-type of GC, whereas genetic abnormalities are more commonly implicated in the diffuse type (Machlowska et al., 2020). The exact molecular pathways guiding GC progression remain unclear. Currently, most epidemic GCs are attributed to inflammation, highlighting their environmental etiology (Correa, 2013; Yakirevich and Resnick, 2013).

Because of this infectious etiology, GC stands as one of the highly lethal but preventable malignancies. Chronic gastric inflammation leads to changes in the microenvironment that result in atrophy and metaplasia of the mucosa, which, along with other molecular alterations, can culminate in neoplasia (Nagtegaal et al., 2020). The sequence of inflammation–atrophy–metaplasia–dysplasia–carcinoma, known as the Correa cascade, culminates in intestinal-type gastric adenocarcinoma (Correa, 2013; Pimentel-Nunes et al., 2019) (**Figure 3**).
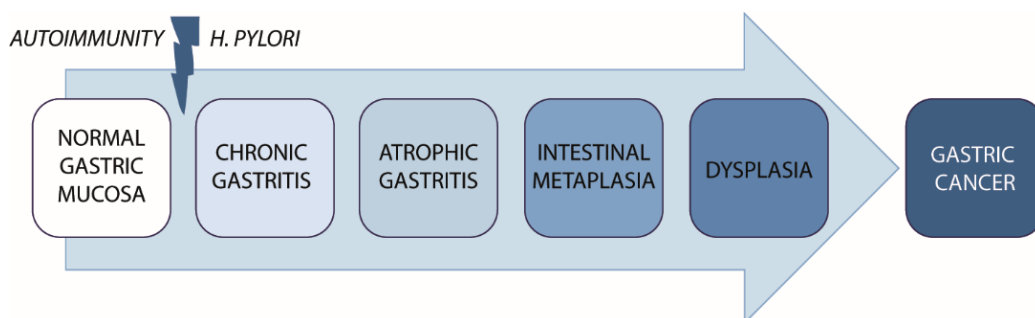
FIGURE 3. ***Correa sequence.*** *Gastric carcinogenesis progressed through different stages, from chronic gastritis and intestinal metaplasia to dysplasia and, ultimately, GC. Understanding the Correa Sequence is critical for early detection and intervention in GC development.*

Chronic atrophic gastritis and intestinal metaplasia are recognized precancerous conditions that independently confer GC risk, providing a backdrop for dysplasia and adenocarcinoma development (Battista et al., 2021). Several attempts have been made to classify affected individuals according to the severity and extent of these changes. The advanced stage of atrophic

gastritis includes significant (moderate to marked) atrophy or metaplasia. Gastric dysplasia represents the penultimate stage within the complicated sequence of gastric carcinogenesis. This condition is characterized by a histological distinct neoplastic epithelium that shows no evidence of tissue invasion, and thus represents a direct precursor lesion for neoplastic transformation. The understanding of histological features of GC subtypes provides valuable insights into the patterns and mechanisms of disease progression (Yakirevich and Resnick, 2013). For instance, the presence of well-defined glandular structures in intestinal-type cancer suggests a propensity for lymphatic metastasis to regional lymph nodes, whereas the diffuse subtype, with its infiltrative growth, have a higher propensity for peritoneal dissemination (Riihimäki et al., 2016). These findings help in predicting the routes of disease spread and establishing surveillance strategies (Kinami et al., 2022).

In the last decade, several molecular classification systems for GC have been introduced, often aiming to establish links between molecular attributes, histological traits, and clinical characteristics. In 2014, a milestone was reached with the publication of the results of a very comprehensive genome-wide analysis conducted by The Cancer Genome Atlas (TCGA) research network (Bass et al., 2014). This study proposed the existence of four distinct molecular subtypes in GC: Epstein-Barr virus-positive (EBV+), microsatellite unstable (MSI), genomically stable, and chromosomally unstable (CIN). Although molecular features rather than morphology may be critical for future development of therapies, Laurén's classification remains the most commonly used for subgroup analyses in clinical trials. Thes, additional molecular subgroup testing is not yet performed in routine clinical practice (Smyth et al., 2020).

Dissemination

GC can spread both hematogenously and lymphatically, and the preference for a particular route of dissemination may depend on numerous factors that include cancer stage and individual patient characteristics (Lee et al., 2023). Predominant sites of metastasis in GC via the bloodstream are represented by the liver, lung, peritoneum, and distant lymph nodes.

At the same time, lymphatic metastasis represents another prominent avenue for the spread of GC. Cancer cells are able to infiltrate and propagate through lymphatic vessels (LVs), often reaching regional and occasionally distant lymph nodes (Akagi et al., 2011; Brown et al., 2018). Lymphatic dissemination is typically an early event in the progression of GC and is closely associated with lymph node involvement (Bausys et al., 2017; J. Chen et al., 2020). Detection of

cancer cells in lymph nodes has profound prognostic implications and significantly influences therapeutic decision-making (Z. Li et al., 2021).

The propensity for either mode of dissemination depends on a number of factors, including the anatomic location, size, and aggressiveness of the tumor, as well as the patient's immunological response and genetic predisposition (Lee et al., 2023). Nonetheless, in the clinical setting, evaluation of lymph node involvement and identification of distant metastases play a critical role in staging GC and formulating optimal treatment strategies. Consequently, understanding the intricate mechanisms underlying lymphatic spread is of paramount importance, especially for improving therapeutic approaches in the early stages of the disease (Deng and Liang, 2014).

The journey begins at the site of the primary tumor, where cancer cells undergo various changes that allow them to invade and reach LVs (**Figure 4**).
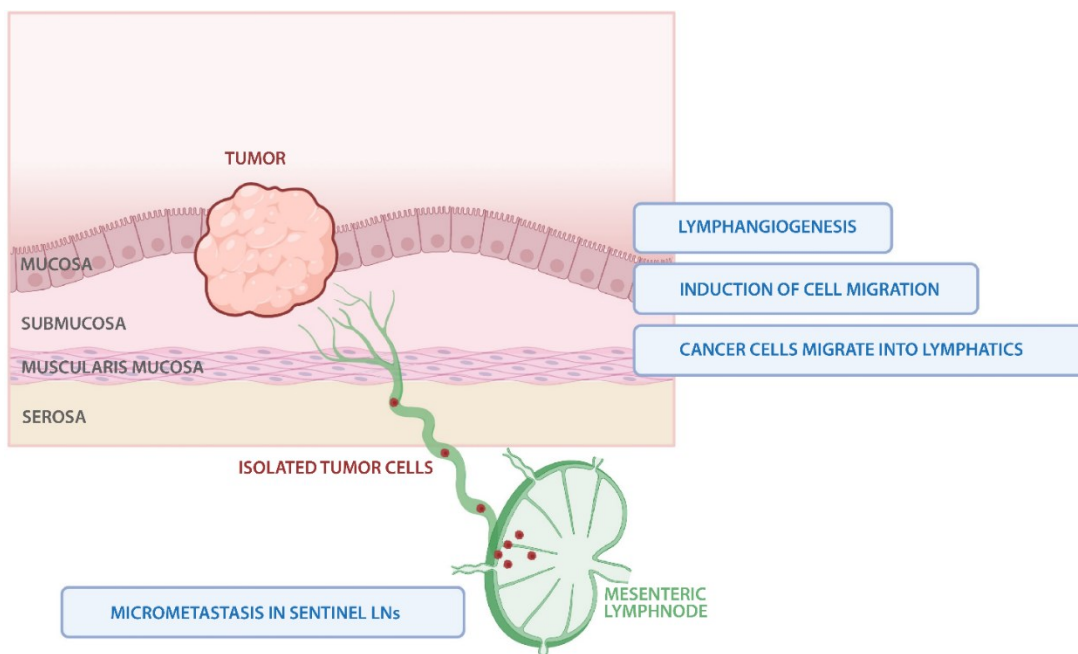
FIGURE 4. **Lymphatic Dissemination of GC Cells.** *This schematic diagram illustrates the multilayered process of lymphatic dissemination in GC. It includes key stages such as lymphangiogenesis, induction of cell migration, invasion of LVs by cancer cells, and formation of micro-metastases in sentinel lymph nodes, thus highlighting the intricate mechanisms that drive disease progression. Created with BioRender.com.*

The stomach has abundant lymphatic vasculature (Alexander et al., 2010; Lirosi et al., 2017), and cancer cells acquire the ability to infiltrate LVs through a combination of molecular alterations and interactions with the lymphatic endothelium. These interactions are influenced by factors such as lymphangiogenic growth factors (like VEGF-C and VEGF-D) and adhesion molecules (such as E-cadherin, ICAM-1 and VCAM-1) (Stachura et al., 2016; Velikova et al., 1997). Tumors promote changes in the lymph nodes such as enhanced lymphangiogenesis, induction of an immunosuppressive environment, and increased vascular flow. These changes precede

metastatic colonization (Gillot et al., 2021; Tian et al., 2023). Successful colonization of lymph nodes by cancer cells leads to the formation of metastatic foci. Here, cancer cells can proliferate and form secondary tumor deposits in the lymph nodes (Zhu et al., 2018).

The intestinal subtype of GC often exhibits a predilection for lymphatic metastasis (J. Chen et al., 2020). Indeed, metastasis to regional lymph nodes is a specific feature in early-stage intestinal GC (Bausys et al., 2017). Although less common than lymphatic metastasis, the intestinal subtype can lead to hematogenous spread to distant organs such as the liver and lungs in advanced stages of the disease, which is associated with a worse prognosis (Pereira et al., 2018). In these cases, peritoneal dissemination may also be observed (Manzanedo et al., 2023). In summary, the ability to follow the progression of intestinal histotype GC through different preneoplastic stages and to detect involvement of lymph nodes facilitates diagnosis in the early phase.

On the other hand, diffuse GC has been shown to have the worse prognosis than the other two forms. Several prospective and retrospective studies have demonstrated a higher 5-year risk of death in patients with diffuse GC (Lee et al., 2017; Liu et al., 2013; Petrelli et al., 2017). This type of GC is asymptomatic and difficult to detect. Despite the presence of many early lesions, patients typically develop only a single advanced tumor over the course of years or decades, which is larger and has invaded the submucosa and deeper tissue layers (Monster et al., 2022). A hallmark of the diffuse subtype is a predilection for peritoneal dissemination (Y. Chen et al., 2020; Kanda and Kodera, 2016). These malignant tumors consist largely of poorly differentiated cells that are highly migratory and may metastasize to the peritoneum, bone, lung and liver. Although distant metastases are less common in the diffuse subtype than in the intestinal subtype, they can still occur and present a very difficult prognosis (Lee et al., 2017; Li et al., 2020). In diffuse GC, epithelial cells are triggered to delaminate into the mesenchyme, facilitating the transmigration and spread of malignant cells. Moreover, the increase of undifferentiated tumor cells in advanced diffuse GC enables rapid tumor growth.

Some gastric carcinomas have mixed histological features that combine elements of both intestinal and diffuse subtypes. In these cases, metastatic patterns may vary depending on the predominant components within the tumor (Zheng et al., 2008).

The intricate interplay within the gastric TME shapes lymphatic metastasis through processes such as inflammation, lymphangiogenesis, ECM remodeling, and chemotactic signaling. These complex interactions create a permissive environment that enables cancer cells to invade LVs and disseminate to regional lymph nodes, ultimately impacting disease progression and patient outcomes (Pellino et al., 2019; Wang et al., 2020).

Tumor microenvironment

The TME includes all non-cancerous components, their metabolites, and secretions within the tumor milieu (Li et al., 2007). It is an extremely complicated system consisting mainly of infiltrating immune cells (such as macrophages, dendritic cells, and lymphocytes), cancer-associated stromal cells (such as cancer-associated fibroblasts), endothelial cells and adipocytes, as well as the ECM and several signaling molecules (Oya et al., 2020) (**Figure 5**).

Recent studies have clearly shown that the TME exerts a profound influence on crucial malignant phenotypes, including tumor growth, invasiveness, metastatic potential, drug resistance, and evasion of immune surveillance (Giraldo et al., 2019).
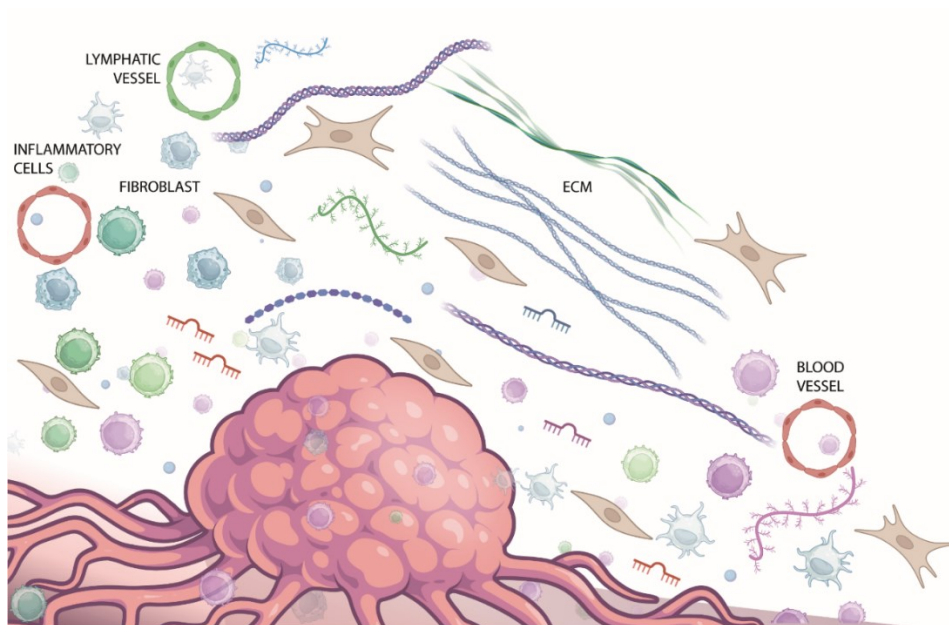
*FIGURE 5. **Tumor Microenvironment Complexity.** This picture portrays the intricate tumor microenvironment, characterized by a dynamic interplay of ECM, lymphatic vessels, blood vessels, fibroblasts, and inflammatory cells. Created with BioRender.com*

In the initial stages of tumor development, TME exerts predominantly a tumor-suppressive influence. However, as the tumor progresses, the tumor-suppressing microenvironment is increasingly repressed, while the tumor-promoting microenvironment gains the upper hand, which ultimately promotes immune tolerance and favors tumor progression (Liu et al., 2022).

The gastric TME is unique due to the highly acidic nature of the stomach and its distinct endocrine system, both of which together contribute to the specific characteristic of GC (Rojas et al., 2020). Within this complex system, the immune TME plays a dual role, that includes both tumor-promoting and tumor-suppressing effects (Zhao et al., 2023).

The gastric TME is composed of a complex interplay of components, including the ECM, fibroblasts, endothelial cells, mesenchymal stem cells, macrophages, lymphocytes, neutrophils, and other cellular elements. In addition, the metabolites and cytokines secreted by these components, which include GC cells themselves, contribute critically to TME. These components are actively involved in shaping the immune tolerance landscape and ultimately promote GC progression (Liu et al., 2022). In traditional paradigms, histological classification of GC has primarily focused on the features of the epithelial tumor component. However, emerging evidence suggests that other histological features within the TME, such as the presence of tumor infiltrating lymphocytes and the proportion of intratumoral stroma, have significant potential as clinically relevant prognostic or predictive factors (Ni et al., 2021; Zeng et al., 2019; Zhang and Huang, 2011).

Angiogenesis and lymphangiogenesis

Angiogenesis is a multifaceted and highly regulated process that plays an important role in tumor progression (Jiang et al., 2020). Tumors initiate and sustain angiogenesis by producing a plethora of pro-angiogenic factors, with vascular endothelial growth factors (VEGFs) standing out as key mediators. These factors stimulate the sprouting of new blood vessels from pre-existing ones, primarily postcapillary venules and capillaries. Tumor angiogenesis is characterized by several distinctive features. Firstly, angiogenic vessels often exhibit structural abnormalities, including irregular diameters, tortuous paths, and uneven distribution (Lugano et al., 2020). The architectural irregularities contribute to enhanced vascular permeability, resulting in leaky vessels that allow for the extravasation of plasma proteins and interstitial fluid. Consequently, elevated interstitial fluid pressure within the TME can hinder efficient drug delivery and immune cell infiltration. The newly formed tumor vasculature serves as a critical lifeline for the expanding neoplastic mass, ensuring a constant supply of oxygen and nutrients necessary for efficient tumor growth. It also provides a conduit for cancer cells to intravasate into the bloodstream, facilitating metastatic spread to distant organs (Hanahan and Weinberg, 2011).

In addition to tumor angiogenesis, the TME actively promotes lymphangiogenesis, reflecting the interplay between these processes (Paupert et al., 2014). While angiogenesis ensures a robust blood supply for tumor growth and metastasis, lymphangiogenesis provides conduits for cancer cells to disseminate to regional lymph nodes and distant sites. This intricate connection underscores their joint impact on cancer progression and clinical outcomes (Paduch, 2016). In the microenvironment, lymphatic sprouting and lymphangiogenesis occur through the influence of

biochemical factors derived from both the tumor and surrounding stromal cells, which stimulate the migration and proliferation of lymphatic endothelial cells (LECs) (Chen et al., 2015; Cho et al., 2021). The newly formed LVs are enlarged, leaky, and physiologically dysfunctional, but serve as conduits for the dissemination of cancer cells to regional lymph nodes and distant sites, which strongly influences the clinical course of GC (Gao et al., 2009) (**Figure 6**).
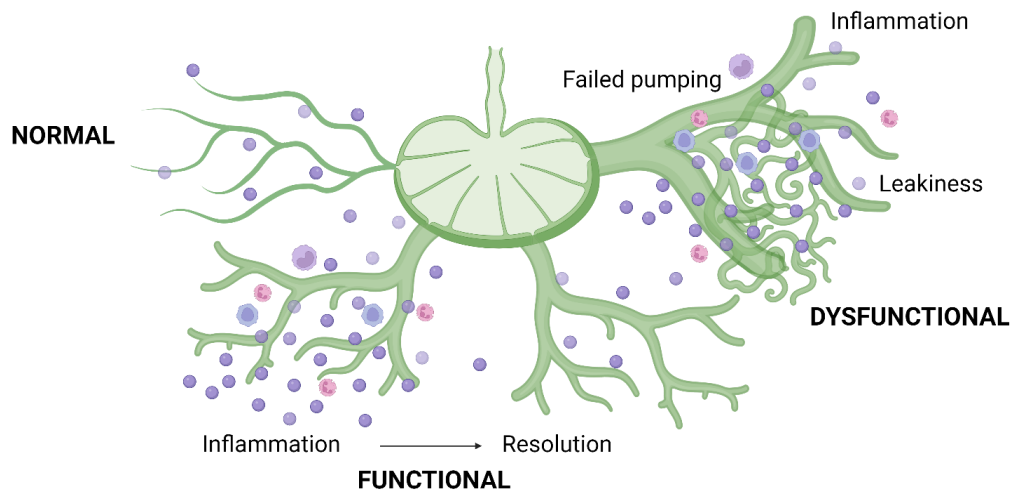

*FIGURE 6. **LVs in health and disease.** Illustration shows normal LV, functional LV in inflammation (where homeostasis is restored), and dysfunctional LV in cancer characterized by a tortuous and aberrant morphology with reduced inflammatory clearance and increased vessel abundance. Adapted from (Abouelkheir et al., 2017) and created with BioRender.com.*

Increased LV density enhances the likelihood that cancer cells have access to them. LECs lining the LVs interact with cancer cells in the TME. These interactions are mediated by adhesion molecules and chemokines and promote cancer cell invasion of LVs (He et al., 2021). Since increased lymphangiogenesis correlates with a higher tumor metastasis rate, it is not surprising that various lymphangiogenic growth factors are found in the TME to facilitate proliferation and morphological change of LECs (Pak et al., 2015). The strongest stimulatory factor for LEC growth has been shown to be VEGF-C, which correlates with lymphangiogenesis, lymph node metastasis, and poor tumor prognosis, as demonstrated by supplementing or blocking VEGF-C in mouse models of human cancer (Eklund et al., 2013). VEGF-C, along with the less potent ligand VEGF-D, binds to the receptor tyrosine kinase VEGFR-3, which later triggers protein kinase C (PKC)-dependent activation of p42/p44 MAPK and Akt phosphorylation. Downstream signaling then leads to increased survival, growth, and migratory ability of LECs, resulting in vessel sprouting and proliferation. Consistent with this, VEGF-C-induced lymphangiogenesis and tumor progression can be completely inhibited by blocking VEGFR-3, highlighting the key role of the VEGF-C/D-VEGFR-3 axis in LEC growth (Chen et al., 2015). In addition, the transcription factor Prox1 and the membrane glycoprotein podoplanin are essential for LEC differentiation and maintenance. Dysregulation of these factors can promote growth of LVs in GC (He et al., 2021).

Moreover, remodeling of the ECM by Matrix Metalloproteinases (MMPs) may loosen the structural support of LECs and thus promote LV sprouting. MMP-2 and MMP-9 have been implicated in GC lymphangiogenesis (Li et al., 2018). When the number and density of LECs increase in and around the tumor mass, the contact opportunities between them and tumor cells increase, and cancer spreading is promoted. Therefore, targeting lymphangiogenesis in cancer is a promising therapeutic strategy to interrupt the spread of cancer cells through LVs, potentially improving patient outcomes (Wang and Chu, 2022).

Inflammatory microenvironment

Chronic inflammation is a major contributor to the development and progression of GC, and has profound effects on the TME and clinical outcomes (Bockerstett and DiPaolo, 2017). The complex interplay of inflammatory processes in the context of GC is determined by a variety of factors that include Helicobacter pylori infection, dietary patterns, and lifestyle determinants (Wessler et al., 2017).

Helicobacter pylori, a persistent resident of the gastric mucosa, is a well-established risk factor for GC. Its presence triggers a chronic inflammatory response characterized by the recruitment in the gastric mucosa of immune cells, particularly neutrophils and lymphocytes (Jaroenlapnopparat et al., 2022). In response to H. pylori, these immune system sentinels orchestrate the release of proinflammatory cytokines and the generation of reactive oxygen species. This cascade of molecular events collectively forges an inflammatory microenvironment conducive to oncogenic transformation. In addition to the realm of microbial influence, dietary factors have a significant impact on triggering GC-related inflammation.

The inflammatory background of GC microenvironment shapes the behavior of tumor cells. It fuels genomic instability by favoring DNA damage and triggering mutations in critical oncogenes and tumor suppressor genes. These genetic aberrations accelerate the transition from normal gastric tissue to precancerous dysplasia, which eventually culminates in an invasive cancer phenotype. Moreover, chronic inflammation drives angiogenesis/lymphangiogenesis, stimulates tissue remodeling, and orchestrates the recruitment of immune cells, overall creating a favorable niche for tumor growth, invasion, and metastasis (Kim et al., 2014).

The presence of immune cells, such as tumor-associated macrophages and neutrophils, further contributes to the inflammatory microenvironment (Rihawi et al., 2021). These immune effectors do not impede tumor growth, but often enhance the evasion of the tumor immune system. They

create an environment rich in cytokines and growth factors that further enhance the tumor friendly scenery (Liu et al., 2022).

Tumor-associated neutrophils, which represent a nuanced dichotomy of tumor-suppressing N1 cells and tumor-promoting N2 cells, underscore the dynamic nature of the inflammatory microenvironment. Transforming growth factor-beta (TGF-β) emerges as a central molecular regulator, orchestrating the polarization of N1 to N2 phenotypes (Fridlender et al., 2009). Clinical data confirm the importance of tumor-associated neutrophils, with studies demonstrating a correlation between their increased infiltration in GC tissue and increased risk of lymph node metastasis, underscoring their role in GC progression (Wang et al., 2020).

Extracellular matrix remodeling

The cellular components of the microenvironment are incorporated into a structural framework which is the ECM, a heterogeneous ensemble that includes collagens, elastin, proteoglycans, and glycoproteins. This ECM is not only a passive structural scaffold that supports and maintains epithelial cell structures, but also exerts profound regulatory effects on a spectrum of cellular behaviors, including growth, differentiation, motility, and viability (Hynes, 2009). Furthermore, ECM molecules serve as reservoirs for important regulatory molecules such as growth factors, cytokines, MMPs, and processing enzymes. Perturbations in the ECM, as seen in processes such as wound healing or tumor progression, can dynamically affect the availability of these critical elements.

The core of the gastric ECM is composed by a series of fibrous proteins, which include collagens, elastin, and fibronectin. Collagens, the predominant ECM proteins, join to form fibrils, and provide tensile strength to tissues such as tendons, skin, and bone. In contrast, elastin gives elasticity to the tissues and allows them to withstand mechanical stress. Fibronectin, another key ECM protein, facilitates cell adhesion by connecting cells with the ECM itself (Moreira et al., 2020). These ECM components are primarily secreted by fibroblasts, although other cellular inhabitants of the microenvironment also can secrete these vital proteins, such as endothelial cells. The ECM actively regulates cell behavior through interactions with cell surface receptors, particularly integrins. These receptors facilitate crucial processes such as cell adhesion, spreading, and migration, which are essential for development, tissue repair, and immune response. The specific binding sites within the ECM for these receptors mediate the intricate interplay between cells and their microenvironment. In addition, the mechanical properties of the ECM, such as stiffness, influence cell motility and differentiation and are critical for cell fate and tissue morphogenesis,

especially in developmental biology. The ECM plays a significant role in tissue remodeling and repair, with enzymes such as MMPs and their inhibitors (TIMPs) modulating ECM changes during these processes. However, imbalances can lead to pathological conditions, including tissue fibrosis and tumor invasion (Mohan et al., 2020).

The role of ECM in disease is multifaceted. In cancer, ECM remodeling facilitates tumor cell invasion and metastasis, enabling cancer cells to spread to distant sites. ECM is shown to be a triggering factor for the development of GC (Moreira et al., 2022). Studies have unveiled that different GC subtypes have different ECM compositions, with less differentiated forms showing a greater abundance of ECM components, increased cellular metabolism, and higher levels of metabolic reprogramming (Jang et al., 2018). Proteomic analyses have highlighted that while ECM components in tumor tissues are not significantly different from their counterparts in normal tissue, their levels exhibit considerable variation (Yang et al., 2021). This difference manifests primarily in an increase in ECM proteins associated with tumor angiogenesis, invasion, metastasis, and malignant phenotypes. As GC progresses, ECM accumulates and increases in density. These dense matrices directly interact with tumor surface receptors, promoting proliferation, invasion, and metastasis, thus contributing to tumor progression.

Fibroblasts

The functions of fibroblasts in the GC TME encompass a wide range of contributions that together strongly influence tumor behavior and clinical outcomes (Gu et al., 2023; Mak et al., 2022). Fibroblasts are the major producers of ECM components, including collagens, fibronectin, and proteoglycans. These cells are instrumental in the formation of tumor stroma, a supportive environment surrounding cancer cells (Truffi et al., 2020). Moreover, they play a key role in the desmoplastic response commonly observed in GC, which is characterized by the accumulation of fibrous tissue in the tumor stroma (Kemi et al., 2018). This fibrotic reaction can provide cancer cells access to LVs. Fibroblasts are also involved in ECM remodeling, by secreting MMPs, allowing cancer cells to invade surrounding tissues and migrate to distant sites (Mohan et al., 2020).

In a malignant environment, fibroblasts can transform into cancer-associated fibroblasts (CAFs). CAFs are known to be potent drivers of cancer progression (Ucaryilmaz Metin and Ozcan, 2022). They secrete a variety of factors, including growth factors, cytokines, and chemokines, which create a nurturing milieu for cancer cells. These soluble mediators promote tumor cell survival, proliferation, and invasion, thereby facilitating GC spread and growth (Mao et al., 2021). CAFs are associated with chemoresistance in GC (Liu et al., 2022). They form a protective niche for cancer

cells, hinder chemotherapeutic drug penetration, and contribute to treatment resistance. The interaction between fibroblasts and cancer cells is reciprocal. Cancer cells can activate fibroblasts, inducing their transformation into CAFs through the secretion of various signaling molecules. In turn, CAFs enhance cancer cell survival and migration, fostering a symbiotic relationship that fuels tumor progression (Sun et al., 2022). Furthermore, CAFs have been shown to play an immunomodulatory role in other tumors such as breast cancer, where the Yes-associated protein (YAP) pathway promotes fibroblast-induced ECM hardening, favoring breast cancer progression and immune tolerance (Calvo et al., 2013). Tumor therapy strategies targeting fibroblasts have been tested in pancreatic cancer, breast cancer, and other tumors (Chen and Song, 2019). Nevertheless, research in this area is still insufficient in GC. There is compelling evidence that CAFs are essential in GC, as there is a remarkable correlation between elevated CAF levels in TME and more aggressive tumor behavior and poorer patient prognosis. Understanding the unique CAF signatures in different cancer types is important to unravel the complex interactions between CAFs and cancer cells, which can significantly influence various aspects of cancer progression, including tumor growth, metastasis, and response to therapy. Moreover, the identification of specific CAF signatures also holds the potential for the development of targeted therapies aimed to disrupt these interactions and improve the efficacy of cancer treatments (Mao et al., 2021).

Enzymes

As mentioned earlier, in the context of cancer and other pathological conditions, the ECM undergoes extensive remodeling, resulting in a TME that supports tumor growth, invasion, and metastasis (McMahon et al., 2021). A number of enzymes, particularly proteases, play a central role in ECM remodeling and degradation and are a critical component of the TME (Mohan et al., 2020). Proteases catalyze the cleavage of peptide bonds in proteins, including those that form the ECM (Park et al., 2020). They are classified into several families based on their catalytic mechanisms, including serine proteases, cysteine proteases, aspartic proteases, and MMPs (Vizovisek et al., 2021). These enzymes can be released by cancer cells themselves, CAFs, inflammatory cells, or endothelial cells. The secretion of proteases by these different cell types underscores the complexity of the TME and its role in tumor progression.

MMPs are a family of zinc-dependent endopeptidases that critically regulate ECM turnover (Chang and Werb, 2001). They play an essential role in maintaining tissue homeostasis by controlling the turnover of ECM components under normal physiological conditions (Klein and Bischoff, 2011). However, in the context of GC, MMPs become central players in orchestrating

pathological alterations within the TME. One peculiar feature of cancer is the dysregulated degradation of ECM components (Winkler et al., 2020). MMPs are instrumental in this process, as they can degrade structural proteins such as collagen, fibronectin, and laminin, that provide mechanical support to tissues. By cleaving these components, MMPs create paths for cancer cells to infiltrate surrounding tissues and enter the vasculature, facilitating their dissemination to distant sites. Within the gastric TME, cancer cells and stromal cells release MMPs, particularly MMP-2 and MMP-9 (Bonnans et al., 2014).

Neutrophil elastase (NE) is a serine protease found predominantly in granules released by neutrophils. It plays a critical role in innate immunity, particularly in defense against bacterial and fungal pathogens (Krotova et al., 2020). The primary substrate of NE is elastin. This protease also targets other ECM proteins, such as collagen and fibronectin, contributing to tissue damage during inflammatory responses. Dysregulation of NE activity has been implicated in several inflammatory diseases, such as cystic fibrosis and pulmonary emphysema, where excessive elastin degradation leads to tissue destruction and impaired lung function (Gifford and Chalmers, 2014). In TME, it promotes tumor growth by supporting tissue remodeling, chronic inflammation, immunosuppression, and angiogenesis in the TME (Tagirasa and Yoo, 2022). Its precise role in cancer varies depending on tumor type and stage and is therefore the subject of ongoing research. Very recently, a Chinese group demonstrated that high expression of NE is closely associated with GC progression. The enzyme can stimulate epithelial cells to produce inflammatory cytokines and further activate neutrophils, triggering an acute inflammatory response. Therapeutic strategies targeting NE are currently being explored to potentially prevent its tumor-promoting effects (Jia et al., 2023).

Overall, these proteases are essential for tumor cells to break through the basement membrane and invade surrounding tissues. They cleave ECM proteins, creating pathways for tumor cell migration, while also being able to destroy proteins with a protective role in the TME. Enzymes that remodel the ECM facilitate the intravasation of tumor cells into blood vessels and LVs (Krishnaswamy et al., 2019; Lu et al., 2011; Nawaz et al., 2018).

EMILIN protein family

The EMILIN protein family is a group of ECM glycoproteins, that play several roles in tissue development, homeostasis, and disease. They are characterized by a unique structural composition, which includes a C-terminal globular domain known as gC1q, a short collagenous

sequence, an extended coiled-coil region, and a cysteine-rich N-terminal domain. This structural diversity is crucial for their multifaceted functions within the ECM. In particular, the gC1q domain emerges as a central player in mediating several biological functions of EMILINs, which include cell adhesion, cell signaling, and ECM assembly (Colombatti et al., 2012, 2000). EMILINs have an extensive repertoire of interactions within the ECM, engaging with various ECM proteins such as collagen, elastin, and fibrillin. This ability makes them important players in the organization and assembly of the ECM, contributing to its structural integrity. Furthermore, EMILINs actively participate in several molecular pathways, including the TGF-β signaling pathway, the Wnt signaling pathway, and the Notch signaling pathway.

These complex pathways govern a variety of cellular processes, including cell growth, differentiation, and migration (Colombatti et al., 2012). The importance of EMILINs also extends to their involvement in several human diseases, including cardiovascular disease, cancer, and inflammation (Adamo et al., 2022; Pivetta et al., 2022). In cancer, EMILIN-1, a member of this protein family, is frequently downregulated and has been shown to inhibit tumor growth and metastasis (Amor López et al., 2021; Capuano et al., 2019a; Danussi et al., 2012).

EMILIN-1

Elastin Microfibrillar Interface-Located protein-1 (EMILIN-1) is a large, multidomain glycoprotein of approximately 140 kDa that plays a variety of roles in tissue development, homeostasis, and disease. It is highly expressed in multiple tissues, including the skin, blood vessels, heart, intestine, lymph nodes, lymphatic capillaries, and lung. The gene is located in chromosome 2 in humans and chromosome 5 in mice, sharing a homology higher than 90%. EMILIN-1 is particularly abundant in elastic tissues, such as the aorta and skin (Danussi et al., 2008; Doliana et al., 1999). EMILIN-1 plays a crucial role in the development and maintenance of elastic tissues by interacting with collagen and elastin to form fibrils. These fibrils provide structural support and elasticity to the ECM (Zanetti et al., 2004).

Structure

EMILIN-1 is characterized by an amino-terminal EMI domain, a long coiled-coil region, a short collagenous sequence, and a gC1q globular domain at the carboxyl-terminal end. It-1 is homotrimeric and assembles into high molecular weight multimers (**Figure 7**).

The N-terminal EMI domain of EMILIN-1 is cysteine-rich and contains a variety of motifs that are involved in protein-protein interactions (Doliana et al., 2000; Zacchigna et al., 2006). The C-terminus contains a C1q-like globular domain, a subunit that is found in a variety of proteins, including complement proteins and some other ECM proteins. (Ghebrehiwet et al., 2012; Ressl et al., 2015).
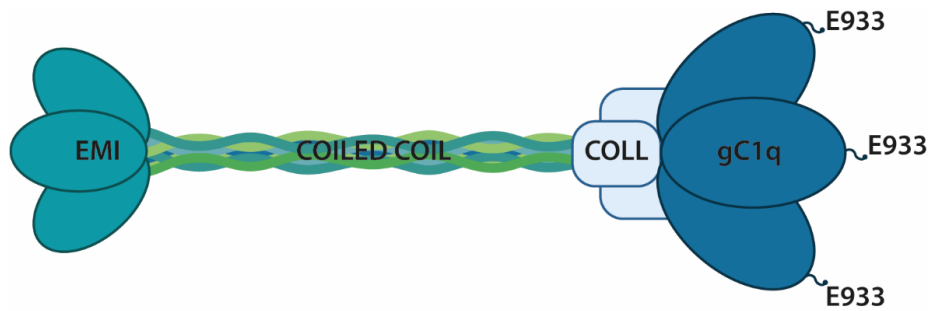

*FIGURE 7. **Structural Overview of EMILIN-1**. The structure of protein with all its functional domains.*

Uniquely within the C1q family, the gC1q domain of EMILIN1 adopts a nine-stranded β-sandwich fold, with the tenth strand replaced by an unstructured segment containing nineteen residues at the apex of the gC1q domain. This unstructured loop exposes the essential acid residue E933 to solvent, playing a pivotal role in mediating the interaction with α4β1 integrin (Verdone et al., 2009). Experimental evidence confirms that all three E933 residues (one from each monomer) are essential for ligand binding. In addition, R904 was identified as a synergistic residue for enhancing cell adhesion. This type of interaction contributes to a more robust and durable α4β1-gC1q interaction compared with other ligands, such as the CS1 region of fibronectin. A distinctive feature of EMILIN-1 among integrin/ligand pairs is that each trimeric gC1q domain exposes three copies of the active tripeptide, suggesting a mode of interaction based on three-dimensional folding with its counterpart (Capuano et al., 2018).

Function

EMILIN-1 is a multifunctional protein that can be involved in tissue structure, cell behavior, and regulation of processes such as cell adhesion, migration, proliferation, and blood pressure control (**Figure 8**). Its functions may have significant implications for vascular health, lymphatic system integrity, and potentially cancer progression (Capuano et al., 2018, 2019a, 2019a; Danussi et al., 2011).

EMILIN-1 is closely associated with elastic fibers and microfibrils in vessels. It contributes to the stabilization of elastic fibers and thus to the elasticity and structural integrity of blood vessels through molecular interactions. EMILIN-1 interacts with elastin and fibulin-5, and this connection influences the arrangement the two (Zanetti et al., 2004).

EMILIN-1 exhibits several functions mediated by its distinct domains, with its EMI domain regulating TGF-β maturation and the gC1q domain maintaining LVs integrity and exerting anti-proliferative effects through its interaction with α4/9β1 integrins.
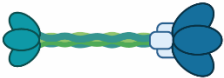
DOMAINS		BIOLOGICAL FUNCTIONS	REFERENCE
EMI		Blood pressure homeostasis, regulation of TGF-β maturation	Zacchigna et al, 2006
Coiled-coil region		Homotrimerization	Colombatti et al, 2000; Mongiat et al, 2000; Verdone et al, 2008
Collagenous region		Homotrimerization	Mongiat et al, 2000
gC1q		Homotrimerization, cell adhesion and migration, cell proliferation and homeostasis, interaction with integrins α4β1/α9β1, control of skin and colon carcinogenesis, structural and functional regulation of lymphatic vessels, NE cleavage site	Mongiat et al, 2000; Spessotto et al, 2006; Danussi et al, 2011; Spessotto et al, 2003; Verdone et al, 2008; Capuano et al, 2018; Danussi et al, 2012; Capuano et al, 2018; Danussi et al, 2008; Danussi et al, 2013; Pivetta et al, 2016; Capuano et al 2018-19; Pivetta et al, 2014; Maiorani et al, 2021
		Homotrimerization, elastogenesis and maintenance of vascular morphology, lymphangiogenesis, tumor and metastasis suppressive-like properties in melanoma, prevention of chronic inflammation	Zanetti et al, 2004; Danussi et al, 2008; Amor Lopez et al, 2021; Pivetta et al, 2022

*FIGURE 8. **Functional Diversity of EMILIN-1**. EMILIN-1 multiple domains govern various cellular processes, including TGF-β maturation, LVs integrity, and anti-proliferative effects via interactions with α4/9β1 integrins.*

As mentioned previously, EMILIN-1 controls the maturation of TGF-β through its N-terminus EMI domain (Zacchigna et al., 2006). Indeed, EMILIN-1 prevents the proteolytic cleavage of proTGF-β, a key event for TGF-β availability. Briefly, TGF-β is synthesized as a homodimeric inactive proprotein (proTGF-β). After cleavage, the propeptide, known as latency-associated protein (LAP), remains noncovalently bound to TGF-β in a latent complex. This binding prevents TGF-β from interacting with its receptor until LAP is removed from the complex. The release of TGF-β from LAP is achieved through the action of thrombospondin-1, integrins, and other proteins. EMILIN-1 specifically interacts with the immature form of TGF-β, known as proTGF-β, via its EMI domain, whereas it does not interact with the latent form of TGF-β bound to LAP. Overexpression of EMILIN-1 promotes accumulation of unprocessed proTGF-β at the expense of mature TGF-β; conversely, proTGF-β1 is readily cleaved in mutant EMILIN-1 cells. EMILIN-1, as is typical for an ECM molecule, impedes the processing of proTGF-β in the extracellular space. EMILIN-1 is unique in that it recognizes immature TGF-β before it is cleaved by LAP thus acting as one of the earliest

extracellular regulators of TGF-β signaling. The discovery of EMILIN-1 as a regulator of TGF-β processing and activation is relevant to many pathological conditions in which TGF-β plays a role, including atherosclerosis, inflammation, tissue repair, fibrosis, and cancer. TGF-β is a key driver of fibrosis and promotes the accumulation of ECM proteins. Following the loss of EMILIN-1, the increased availability of TGF-β leads to severe fibrotic conditions (Angel et al., 2017; Munjal et al., 2014; Pivetta et al., 2022; Schiavinato et al., 2016).

Many of EMILIN-1 functions are modulated by ligand-receptor interactions involving the gC1q domain. The NMR-solved structure of the gC1q domain of EMILIN-1 reveals unique features compared with other gC1q domains, in particular a highly dynamic protruding loop formed by an insertion of nine residues (Verdone et al., 2009, 2008). Integrins α4 and α9 exhibit both unique and overlapping functions *in vivo*, despite their 39% amino acid identity and shared binding capability to the β1 subunit. They interact with common ECM ligands (Cox et al., 2010). α4β1 is expressed on several hematopoietic cell types, including lymphocytes, monocyte/macrophages, and eosinophils, and drives processes such as proliferation, survival, and migration. α4β1-mediated interactions support initial cell adhesion and spreading, promoting cell motility while reducing strong adhesion properties such as focal adhesion and stress fiber formation. This integrin indirectly facilitates tumor cell dissemination by promoting tumor-induced lymphangiogenesis and metastasis to lymph nodes via its expression in LECs and interaction with fibronectin ligand (Imai et al., 2010). Integrin α9β1 is widely expressed in various cell types and plays important roles in cell adhesion and migration, lymphatic vascular system and lung development, and wound healing. In tumor research, α9β1 is associated with reduced metastasis-free and overall survival in breast cancer patients, suggesting a role in tumor cell invasion (Gupta and Vlahakis, 2010; Kon and Uede, 2018). Moreover, α9β1 contributes to epithelial-mesenchymal transition favoring tumor growth and metastatic spread (Gupta et al., 2013). In summary, both α4 and α9 integrins have the propensity to promote tumorigenesis when interacting with ECM ligands, making them important contributors to cancer biology. The interaction between EMILIN-1 and integrins is remarkably efficient, allowing strong adhesion and migration capabilities even at extremely low ligand concentrations. Moreover, EMILIN-1 engagement with α4/α9 integrins has peculiar implications for proliferation (Capuano et al., 2019b; Danussi et al., 2012). Remarkably, in contrast to typical integrin occupancy, which often upregulates cell growth (Liu et al., 2023), the binding of gC1q to integrins leads to a decrease in the proliferative capacity of cells, a novel function attributed to α4 and α9 integrins (Capuano et al., 2018). In EMILIN-1 knock out mice, the lack of integrin occupancy by EMILIN-1 leads to increased cell proliferation in the epidermis and dermis, with a molecular mechanism involving PTEN and inhibition of Erk in the TGF-β pathway (Danussi et al., 2011) (**Figure 9**).
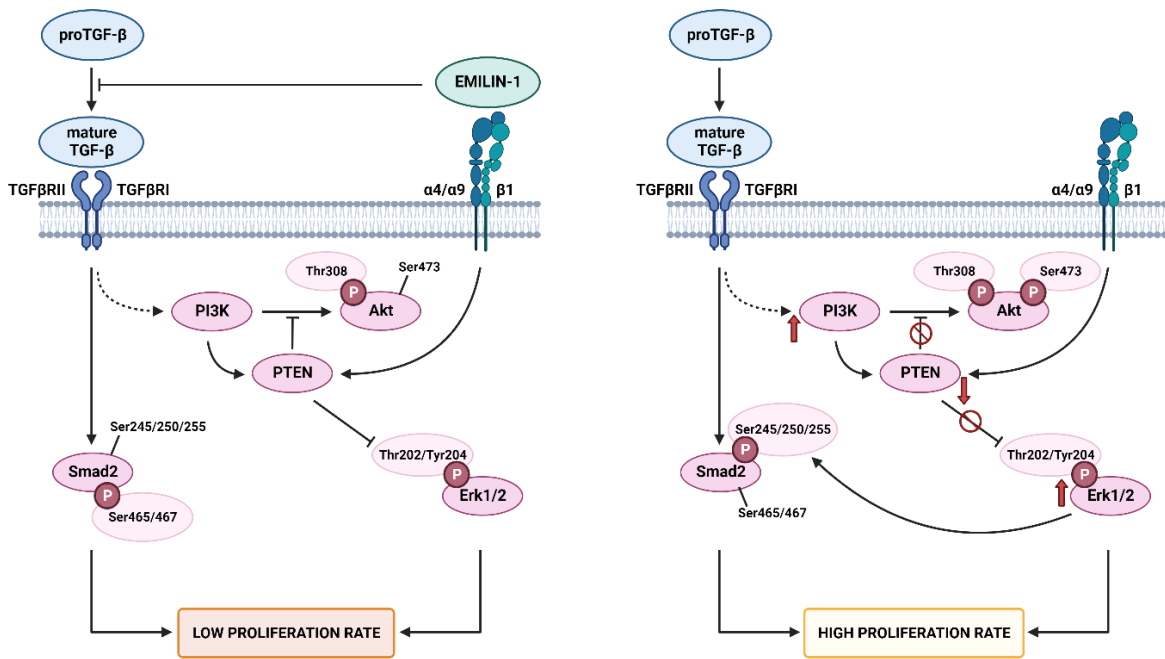
FIGURE 9. **EMILIN-1-mediated regulation of proliferation.** *EMILIN-1 interacts with α4β1/α9β1 integrins, activating PTEN and inhibiting pErk1/2, thereby suppressing TGF-β-induced proliferation. Conversely, reduced EMILIN-1 levels result in PTEN downregulation, facilitating pro-proliferative pathways. Created with BioRender.com.*

The engagement between EMILIN-1 and integrins has proved to be a critical factor for efficient lymphatic function (Capuano et al., 2019a). EMILIN-1 regulates lymphatic capillary growth, valve formation, and lymphatic collector maintenance through the interaction with integrin α9β1(Danussi et al., 2013). EMILIN-1 is part of anchoring filaments, structural elements that connect LECs to the ECM, and its integrity is necessary to ensure the stability of LEC junctions (Maiorani et al., 2017). Deficiency of EMILIN-1 leads to hyperplasia, enlargement, irregular patterns in superficial and visceral LVs, and significant reduction of anchoring filaments (Danussi et al., 2008). These morphological changes in the LVs are associated with functional defects, including mild lymphedema, significant reduction of lymph drainage, and increased lymph leakage. The phenotype observed in EMILIN-1 Knock Out (KO) mice represents the first abnormal lymphatic pattern associated with deficiency of an ECM protein and highlights the role of EMILIN-1 as a local regulator of lymphangiogenesis.

The regulatory control of EMILIN-1 over LECs is associated with its functional domain gC1q. Evidence that all signaling depends on gC1q was provided by establishing an EMILIN-1 transgenic mouse model carrying an E933A mutant of EMILIN-1 that prevents binding to integrin α4/α9β1(Capuano et al., 2019a). Generation of these transgenic mouse models was expected to preserve EMILIN-1-mediated functional control of TGF-β maturation via the EMI domain while losing the ability to interact with α4/α9β1 integrin. This strategy separated the effects linked to the regulation of TGF-β by the EMI domain from those dependent on the EMILIN-1/integrin

interaction. The lymphatic phenotype associated with the absence of the entire molecule, as in the KO mouse, may result from a combinatorial effect due to different regulatory regions. The unaltered levels of TGF-β in E933A transgenic mice suggest that all lymphatic alterations and the consequent functional anomalies associated with EMILIN-1 deficiency are due exclusively to the regulatory sequence of the gC1q domain. This mouse model provided valuable insights into the importance of the gC1q/integrin interaction in controlling the lymphangiogenic process mediated by EMILIN-1, as evidenced by the striking similarity in lymphatic phenotype between E933A transgenic and KO mice (Capuano et al., 2019a). The presence of the E933 residue in the gC1q domain alone is sufficient to regulate the dissemination of cancer cells to lymph nodes through integrin interactions, independent of the involvement of other EMILIN-1 domains. The role of the ECM, in which lymphatics are embedded, is considered important for lymphatic function and, in particular, for the formation of new LVs in response to physiological and pathological stimuli (Wiig et al., 2010). Nevertheless, the direct link between ECM and lymphangiogenesis has been documented for only a few matrix proteins (Bazigou et al., 2009; Morooka et al., 2017; Ou et al., 2010; Podgrabinska et al., 2002; Steele et al., 2011) and EMILIN-1 is one of them.

EMILIN-1 and cancer

EMILIN-1 goes beyond its role as a scaffold molecule, with its importance in the context of cancer highlighted by several findings. EMILIN-1 involvement in the TME has been shown to regulate cell growth and metastatic spread (Danussi et al., 2012). Moreover, EMILIN-1 has oncosuppressive properties as demonstrated in models of skin and colon carcinogenesis (Amor López et al., 2021; Capuano et al., 2019b). Initial investigations on lymphatic phenotypes indicated that an EMILIN-1-deficient microenvironment predisposes to tumor development. EMILIN-1 KO mice developed larger lymphangiomas than their WT counterparts, and further studies confirmed accelerated tumor development in EMILIN-1 KO mice exposed to skin carcinogenesis protocols (Danussi et al., 2012). These skin tumors exhibited increased cell proliferation as showed by the high number of Ki67-positive cells. Functional studies showed that PTEN, a major tumor suppressor, was expressed at lower levels in EMILIN-1 KO skin tumors, along with increased levels of pErk 1/2, PI3K, and pAkt. The increased LV density in tumors and draining lymph nodes of EMILIN-1 KO mice suggests that the anti-proliferative effect typically associated with the interaction of EMILIN-1 with α4-α9 integrins is absent. (Capuano et al., 2019a). In the context of colon cancer, EMILIN-1 act as a tumor suppressor by inhibiting cell proliferation, migration, and invasion. The loss of EMILIN-1 in colorectal cancer tissues is associated with more advanced disease stages and poorer

patient prognosis. Moreover, animals expressing EMILIN-1 had smaller tumors and fewer metastatic lesions compared with transgenic ones (Capuano et al., 2019b).

Expression analyses have revealed that EMILIN-1 expression levels correlate with lower proliferation rates in lung cancer (Edlund et al., 2012) and predict response to doxorubicin-based therapy in breast cancer (Koike Folgueira et al., 2005). Studies of EMILIN-1 expression in ductal invasive breast cancer showed decreased production of EMILIN1 mRNA and protein in tumors of grade II and III compared with control (Stegemann et al., 2013).

In contrast however, EMILIN-1 was found to be upregulated in low-grade brain tumors/gliomas (Zhao et al., 2020). This suggests that the role of EMILIN-1 in cancer may be context-dependent or influenced by tissue-specific factors. Another possibility is that EMILIN1 gene expression increases in tumors but, the functionality of the protein may be impaired. Tumor and microenvironment cells could release specific proteolytic enzymes that degrade EMILIN-1, leading to uncontrolled cell proliferation. EMILIN-1 can indeed be digested *in vitro* by proteolytic enzymes, including NE, which has profound effects on cancer growth (Maiorani et al., 2017). As mentioned previously, inflammatory cells such as neutrophils are common in the TME and release proteases that can fragment EMILIN-1. Functional properties of EMILIN-1 are mainly affected by enzymes capable of digesting gC1q, NE being the only one among the studied enzymes that specifically cleaves this regulatory domain of EMILIN-1, thus affecting its integrity and its suppressive role. The activity of other proteases present in the TME, such as MMPs that do not digest the recombinant gC1q domain, was restricted to the rest of EMILIN-1 (Maiorani et al., 2017). Therefore, MMPs were unable to interfere with adhesion or proliferation of cells seeded on EMILIN-1 after enzymatic treatment. However, the proteolytic action of MMPs could be essential in some pathological conditions of vessels and may contribute to the weakening of the vascular wall through their ability to digest basic structural ECM components of elastic fibers. EMILIN-1 degradation could be a critical aspect in inflammatory and degenerative processes, as well as tumor growth in humans. In conclusion, the structural integrity of EMILIN-1 appears to be critical for tumor behavior, including tumor quiescence and metastatic niche formation.

An EMILIN-1-negative microenvironment appears to promote both tumor cell proliferation (directly) and spread to lymph nodes (indirectly). The absence or dysfunction of EMILIN-1 can alter cell-ECM architecture, thereby enhancing opportunities for tumor cell proliferation and migration through disrupted barriers in LVs. Considering that EMILIN-1 engagement with α4/α9β1 integrins appears to be central in suppressing tumor cell growth and lymphangiogenesis, it is plausible that the suppressive role of EMILIN-1 involves a combination of structural and signaling-mediated functions.

Recently, EMILIN-1 was found to synergistically enhance the tumor suppressive effect of Tetraspanin9, a transmembrane protein that regulates the secretion of MMP-9 through the ERK1/2 pathway, thereby inhibiting GC cell proliferation, migration, and invasion (Qi et al., 2019). Moreover, EMILIN-1 was identified as a candidate gene that may be involved in GC cell proliferation and differentiation (Chen et al., 2018). In this study EMILIN-1 expression level correlated with pathological T stage and histological grade influencing the overall survival of GC patients. However, histological validation and localization of EMILIN-1 in gastric tissues are still pending and its role in tumor progression remains to be elucidated.

Unmet needs in gastric cancer research

Although the incidence of GC in developed countries has steadily declined in recent decades, outcomes in Western countries remain poor, primarily due to the advanced stage of the disease at presentation (Lordick et al., 2014). While earlier diagnosis would help to improve outcomes for GC patients, a better understanding of the biology of the disease and the advances in therapy are also needed. Indeed, progress in treating GC has been limited, largely due to its genetic complexity and heterogeneity (Rha et al., 2020).

There are still several unmet needs in the field of GC research, particularly with regard to the complicated interactions between the components of the TME (Zeng et al., 2019). The first issue is a comprehensive understanding of the role of the ECM in GC progression. ECM remodeling is pivotal in cancer invasion and metastasis, but the precise mechanisms and potential therapeutic targets within the ECM have not been fully elucidated in GC. Another important need is in the area of lymphangiogenesis, as the mechanisms controlling LV formation in GC remain a subject of active investigation. A more detailed understanding of how lymphangiogenesis contributes to disease progression is essential for the development of targeted therapies that interrupt this process and limit metastasis (Wang and Chu, 2022). Furthermore, the role of Cancer-Associated Fibroblasts (CAFs) within the gastric TME is a complex and evolving area of research. Deciphering the molecular signatures and functional contributions of CAFs in GC is essential for developing innovative strategies targeting these cells to effectively impact tumor growth and metastasis (Mak et al., 2022; Ucaryilmaz Metin and Ozcan, 2022).

Answering these unresolved questions related to TME not only improves our basic understanding of GC but also paves the way for the development of more precise and effective therapeutic interventions.

AIM OF THE STUDY

The aim of this study is to explore the complexity of GC, with particular emphasis on deciphering the role of EMILIN-1 as a molecular regulator of its development and progression (**Figure 10**).
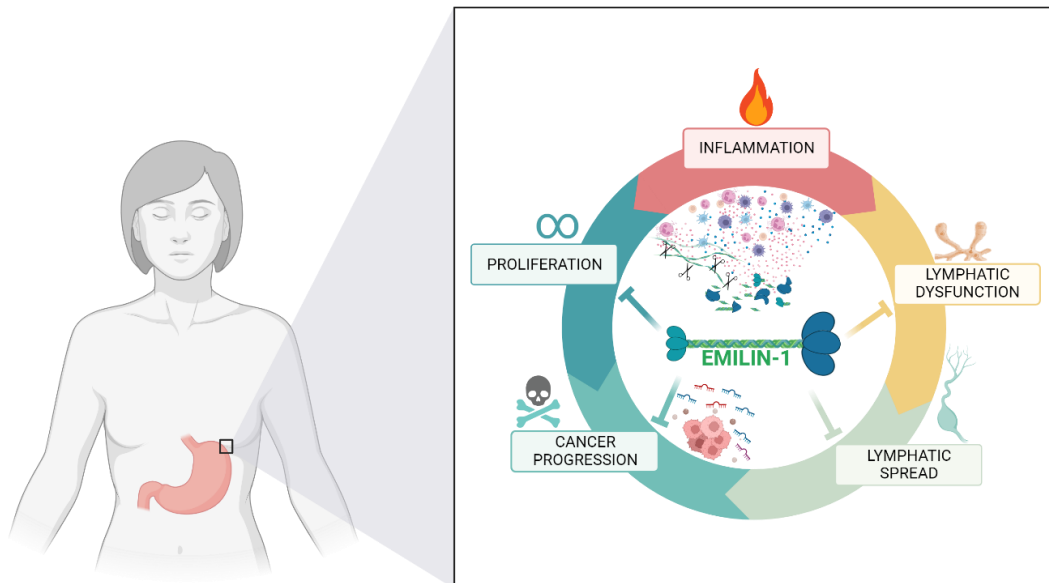

*FIGURE 10. **Rationale of the study**. Interplay between different actors in the multifaceted gastric environment. Created with BioRender.com.*

Lymphatic metastasis is the main dissemination pathway of GC and plays a critical role in determining clinical outcome (Deng and Liang, 2014). The complicated dynamics of GC progression involve significant changes in the lymphatic vasculature, which are closely associated with the metastatic potential of GC cells. Consequently, lymphatic metastasis emerges as a critical factor in disease progression. Moreover, dysregulation of lymphangiogenesis, which traditionally serves to solve inflammation and clear inflammatory cells, may lead to persistent inflammation, contributing to the maintenance of malignant gastric cells (Kim et al., 2014). This study places particular emphasis on recognizing the critical role played by the GC TME. As reported in the introductory section EMILIN-1 is a key player controlling tumor growth and lymphangiogenesis. Furthermore, EMILIN-1 exhibits remarkable anti-proliferative properties, due to its interaction with α4β1 integrin. The observation that α4 integrin is transcriptionally repressed in GC suggests an additional and important mechanism involving integrin/EMILIN-1 recognition in the suppression of cell proliferation (Park et al., 2004a). Previous findings from our research have already provided compelling evidence that the absence of EMILIN-1 accelerates tumor development, resulting in a greater number and size of colon tumors (Capuano et al., 2019b). Conversely, the presence and expression of EMILIN-1 exert control over cell proliferation while attenuating lymphatic dysfunction. This leads to the convincing hypothesis that EMILIN-1 may also exert an oncosuppressive role in the gastric microenvironment, where inflammation,

lymphangiogenesis, and alterations in ECM constituents represent important pathogenic mechanisms.

In summary, the overall goal of this study is to comprehensively investigate the multifaceted interactions between EMILIN-1, the TME, and GC progression. By examining these complex mechanisms in detail, we aim to gain valuable insights into the development and progression of GC, potentially opening new avenues for research and treatment strategies in this area.

MATERIAL AND METHODS

Patients

Gastric biopsies were obtained during endoscopy from 20 patients from the Oncologic Gastroenterology Unit of IRCCS CRO Aviano, with written informed consent. Experienced gastroenterologists and pathologists classified the lesions according to histopathological diagnostic criteria. Patients were of both sexes and similar age. Control specimens were adjacent healthy tissue. All biopsy samples were embedded in OCT. Some patients in the same cohort underwent surgery. FFPE sections were then obtained from surgical specimens.

In vitro procedures

Chemicals and reagents

Recombinant gC1q WT and E933A domains were prepared and purified as previously described (Spessotto et al., 2003). EMILIN-1 As556 rabbit polyclonal antibody was prepared and purified as previously described (Spessotto et al., 2003). Integrin α4 blocking antibody (P1H4) was provided by Millipore (Sigma). Commercial primary antibodies used for western blot and immunofluorescence are listed in **Table 1**.

TABLE 1

ANTIGEN	COMMERCIAL NAME	COMPANY	ID
α-SMA	Mouse monoclonal to α-CMA, Cy3™	Sigma-Aldrich	C6198
CD31	Mouse monoclonal to CD 31	Abcam	ab9498
CD45	Mouse monoclonal to CD45 (2B11/PD7/26)	Dako	GA75161-2
EMILIN-1	Rabbit Polyclonal EMILIN1 antibody	Abcam	ab243324
FIBRONECTIN	Rabbit polyclonal to Fibronectin	GeneTex	GTX112794
GAPDH	Mouse monoclonal to GAPDH	Millipore	MAB374
INTEGRIN α4	Rabbit monoclonal to integrin α4	Cell Signaling	8440
LYVE1	Rabbit polyclonal to LYVE1	Abcam	ab14917
NEUTROPHIL ELASTASE	Rabbit polyclonal to Neutrophil elastase	Abcam	Ab21595
PODOPLANIN	Mouse monoclonal [D-240] to podoplanin	Abcam	Ab11936

| P54 | Mouse monoclonal to p54[nrb] | BD Biosciences | 611279 |
| VINCULIN | Goat polyclonal to vinculin | Santa Cruz | Sc-7649 |

Commercial secondary antibodies used for western blot were HRP conjugated (Bethyl). Alexa Fluor conjugated antibodies were used for immunofluorescence (Invitrogen).

Cell lines and primary cells

All cells (summarized in **Table 2**) were cultured at 37 °C in a 5% CO2 atmosphere in a HERA cell 240 incubator (ThermoFisher). GES-1 (courtesy of Prof. Marina de Bernard, University of Padova) were cultured in RPMI medium (Gibco) supplemented with 10% Fetal bovine Serum (FBS) and 100 U/mL penicillin/streptomycin (Gibco). NCI-N87 (ATCC) were cultured in RPMI medium (Gibco) supplemented with 10% FBS and 100 U/mL penicillin/streptomycin (Gibco). Hs 746.T (ATCC) were cultured in DMEM 4.5 mg/L glucose medium (Gibco) supplemented with 1 mM Sodium Piruvate (Gibco) 10% FBS and 100 U/mL penicillin/streptomycin (Gibco). AGS (ATCC) were cultured in F-12K medium (ATCC) supplemented with 10% FBS and 100 U/mL penicillin/streptomycin (Gibco). Normal Human Dermal Fibroblasts (Lonza) were cultured in FBM medium (Lonza) supplemented with FGM™ -2 Fibroblast Growth Media Bullet Kits™ (Lonza). Bj-5ta (ATCC) were cultured in 4:1 mixture of DMEM 4.5 mg/L glucose and M199 medium (Gibco) supplemented with 10% FBS and 0.01 mg/mL hygromycin B (Invitrogen). Human Dermal Lymphatic Endothelial Cells (Lonza) were cultured in EBM™-2 supplemented with EGM™-2 MV Microvascular Endothelial Cell Growth Medium-2 Bullet Kit™ (Lonza). YNT16 (courtesy of prof. Sachiyo Nomura, University of Tokyo) were cultured in DMEM 4.5 mg/L glucose medium (Gibco) supplemented with 10% FBS (Gibco), 100 U/mL penicillin/streptomycin (Gibco) and MITO+ serum extender (Corning). Primary fibroblasts (courtesy of Dr. Danilo Ranieri, St. Andrea Hospital, Rome). Jurkat (ATCC) were cultured in RPMI (Gibco) supplemented with 10% FBS and 100 U/mL penicillin/streptomycin (Gibco).

TABLE 2

CELL	TYPE	COMPANY
AGS	Gastric adenocarcinoma, intestinal histotype	ATCC
GES-1	Normal gastric epithelium	Courtesy of Prof. M. de Bernard
Hs 746.T	Gastric carcinoma, metastatic, diffuse histotype	ATCC
NCI-N87	Gastric carcinoma, metastatic	ATCC

HDLEC	Human dermal lymphatic endothelial cells	Lonza
NHDF	Normal human dermal fibroblasts	Lonza
FIBROBLASTS	Primary human fibroblasts	Courtesy of St. Andrea hospital
Jurkat	Immortalized T lymphocyte cell line	ATCC
YTN16	Murine gastric carcinoma	Courtesy of S. Nomura

Cell transfection

AGS cells were transfected using the Fugene HD reagent method (Promega), according to the manufacturer's instructions. Briefly, cells were seeded into six well plates and grown to 80% confluence. 10 μg of the empty vector pcDNA or the α4-pcDNA plasmids were used. 48 hours post-transfection G418 antibiotic (Roche) was added to culture media for transfectant clone selection. Empty pCDNA or α4-pCDNA plasmids were used as previously described (Modica et al., 2017). Single cell cloning was followed to obtain cell clones for functional assays. Cells were then cultured in F-12K medium (ATCC) supplemented with 10% FBS and 0,5 mg/ml G418 (Roche).

RT-PCR analysis

Total RNA was extracted using NucleoSpin RNA II (MachereyNagel, Germany) according to the manufacturer's instructions and the concentration was determined using a spectrophotometer (Nano-Drop ND-1000, ThermoFisher scientific). Reverse transcription was performed using 1 μg of total RNA. The cDNA products were amplified using iQ SYBRGreen Supermix (Bio-Rad Laboratories, Italy) with the primers reported in **Table 3**. qRT-PCR was performed using CFX96 qPCR (Bio-Rad) and data were analyzed with CFX Maestro dedicated software (Bio-Rad).

TABLE 3

GENE	**FORWARD PRIMER (5′ › 3′)**	**REVERSE PRIMER (5′ › 3′)**
ACTA2 (α-SMA)	TATCCCCGGGACTAAGACGG	CACCATCACCCCCTGATGTC
COL1A1	GGAATGAAGGGACACAGAGGTT	AGTAGCACCATCATTTCCACGA
EMILIN1	TCCCCAAAGCATCATGTACCG	CACAGTCATCGCCCCCATAA
EMILIN1 intron1	GACTGAGACAGGCCCAGAAA	TCCTGTGTAGCAGGAGCAGA
EMILIN1 exon4-5	GCAACCAAGGACCGTATCAT	TCACAGACACCCTCAAGACG
FIBRONECTIN	GTGTGATCCCGTCGACCAAT	CGACAGGACCACTTGAGCTT

GAPDH	GAGAGACCCTCACTGCTG	GATGGTACATGACAAGGTGC

microRNAs were extracted using Maxwell® 16 miRNA Tissue Kit (Promega) according to manufacturer's instruction by means of Maxwell® 16 instrument (Promega). miRNA expression was assayed using Taqman™ MicroRNA Assays Kit (ThermoFisher scientific) according to manufacturer's instruction.

Western Blot analysis

For ECM extracts cells were seeded into six well plates and grown to confluence. Media were discarded and cells washed with PBS; cultures were then incubated with the Lysis solution NP40 1% in PBS (IGEPAL, Sigma) for 10 minutes. After a wash step with PBS, 80 µl of Laemmli buffer (60 mM Tris [pH 6.8], 2% SDS, 10% glycerol, 5% β-mercaptoethanol, 0.01% bromophenol blue) were added to each well and cells were scratched and harvested. Lysates were denatured at 90 °C for 5 min. For protein extraction, cells were lysed in RIPA buffer (10mM Tris-HCl, pH 8.0; 1mM EDTA; 0.5mM EGTA; 1% Triton X-100; 0.1% Sodium Deoxycholate; 0.1% SDS; 140mM NaCl). Cell debris were removed from the homogenates by centrifugation at 10,000 g for 20 min. Cell lysates were quantified using the Bradford assay (Bio-Rad). Lysates were denatured in Laemmli buffer (60 mM Tris [pH 6.8], 2% SDS, 10% glycerol, 5% β-mercaptoethanol, 0.01% bromophenol blue) at 90 °C for 5 min. Equal amounts of sample were separated by electrophoresis on a 4–20% SDS polyacrilamide gels (Criterion Precast Gel, BioRad) and transferred onto nitrocellulose membranes (Amersham Hybond-ECL, Amersham Pharmacia Biotech, UK). Membranes were blocked with the everyBlot Blocking Buffer (BioRad) and incubated overnight at 4 °C with primary antibodies. After washing with TBS-Tween, membranes were incubated with the appropriate secondary HRP conjugate antibodies (Bethyl). Chemiluminescent signals were visualized using Chemidoc Touch Imaging System (BioRad).

CRISPR/Cas9 system

Knockout of EMILIN1 in Bj-5ta cells was generated by CRISPR-Cas9 system, according to Ran et al. (Ran et al., 2013). To obtain KO fibroblasts, four different single guide RNAs (sgRNA) were used (as reported in **Table 4**) spanning approximately 511 bp of exon 1 of EMILIN1.

TABLE 4

Gene		Sequence 5'-3'
EMILIN1	RS_CRISPR_132_S	ttgtttgTGGGCGGGATGAGTCTCTGA
EMILIN1	RS_CRISPR_132_AS	aaacTCAGAGACTCATCCCGCCCAcaa
EMILIN1	RS_CRISPR_133_S	caccgCTGTGGAGCGCCCCGCCATG
EMILIN1	RS_CRISPR_133_AS	aaacCATGGCGGGGCGCTCCACAGc
EMILIN1	RS_CRISPR_134_S	tcccaAGAGTCTGGATCCCAGCCCG
EMILIN1	RS_CRISPR_134_AS	aaacCGGGCTGGGATCCAGACTCTt
EMILIN1	RS_CRISPR_135_AS	cctcgCTGCTGTGTCCGCTAATGCA
EMILIN1	RS_CRISPR_135_S	aaacTGCATTAGCGGACACAGCAGc

Briefly, sgRNAs were cloned into pLV hUbC-Cas9-T2A-GFP (AddGene). Bj-5ta cells were transduced with this lentiviral system and an empty control (pLV hUbC-Cas9-T2A-GFP without sgRNAs) and were sorted by flow cytometry. To test CRISPR/Cas9 efficiency, genomic DNA was extracted using Gentra Puregene Cell Kit (Qiagen Sciences, Germantown, MD, USA) according to manufacturer's instructions and sequenced using MiSeq system by Illumina (Illumina, San Diego, CA, USA) as per manufacturer's instructions (Primer MiSeq table 4). Sequencing reads were visualized using the Integrative Genomics viewer (IGV, Broad Institute, Cambridge, MA, USA) to confirm genetic deletion. Cell clones were grown after cell sorting by Flow cytometry. DNA was extracted and clones screened by PCR, using specific primers (**Table 5**).

TABLE 5

PRIMER	Sequence 5'-3'
MiSeq_ F	tcgtcggcagcgtcagatgtgtataagagacagGGGGGCTATCAGAAGGAAAC
MiSeq_ R	gtctcgtgggctcggagatgtgtataagagacagCCTAGGTGACCCAAGGAACA
EMILIN1_KOscreen_ F	ACCCTCTGGAGCTGCTACCT
EMILIN1_KOscreen_ R	CCCCACTGGAACCTGTGTA

Immunofluorescence

Cells were grown on cover glass slides for three days, then were fixed with 4% (w/v) PFA, blocked with 2% BSA and incubated with the appropriate antibodies. Slides were finally mounted in Mowiol containing 2,5% (w/v) of 1,4-diazabicyclo-[2,2,2]-octane (DABCO). For nuclei staining

ToPro3 (Invitrogen) was used. Images were acquired with a confocal system (Leica Microsystems). Images were assembled using Adobe Illustrator CS6 and Adobe Photoshop CS6.

Mouse tissues were excised, embedded in OCT (Kaltek, Padova, Italy), snap frozen and stored at -80°C. Cryostat sections of 7μm were then prepared, air dried at room temperature, hydrated with PBS for 5 min and fixed with PFA 4% for 15 min. Then the sections were permeabilized with a PBS solution containing 1% BSA, 0.1% TRITON X-100 and 2% FCS for 5 min and saturated with blocking buffer (PBS-2%BSA) and incubated with the appropriate antibodies. Images were acquired with a confocal system (TCS SP8, Leica Microsystems). Images have been assembled using Adobe Illustrator CS6 and Adobe Photoshop CS6.

Cytonuclear fractionation protocol

Cell processing and fractionation were performed as follows. Cells were harvested, and the resulting pellet was lysed using 500 μl of RSB lysis buffer (Tris-HCl 10 mM pH 7,4; NaCl 50 mM; $MgCl_2$ 10 mM) containing 0.034% NP-40. Following lysis, the suspension underwent centrifugation. From the upper phase, corresponding to the cytoplasmic fraction, 300 μl were reserved for western blot analysis, while 200 μl were resuspended in 800 μl of TRIzol™ LS (Invitrogen, ThermoFisher) for subsequent RNA extraction. The pellet was then washed with the lysis buffer. From the pellet, 5 μl were lysed using SDS lysis buffer for western blot analysis, and an additional 10 μl were resuspended in TRIzol™ (Invitrogen, ThermoFisher) for RNA extraction, following the manufacturer's instructions. Gene expression analysis was performed as previously described (qRT-PCR). To quantify the cytoplasmic fraction, the Bradford assay (Bio-Rad) was employed. Protein lysates were denatured in Laemmli buffer (composition previously reported) at 90 °C for 5 minutes. Subsequently, 15 μg of protein extract were loaded for western blot analysis.

The relative amount of nuclear material for western blot analysis was determined as a proportion, with 'x' representing the number of cells in the desired volume of cytoplasm.

$$number\ of\ harvested\ cells: 500\mu l = x: volume\ loaded\ on\ gel$$

The number of cells contained within 5 μl of nuclear fraction was determined as volume ratio, and the concentration was established. Then, the volume of the nuclear fraction to be loaded was determined, with 'y' representing the volume from the nuclear fraction that equaled that of the cytoplasmic fraction.

$$y = \frac{x}{\frac{cell}{\mu l} nuclear\ fraction}$$

This approach allowed precise calculations and comparisons between the nuclear and cytoplasmic fractions. It is important to note that the western blot analysis primarily serves as a quality index for the cytonuclear fractionation process.

FACS analysis

Analysis of AGS clones: cells were detached with 5 mM EDTA in PBS, centrifuged and the pellet was incubated with a PE-conjugated anti-integrin α4 (CD49d) antibody (clone 9F10, BioLegend) or an anti-IgG (Isotype control) on ice for 15 minutes protected from light. Flow cytometry analysis was performed at the Flow Cytometry core facility of the Hematology Unit of CRO-Aviano with the LSRFortessa X-20 instrument (BD Biosciences).

Bj-5ta sorting: cells were detached with 5 mM EDTA in PBS, centrifuged. The pellet was resuspended in PBS 20% BSA 0,5 mM EDTA (pH 8). Sorting of positive cells was performed through flow cytometry with BD FACSAria™ III Cell Sorter (BD Biosciences). Positive cell clones were selected and grown as described in cell culture section.

Cell adhesion (CAFCA) assay

The quantitative cell adhesion assay CAFCA (Centrifugal Assay for Fluorescence based Cell Adhesion) is based on centrifugation as previously described (Spessotto et al., 2000). Briefly (**Figure 11**), six-well strips of flexible polyvinyl chloride (BectonDickinson, Falcon), covered with double-sided adhesive tape (bottom units), were coated with the different substrates (Collagen type I, Collagen type IV, FN, recombinant gC1q, Laminin). The coating solutions were prepared dissolving protein substrates in PBS, at a concentration of 10 μg/mL. Coated bottom units were incubated overnight at 4°C. The next day the coating solution was removed and the miniplates were incubated with 1% (w/v) BSA blocking solution at room temperature for at least 2 hours. Cells were labelled with the vital fluorochrome Calcein AM (Molecular Probes, Invitrogen) for 15 minutes at 37°C and then aliquoted (50 x 10^3 cells/well) into bottom miniplates (after removing blocking solution). Cells are resuspended in cell-adhesion medium (0.5% Polyvinylpyrrolidone; 2% India Ink in PBS) and then centrifuged at 146 x g (to synchronize the contact of the cells with the substrate). Bottom miniplates were incubated for 20 minutes at 37°C to allow cell adhesion

to substrates. Top CAFCA miniplate were then prepared, filled with adhesion medium and assembled to bottom units. A "reversed" centrifugation step was then applied and the fluorescence signals emitted by cells in wells of the top (unbound cells) and bottom (substrate-bound cells) sides were finally measured independently, using InfinitemM1000 microplate fluorometer (TECAN). The percentage bound cells, out of the total amount of cells introduced into the system, was calculated.
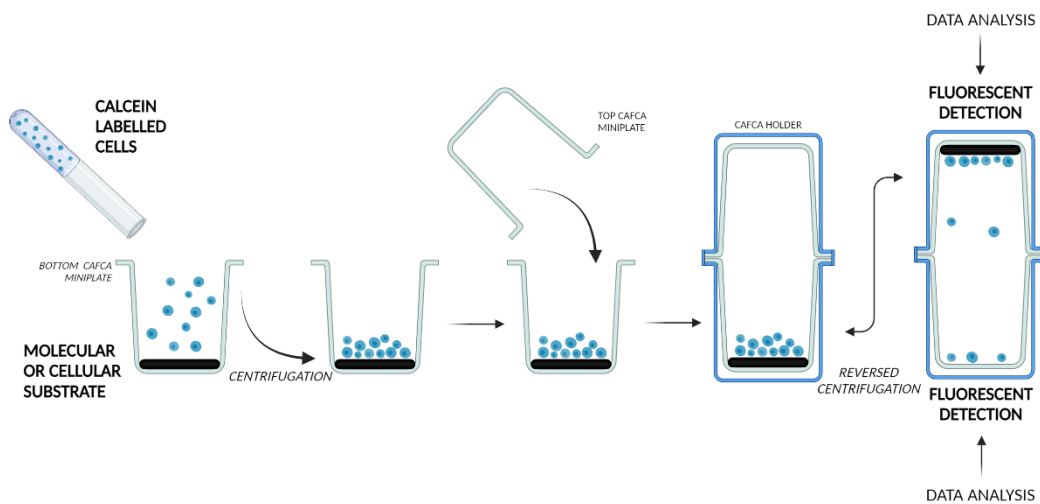

FIGURE 11. **Schematic representation of CAFCA assay.** *CAFCA bottom miniplates were coated with ECM protein. Cells were labeled with the vital fluorochrome Calcein and then aliquoted into the bottom CAFCA miniplates, which were centrifuged to synchronize the adhesion of the cells with the ligand. The miniplates were then incubated for 20 minutes at 37°C and subsequently mounted together with a similar CAFCA miniplate to create communicating chambers for subsequent reverse centrifugation. The relative number of cells which bound or not the ligand was estimated by top/bottom fluorescence detection. Created with BioRender.com.*

xCELLigence technology for adhesion and proliferation assays

To monitor cell adhesion and cell proliferation quantitatively and qualitatively in real time, the xCELLigence technology provided by the Real-Time Cell Analyzer (RTCA) Single Plate instrument (Agilent) was used. The plate used was the 96-well E-plate VIEW 96 (Acea Bioscience); experimental set-up, data acquisition and data analysis were performed using the RTCA Software Pro. The cell index is an arbitrary measure that reflects the total cell number, attachment quality, and cell morphology; it can change over time according to impedance modifications caused by cell attachment attitude and cell number (**Figure 12**). For adhesion experiments, the E-plate 96 was coated with ECM proteins or gC1q domain (10 µg/ml) and saturated with BSA1% in PBS solution. Cells were seeded and monitored every 5 min for 20 hours. For proliferation experiments, cells were seeded in the E-plate 96 and gC1q domain was added (10 µg/ml). Cells were monitored every hour for 5 days.
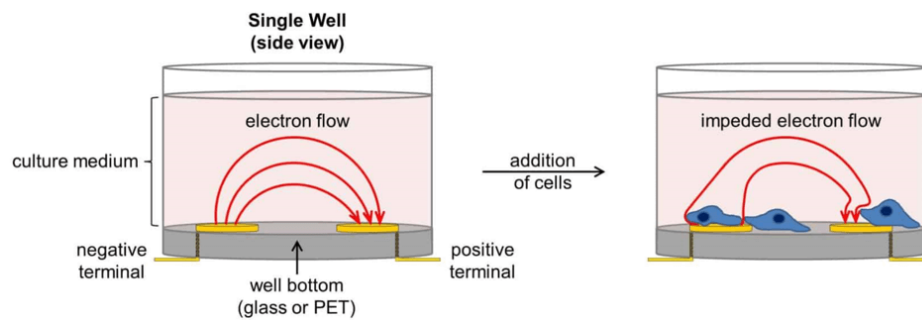
FIGURE 12. **Simplified schematic of the impedance phenomenon.** *Real-time measurement of impedance via the biosensors is correlated with electron flow and depends on the number of cells, their size and shape. The impedance measurement does not affect the health and behavior of the cells and thus provides an opportunity to study cell properties in a non-invasive way.*

In vivo procedures

In vivo experiments were performed using WT, KO and KI mouse models generated in our laboratory as previously described (Capuano et al., 2018). Heterozygous +/E933A animals were also used. Mice genotypes were routinely assessed. Tissues collected from all experiments were sent to pathologists for systematic evaluation. For the invasion score, samples were divided in 6 blocks: 1) spleen, liver and kidneys; 2) lungs, heart, thymus; 3) upper Gi - stomach, duodenum, pancreas; 4) lower Gi - cecum, ileum, colon, mesentery; 5) genitals – uterus, ovaries/accessory sexual glands, testicles, epididymis; 6) diaphragm, abdominal wall.

Syngeneic models

We used three injection methods to transplant the syngeneic YTN16 cell (Yamamoto et al., 2018). In subcutaneous injection (**Figure 13A**) 5×10^6 YTN16 cells were delivered just below the skin surface, into each mouse flank. Animals were sacrificed after 20 days. For intraperitoneal injection (**Figure 13B**), 10×10^6 YTN16 cells were delivered into the peritoneal cavity, representing a more direct and systemic route of administration. Mice were sacrificed 25 days after-injection. For intrafootpad injection (**Figure 13C**), 10×10^6 YTN16 cells were precisely delivered into the footpad region. Animals were sacrificed 21 days after injection.

Chemical carcinogenesis model

The chemical carcinogenesis protocol (**Figure 13D**) took advantage of the potent chemical carcinogen N-Methyl-N-nitrosourea (MNU) administered to mice for 5 weeks (K. Li et al., 2021). In this administration, mice were alternately treated with MNU and saline solution for a total of 10 weeks. The mice were then closely monitored for 20 weeks to track any tumor development or related effects. At the end of the observation period, the mice were sacrificed.
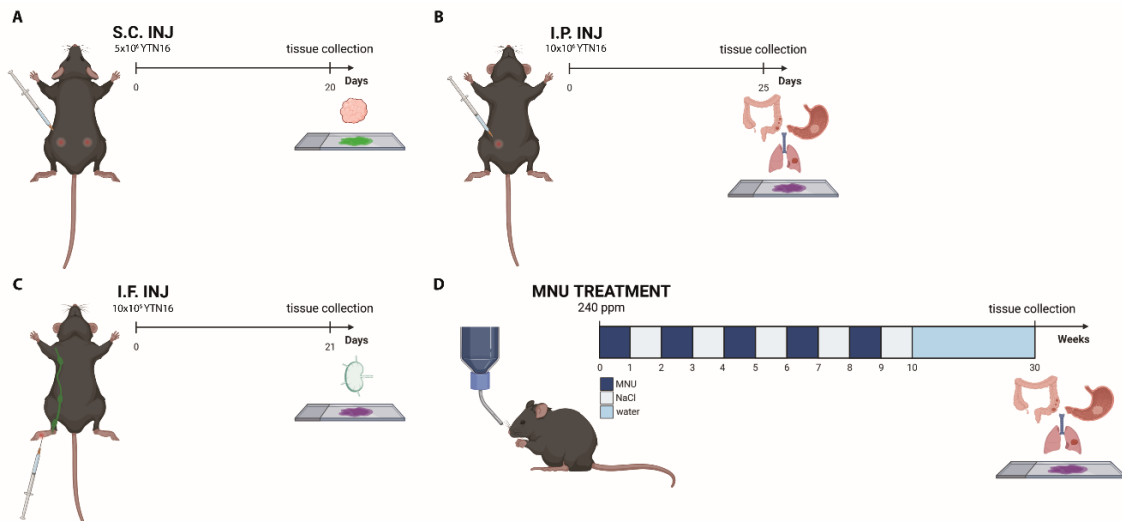

FIGURE 13. **Different GC mouse models used in this study.** *A) Sub-Cutaneous model (S.C.): 5x10^6 cells were injected into each flank of the mice. Animals were sacrificed 20 days after injection B) Intra-Peritoneal (I.P.) model: 10x10^6 cells were injected into the mice. Animals were sacrificed 25 days post injection C) Intra-Footpad model (I.F.): 10x10^{6}cells were injected into the footpads of mice. Animals were sacrificed 21 days post injection. D) MNU chemical carcinogenesis model: administration of 240 ppm of MNU for 5 weeks, alternating with NaCl. Mice were fed with normal drinking water for 20 weeks and sacrificed at week 30. Inj.=injection. Created with BioRender.com.*

Statistical analysis

Graphpad Prism (version 7.02) was used to perform the statistical analyses. The ordinary one-way ANOVA or unpaired t-test was used if the values were normally distributed. P-values <0.05 were considered significant. All measurements are shown as mean ± SD.

RESULTS

Loss of EMILIN-1 in malignant and premalignant gastric samples correlates with the presence of aberrant LVs.

To investigate the role of EMILIN-1 in GC and its impact on lymphatic dysfunction within the TME, we first evaluated the levels of EMILIN-1 in bioptic samples of a small cohort of patients (n= 20).
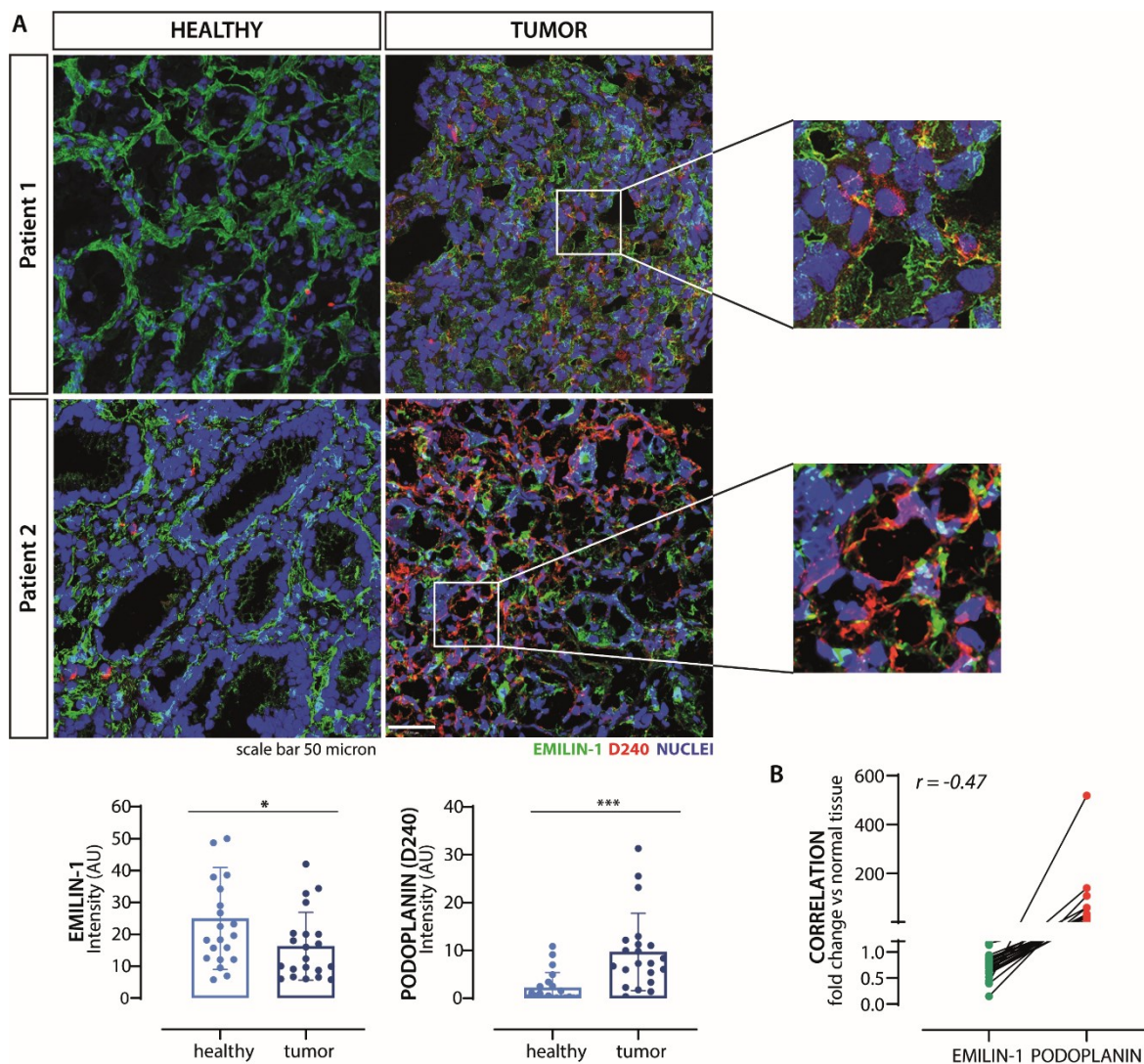

FIGURE 14. **EMILIN-1 is downregulated in human GC mucosa.** *A) Representative images of EMILIN-1 (green) and podoplanin (red) staining of OCT sections of gastric tumor mucosa and adjacent normal tissue of two patients (nuclei pseudo-colored in blue). In healthy tissue EMILIN-1 fibrils decorate the glands. In GC tissues the deposition is reduced and fragmented. Podoplanin expression significantly increases in GC tissue with respect to normal counterpart. Vessels have an aberrant morphology. The associated graphs represent the quantification of EMILIN-1 and podoplanin positive volume in the whole section field examined (20X). For each sample at least five fields were analyzed, and the mean value was reported. The results represent the mean ±SD of 20 patients affected by GC. Scale bars: 50 μm. P values were calculated using two-tailed Student's t-test. *P<0.05, ***P<0,001. B) The graph represents the inverse correlation between EMILIN-1 and podoplanin expression in the patients' cohort. The fold change has been determined comparing intensities in tumor versus normal counterpart, paired samples. Pearson correlation coefficient has been calculated among the two variables. (p<0.05, r=-0,47)*

Our preliminary data from immunofluorescence analysis showed a strong contrast in EMILIN-1 expression between normal and malignant gastric tissue. Interestingly, the decreased levels of

EMILIN-1 in tumor tissues appear to be closely associated with the presence of aberrant LVs, indicating a potentially dysfunctional vasculature within the TME (**Figure 14A** and **14B**). Of particular note are the differences observed in representative images from two patients, although they show some individual variation. Normal gastric mucosa shows a well-defined architectural pattern of EMILIN-1 expression, whereas the malignant samples exhibit both a markedly reduced protein content and a diffuse and fragmented deposition. Although vessel morphology is not maintained in these frozen samples, it is easy to detect their excessive tortuosity and lack of a typical lumen, suggesting alterations in functionality.
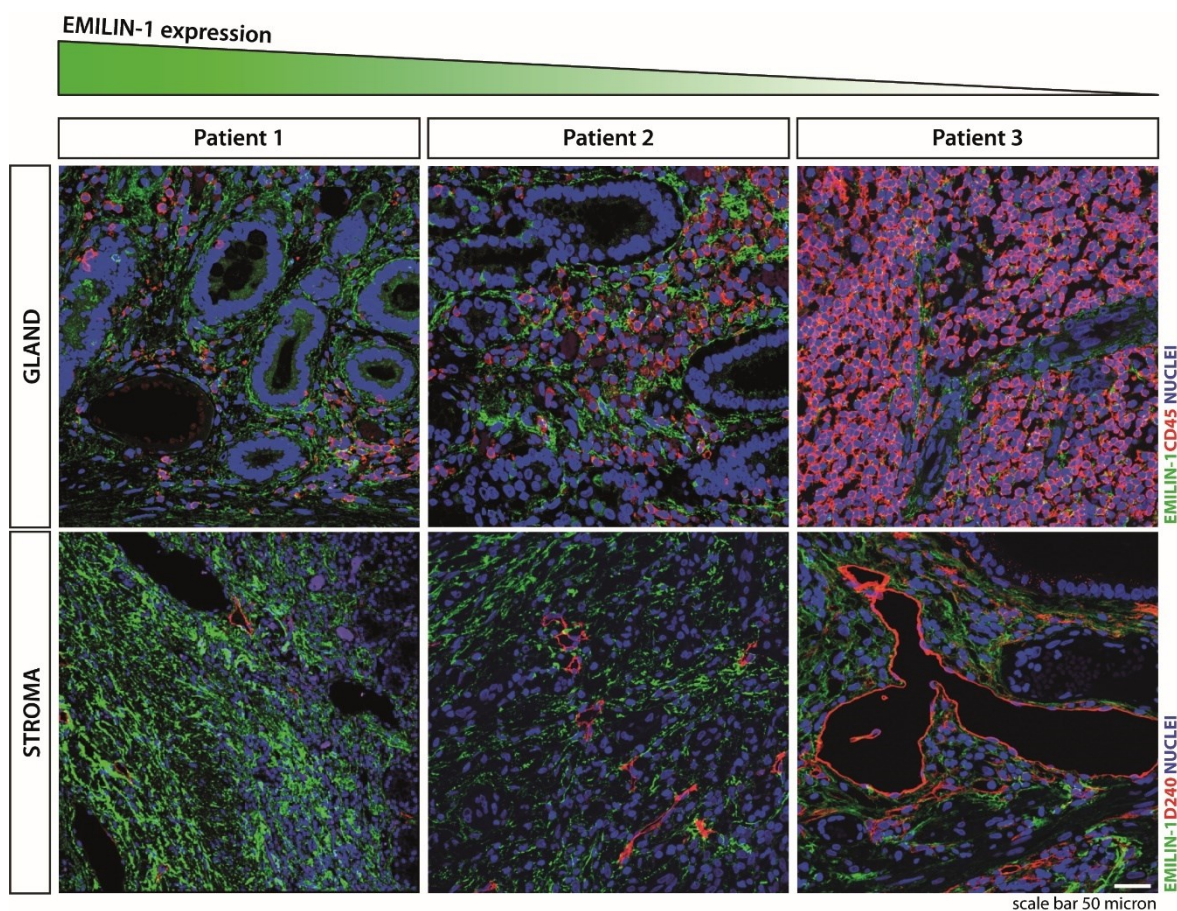

FIGURE 15. *Relationship between the deposition of EMILIN-1 and the architectural changes in the stomach microenvironment. The focus was particularly in the stromal and glandular regions. The decrease in EMILIN-1 (green) levels corresponds to the worsening of stomach architecture in malignant tissues. A concurrent increase in D240 and CD45 (red) levels is observed, suggesting a dynamic interplay between EMILIN-1, immune cell infiltration (CD45), lymphatic vessels (D240) and the structural alterations characteristic of GC. Representative images, not sufficient for statistical evaluation.*

The morphological alterations linked to the decline of EMILIN-1 were more effectively evaluated using representative FFPE- embedded tissue samples from patients who had undergone GC surgery. **Figure 15** suggests a possible relationship between EMILIN-1 deposition and the structural integrity of the stomach, particularly in the stroma and glandular districts. Furthermore, worsening tissue morphology was observed, characterized by compromised glandular architecture, aberrant lymphatic vessel morphology, and a substantial increase in inflammatory

infiltration as cancer progressed. When the structural organization of the stomach changes, EMILIN-1 expression simultaneously decreases. Of note, this architectural decline is accompanied by an increase in levels of podoplanin, a marker of LVs, and CD45, a marker of immune cell infiltration. The increase in podoplanin suggests the presence of a higher number of LVs in the TME, possibly contributing to lymphatic spread in GC. At the same time, the increase in CD45 suggests increased immune cell infiltration, which is likely promoted by tumor-induced de novo lymphangiogenesis.
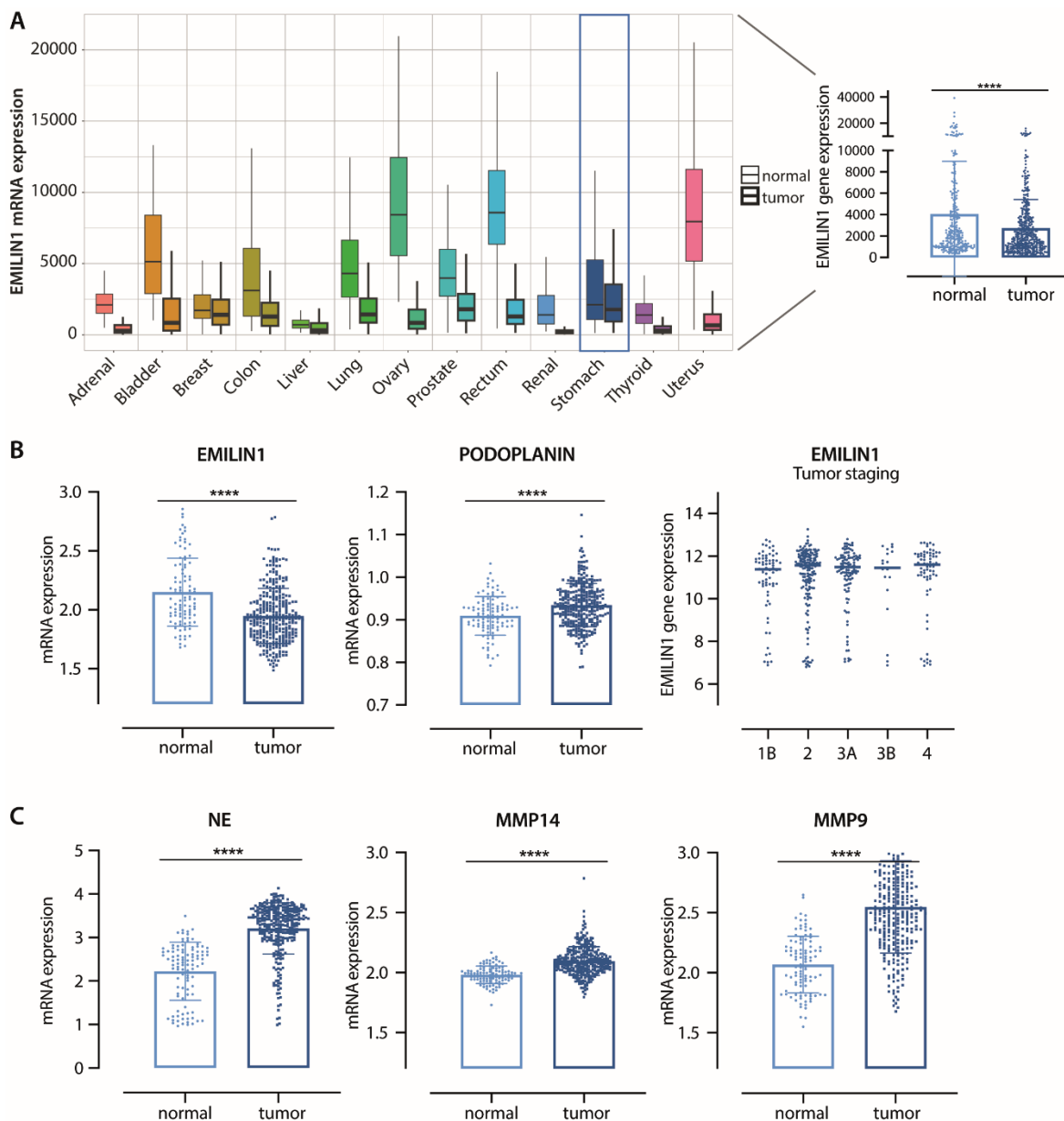

FIGURE 16. **In silico analysis of data from various sources.** *A) TNMplot panel shows reduced EMILIN-1 expression in various tumors, emphasizing GC. B) Analysis of paired samples in GSE 6622 cohort confirms this reduction and reveals an increase in podoplanin expression. The decrease appears significant during early disease stages, with no significant variation in later stages (GSE26253). C) Proteolytic enzymes were assessed in GSE 6622 cohort as potential contributors to EMILIN-1 degradation in ECM remodeling. P values were calculated using two-tailed Student's t-test. ****P<0,0001.*

46

To explore this intriguing relationship in more detail, we initiated an in-silico analysis by mining data from multiple sources. Examination with the online TNMplot tool shed light on the decreased expression of EMILIN-1 in a spectrum of tumor types, with emphasis on GC (**Figure 16A**).

An important confirmation of these results was provided by a GSE cohort analysis including paired normal and tumor samples, in which the decrease in EMILIN-1 expression was clearly validated (**Figure 16B**). Moreover, this decrease is accompanied by a marked increase in podoplanin expression. Notably, the analysis of a different dataset, which included different GC stages, revealed that reduction in EMILIN-1 expression appears to be particularly critical in the early phases of the disease, as no significant differences are observed between disease stages. To fully understand the mechanisms underlying this phenomenon, the presence of proteolytic enzymes was also investigated, indicating their possible role in the degradation of EMILIN-1 as part of the ECM remodeling process (**Figure 16C**). The expression of MMP9, MMP14, and NE, all of which play a role in EMILIN-1 degradation, was significantly increased in GC lesions. These collective findings suggest that multiple mechanisms may impair the protective role of EMILIN-1 in the context of GC and ultimately contribute to tumor growth and cancer dissemination via lymphatic pathways.

Building on our preliminary observations, we looked more closely at the stepwise progression of gastric carcinogenesis, a process that involves chronic gastritis, atrophy, intestinal metaplasia, and dysplasia before culminating in cancer (**Figure 17A**).

For this purpose, several samples were analyzed from each patient. Consistent with our previous results, we observed a gradual decrease in EMILIN-1 levels, even in premalignant tissues. In the middle image, EMILIN-1 is almost absent, coinciding with the appearance of aberrant LVs (**Figure 17B**). These initial observations suggest a possible correlation: decreasing EMILIN-1 levels may contribute to changes in the microenvironment that ultimately lead to aberrant vasculature, a critical factor in GC progression. In addition, our research uncovers a possible link between altered EMILIN-1 status and the increased presence of neutrophils in the GC microenvironment, which is common in this context (**Figure 17C**). Neutrophils are known to release NE, which can efficiently degrade EMILIN-1 (Maiorani et al., 2017). This provides a plausible mechanism for the observed reduction in EMILIN-1 levels, warranting further investigation into the complex dynamics of gastric carcinogenesis (Fu et al., 2016; Jia et al., 2023). NE detected in these scenarios suggests its role in microenvironmental changes driving the shift from pre-cancerous to malignant gastric lesions (Meyer and Goldenring, 2018).
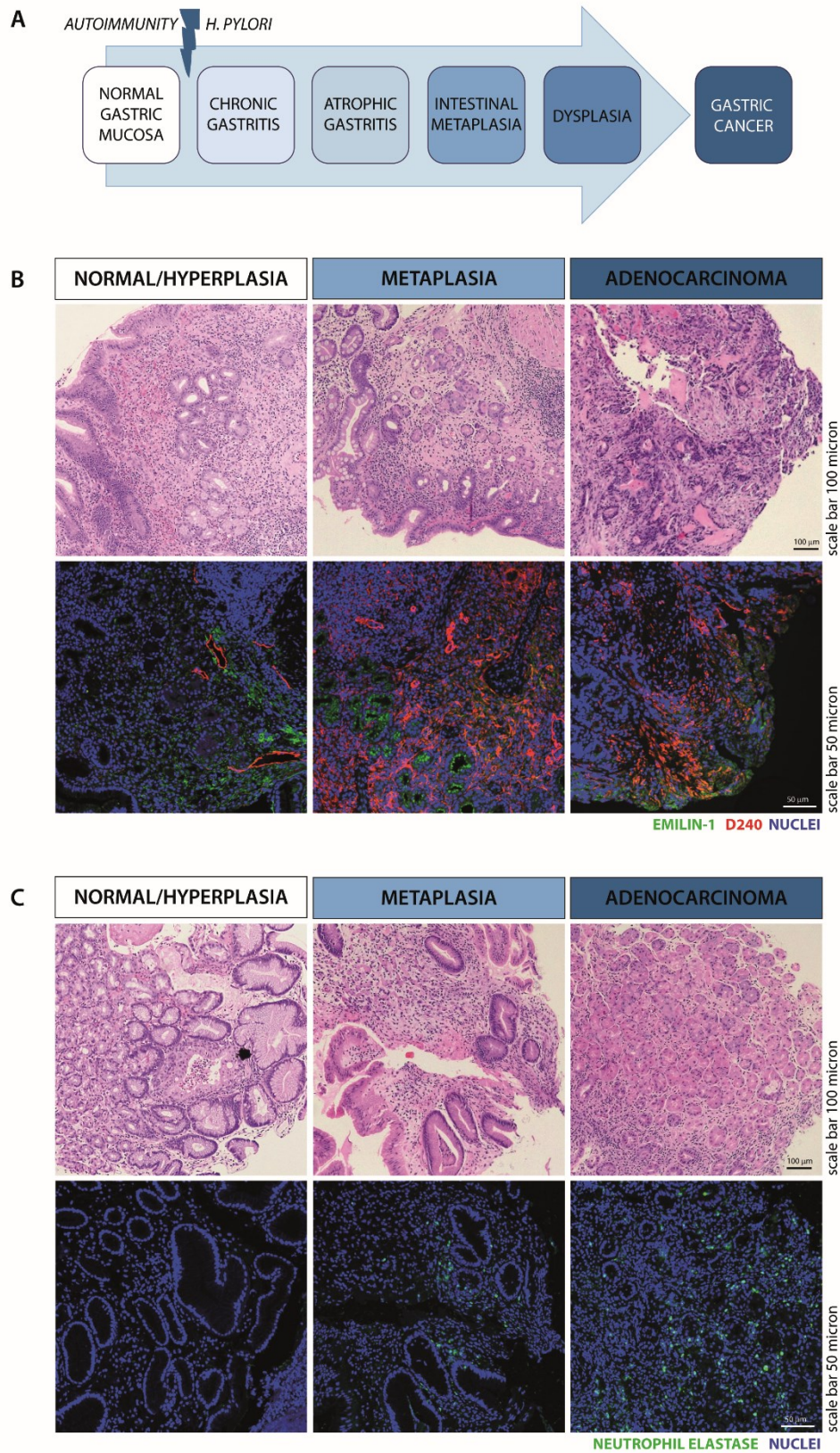
FIGURE 17. **EMILIN-1 and GC Progression.** *A) Correa sequence: progression of gastric carcinogenesis, a stepwise process from chronic gastritis to cancer. B) FFPE samples from a patient at different stages of disease progression. The images show a gradual loss of EMILIN-1 (green), even in pre-malignant tissue, with the concomitant appearance of aberrant LVs (red, D240). C) Increased presence of neutrophils (green), which release elastase and may contribute to the observed EMILIN-1 reduction. Nuclei pseudo-colored in blue.*

EMILIN-1 deficient mice are more permissive to tumor growth.

To further investigate the involvement of EMILIN-1 in tumor development, we performed *in vivo* experiments using different mouse models developed in our laboratory. These models include the C57/BL6J wild-type (WT) mouse, the EMILIN-1 knockout (KO) mouse, and the knock-in (KI) mouse which carries a mutant form of EMILIN-1 (E933A) in the gC1q domain, effectively preventing binding to integrins (**Figure 18A**). Their use allowed us to distinguish between integrin-dependent and -independent effects. Thanks to observations of the phenotype of these mice, we found that the aged transgenic animals showed a thickening of the gastric submucosa, suggesting a possible lymphatic stasis (**Figure 18B**). Moreover, the staining shows a more pronounced inflammatory infiltrate, a condition that can be considered a precursor to tumor development. Thus, the absence of EMILIN-1 or its functional impairment can indirectly exacerbate the inflammatory status for the reduced clearance by dysfunctional lymphatics.
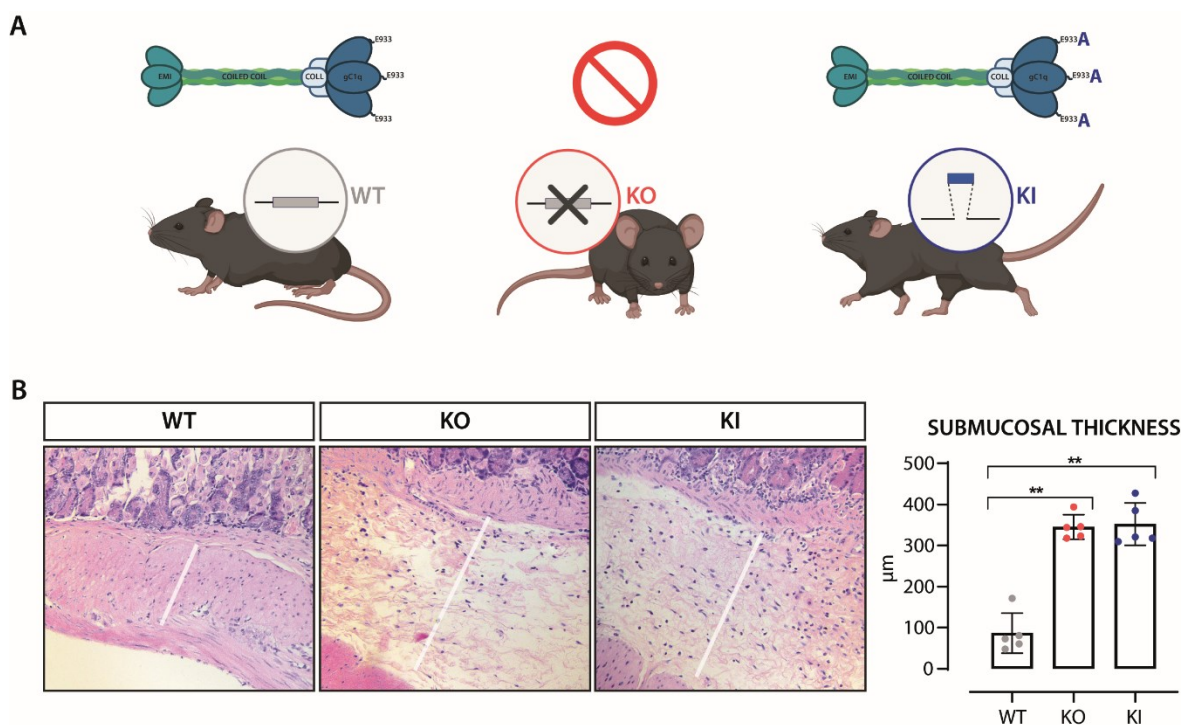

*FIGURE 18. **EMILIN-1 mouse models used in our study.** A) Schematic representation of the different models used: the wild-type C57/BL6J mouse, EMILIN-1 knockout, and the knock-in mouse harboring the E933A mutation in the c1q domain. Created with BioRender.com. B) H&E staining of normal gastric mucosa of 10-months old mice: transgenic animals exhibit thickening of the gastric submucosa. The results represent the mean ±SD of 5 mice/genotype. P values were calculated using two-tailed Student's t-test. **P<0,01.*

At this point, our primary aim was to closely examine tumor development in different genetic backgrounds. For this purpose, we used a syngeneic GC cell line (YTN16) originally derived from p53 heterozygous animals by a research group in Japan (Yamamoto et al., 2018).

We injected these cancer cells subcutaneously into WT and EMILIN-1 transgenic mice. After injection, we observed a marked difference in tumor development between the various genotypes. In particular, transgenic mice (KO and KI) displayed an increased propensity to develop tumors compared with WT mice. To further elucidate these findings, we sacrificed the mice 20 days after injection and performed comprehensive measurements of tumor masses (**Figure 19A**).

The results, as seen in the panel and graph, show a clear difference. Both KO and KI mice had significantly larger tumor masses compared with their WT counterparts. This discrepancy raises interesting questions about the role of EMILIN-1 in regulating tumor growth and progression. To gain deeper insights into the underlying mechanisms, we performed OCT sections to evaluate differences in the TME. Our observations revealed a remarkable increase in the number of LVs, which were distinctly stained green for Lyve-1, in the tumors of the transgenic mice (**Figure 19B**). On the contrary, the density of blood vessels (see lower panel), was unaltered in the different genotypes. The pronounced aberrant lymphangiogenesis observed in the tumors of the transgenic mice led us to consider that EMILIN-1 may play a central role in the tumor growth and *de novo* lymphangiogenesis, which is known to promote tumor dissemination (Danussi et al., 2012).

We then extended our analysis to intra-peritoneal models. Peritoneal metastasis is typically associated with advanced stages of tumor development in human patients. In a preliminary experiment, we found that transgenic mice exhibited greater tumor spread compared with their WT counterparts. This observation highlights the potential impact of EMILIN-1 on tumor dissemination in a clinical context.

To quantitatively assess the extent of metastasis, we involved a pathologist who assigned points for a final score based on the degree of tumor spread to various organs (**Figure 20A**). The total score was significantly higher in transgenic mice than in WT ones. As an example, we show staining of the peritoneum, where the presence of nodules is evident in transgenic mice whereas they are notably absent in WT animals (**Figure 20B**). These findings indicate a complex interplay between EMILIN-1 and tumor dissemination.
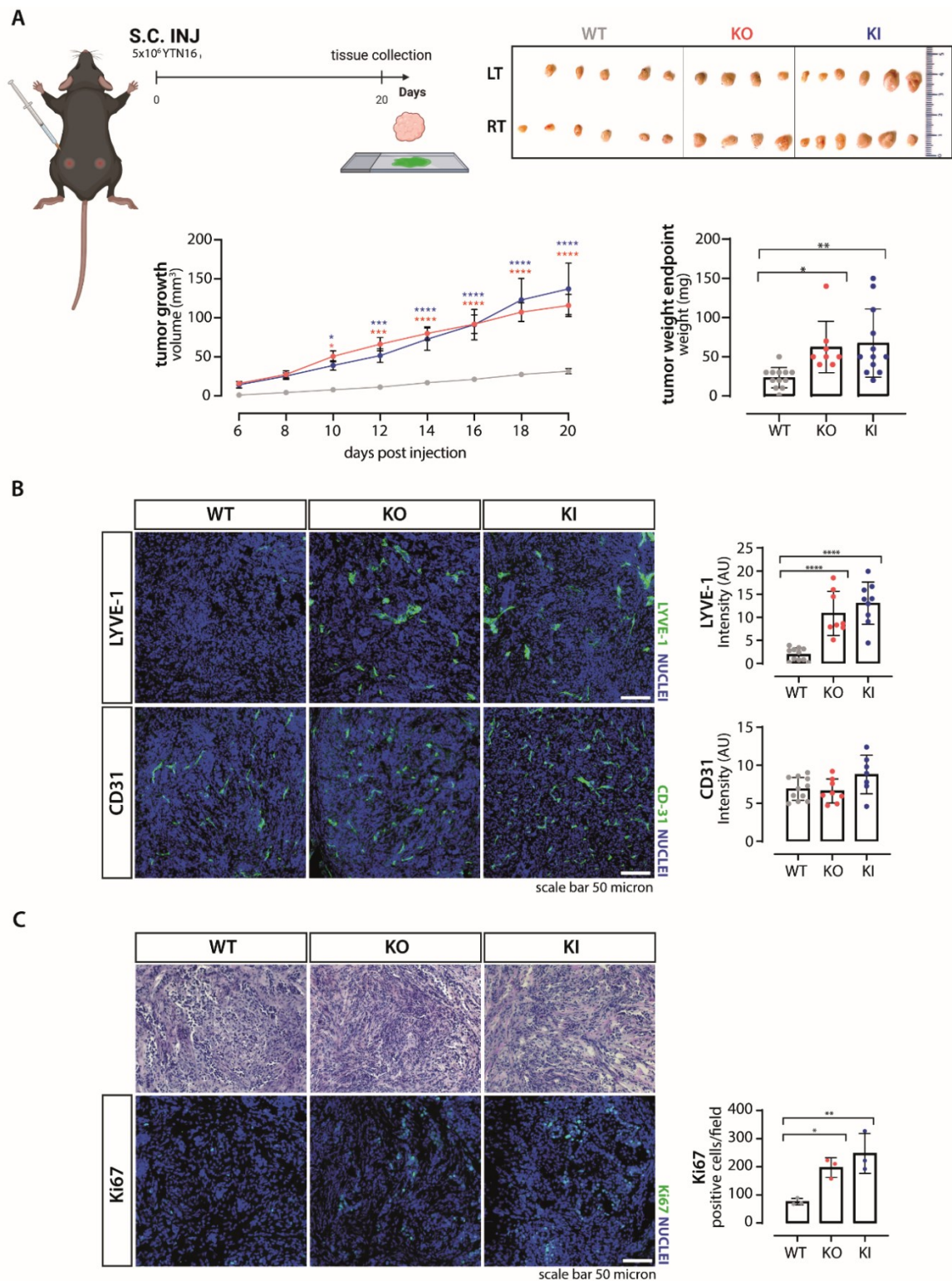
FIGURE 19. **Impact of different EMILIN-1 genetic backgrounds on tumor growth after subcutaneous injection of YTN16 cells.** *A) Schematic representation of the procedure. Created with BioRender.com. In the graphs, KI and KO mice exhibit enhanced tumor development, resulting in significantly larger tumors compared to the wild-type (WT) group. B) KO and KI tumors display increased LVs density, as demonstrated in OCT sections stained for Lyve-1 (green, upper panel). This trend is not mirrored in blood vessels, as evident from CD-31 staining (green, lower panel). The associated graphs represent the quantification of Lyve-1 and CD31 positive volume in the whole section field (20X) examined. For each sample at least five fields were analyzed, and the mean value was reported. C) KO and Ki tumors are more proliferating, as highlighted by Ki67 staining. The number of positive cells/fields was analyzed, and the mean value was reported for 3 mice/genotype. The results represent the mean ± SD of 8-12 mice/genotype. P values were calculated using two-tailed Student's t-test. *P<0.05, **P<0,01, ***P<0,001, ****P<0,0001.*
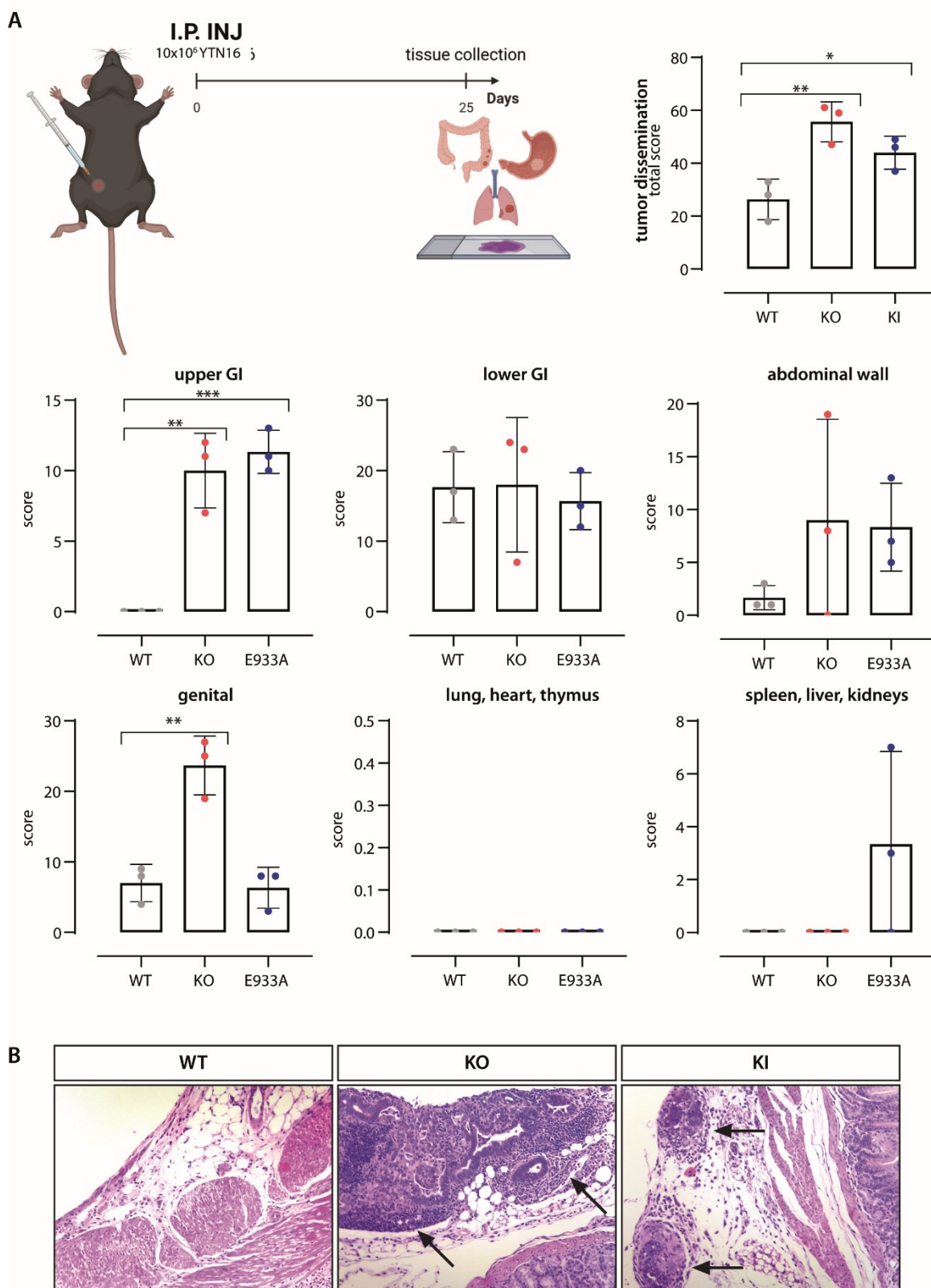
FIGURE 20. **Establishment of an intra-peritoneal model of tumor dissemination.** A) Schematic representation of the procedure. Created with BioRender.com. As shown in the graph, EMILIN-1 KO and KI mice are more permissive to tumor dissemination. The extent of metastasis was evaluated through scores assigned by a pathologist, considering the involvement of various organs. The total score is the sum of the separate score assigned to different organs. The results represent the mean ± SD of 3 mice/genotype. P values were calculated using two-tailed Student's t-test. *P<0.05, **P<0,01. B) Representative images of H&E staining of the peritoneum, where discernible nodules (black arrows) are evident in transgenic mice, but not in WT animals. Magnification 200x.

We also used an intrafootpad model in mice to gain valuable insight into the process of tumor progression. Our findings highlighted a higher tendency for cancer cells to spread especially to the popliteal lymph nodes in transgenic mice (KO and KI) compared with WT, although this does not reach the threshold of statistical significance (**Figure 21A**).
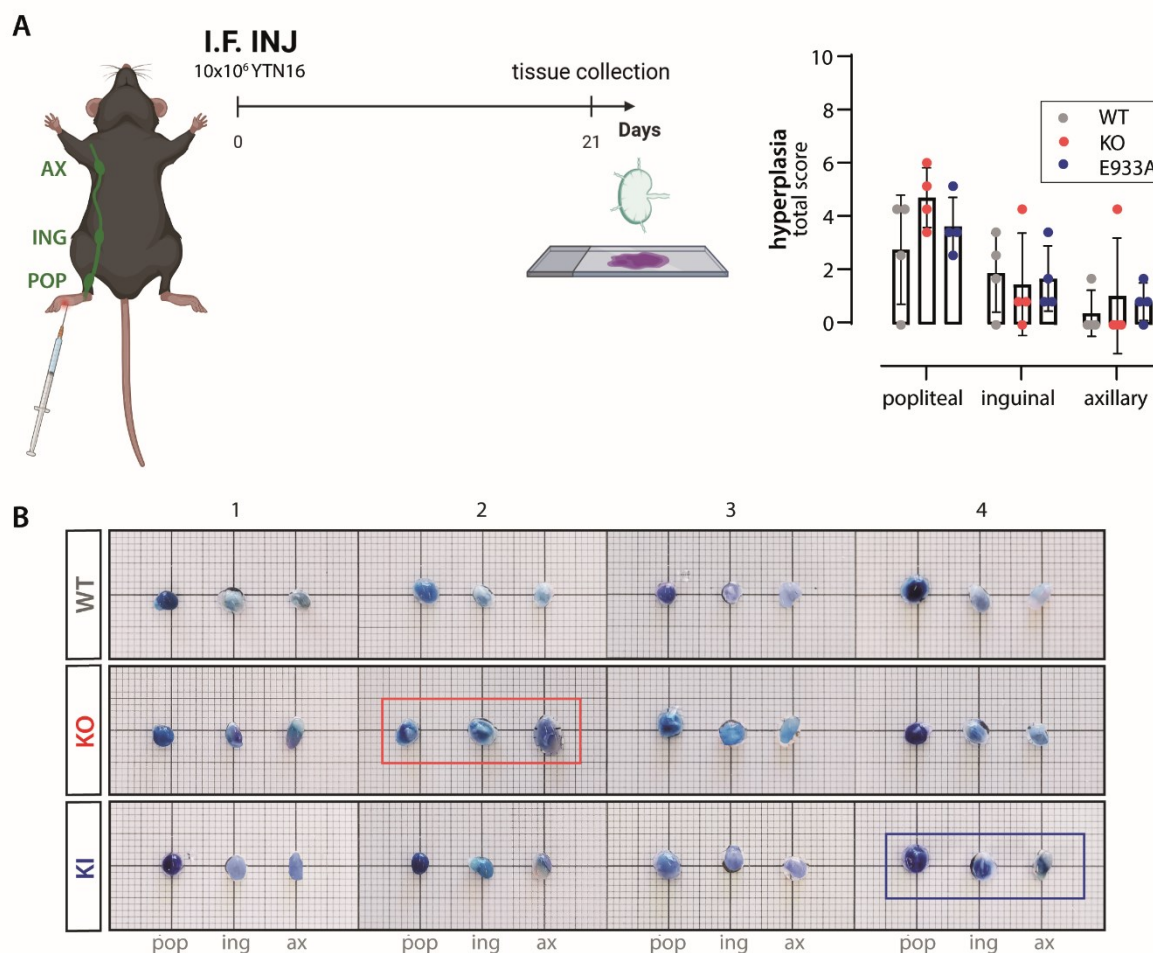

*FIGURE 21. **Intrafootpad model of tumor dissemination.** A) graphical representation of the procedure used for the intrafootpad model. The lymph nodes involved in GC cell dissemination and their collectors are stained in green. Created with BioRender.com. The hyperplasia score for popliteal, inguinal and axillary lymph nodes is reported. Results represent the mean ± SD of 4 mice/genotype. B) Lymph nodes stained with Evans Blue for ease collection. Popliteal (pop), inguinal (ing) and axillar (ax) lymph nodes were collected for each animal. Lymph nodes from KO and KI mice are larger and thicker than those from WT, as shown in the red and blue boxes, respectively.*

There is a tendency for increased hyperplasia in KO and KI lymphnodes. Hyperplasia is a major feature of tumor development and may influence tumor aggressiveness. Indeed, we also noted larger lymph nodes in these mice (**Figure 21B**). Lymph nodes often serve as sites for immune responses against tumor cells. The enlargement of lymph nodes could suggest an enhanced immune response or the presence of more extensive tumor-related changes in the lymphatic system in transgenic animals, as previously demonstrated in melanoma models (Capuano et al., 2019a). Although this trend did not yet reach statistical significance, it encouraged further

exploration of the genetic and immunologic aspects of tumor development in this experimental context.

All the results obtained with this syngeneic mouse model indicated a significant role of EMILIN-1 in GC growth and dissemination. However, the YTN16 experimental model is known for its aggressive behavior, thus limiting our possibility to effectively study tumor onset and early development. To address this gap, we exploited a chemical carcinogenesis model using N-Methyl-N-nitrosourea (MNU), a potent carcinogen. This model, although informative, requires a long timeframe and has low penetration. In our MNU-induced gastric carcinogenesis model, mice were administered MNU ad libitum over a five-week period, alternating with saline solution, for a total of ten weeks. The development of the model was followed for a period of 20-weeks, after which the animals were sacrificed. We removed the gastric tissues and other relevant organs for detailed analysis and consulted a pathologist to evaluate the results (**Figure 22A**).
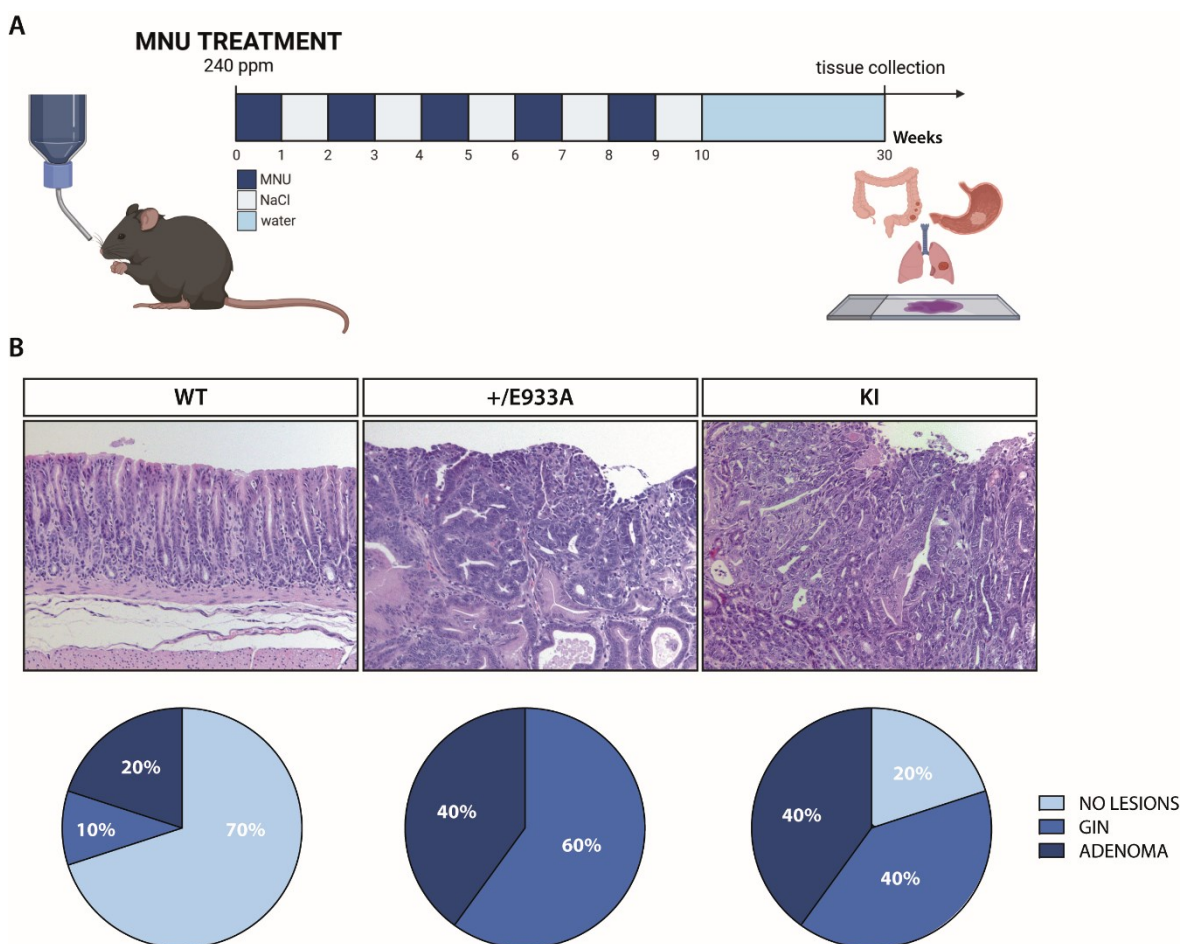
FIGURE 22. **MNU-Induced Gastric Carcinogenesis Model.** *A) Administration regimen of N-Methyl-N-nitrosourea (MNU) to animals. MNU was administered for 10 weeks, alternatively with saline solution (NaCl), followed by a 20-week incubation in which they received normal water. Created with BioRender.com. B) Stomach and organ analysis: visualization of H&E staining of the stomach of different mice. Magnification 200x. The frequency of lesions differs between genotypes: WT (70% no lesions, 20% adenoma, 10% GIN); heterozygous KI (60% GIN, 40% adenoma); KI (40% GIN, 40% adenoma, 20% no lesions). Results represent the relative distribution of the different lesions in 15 mice/genotype.*

It is important to note that this model does not exactly reflect the well-known Correa sequence of gastric carcinogenesis but has a particular pattern with substantial involvement of the stromal component. This feature makes it a particularly valuable model to study the specific role of an ECM protein, such as EMILIN-1, in GC development. A notable aspect of our MNU-induced gastric carcinogenesis model is the occurrence of gastrointestinal intraepithelial neoplasia (GIN) and adenoma formation. We chose to use KI EMILIN-1 mice instead of KO to preserve TGF-β interactions, which allows us to target the effects of E933A modification in the gC1q domain. In addition, the use of heterozygous KI animals provides insight into the penetrance of the modified allele and its role in tumor development. Considering the low incidence of the MNU protocol, we treated equal cohorts of WT, KI and heterozygous animals (25 each) and analyzed 15 mice per genotype. The frequency of lesion development differed between the different genetic backgrounds studied: 70% of WT mice showed no lesions, whereas 20% had adenomas, and 10% GIN; in contrast, heterozygous KI mice displayed a pattern of 60% GIN and 40% adenoma; KI mice demonstrated a distribution of 40% GIN, 40% adenomas, and 20% without lesions (**Figure 22B**).

Examination of mouse gastric tissues included extensive immunohistochemical analysis to elucidate key aspects of their histological features (**Figure 23**). The representative images show untreated mice (referred to as 'cnt') treated WT mice and treated KI mice. In the samples of untreated mice, Periodic Acid-Schiff (PAS) staining displayed remarkable positivity in the gastric pits and foveolae, strongly suggesting active glandular functionality. At the same time, Alcian staining in these sections emphasized positivity within the gastric glands, consistent with the results of PAS. In the WT group of treated mice both PAS and Alcian staining were negative, but PAS positivity was evident in the surrounding non-tumoral mucosa. The KI group had a unique histological profile. In this subgroup, both PAS and Alcian staining were completely negative, indicating the absence of mucin and glandular functionality. As for the assessment of cell proliferation by Ki67 immunostaining, untreated mice showed 30% positivity in the basal layer of the mucosa, underscoring low cell proliferation. In contrast, both treated WT and KI mice displayed a much higher positivity of 60% in the entire area of adenoma and gastric intraepithelial neoplasia (GIN). However, the KI samples exhibited a markedly increased distribution of Ki67 positivity in the surrounding hyperplastic mucosa, further emphasizing the uniqueness of this group of mice. Evaluation of DNA double-strand breaks by H2AX staining unveiled interesting results. Untreated mice had few and weakly stained positive cells in the basal mucosal layer. Treated WT mice displayed strongly stained positive cells distributed throughout the adenoma area. In contrast, the treated KI group was characterized by the conspicuous presence of numerous positive cells throughout the GIN area, indicating an increased level of DNA damage.

These findings underscore the importance of the genetic background in the development of GC and highlight the complex interplay between genetic factors and the ECM in gastric carcinogenesis. The result will be corroborated with a larger group of mice.
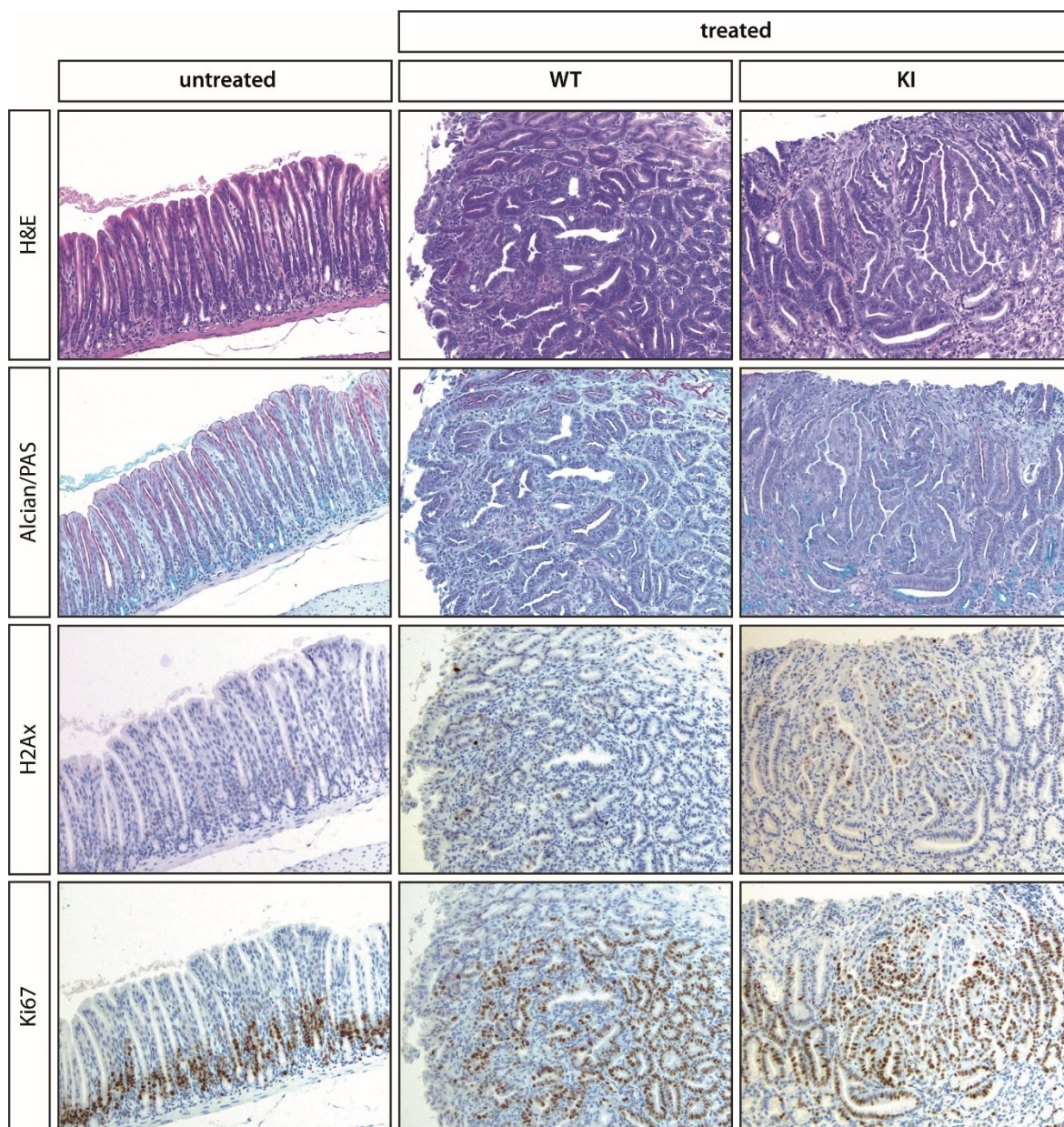

FIGURE 23. **Immunohistochemical staining of mice stomachs.** *Serial sections from the 3 selected cases were stained with hematoxylin and eosin and with Alcian PAS (for mucins-effective gland functionality). Serial sections from the 3 selected cases were immunostained with anti-Ki67 as marker of cell proliferation and anti-H2AX as marker of DNA double-strand breaks. Immunostaining was performed using the Avidin-Biotin Complex (ABC) procedure, an indirect immunoperoxidase staining. Staining results from tissue samples of WT untreated (cnt), Wt and KI mice reveal distinct patterns. In cnt PAS staining demonstrates positivity in gastric pits and foveolae, while Alcian staining indicates positivity in gastric glands. Conversely, the WT displays negative PAS and Alcian staining, with PAS positivity in the surrounding non-tumoral mucosa. In the KI both PAS and Alcian staining are negative. Ki67 immunostaining reflects varying cell proliferation, with 30% positivity in cnt and 60% in WT and KI mice, with increased distribution in surrounding hyperplastic mucosa in KI. H2AX staining shows rare positivity in cnt, a few strongly stained cells in WT and numerous positive cells in KI. Untreated mice showed comparable features, therefore only one is included in this panel (WT mouse). Magnification 200x.*

EMILIN-1 binds integrin α4β1 in models of normal but not neoplastic gastric epithelium.

The regulatory role of EMILIN-1 in proliferation has been well established in previous studies (Capuano et al., 2019b; Danussi et al., 2012, 2011) which showed that the mechanism involves its engagement with α4 and α9 integrins. Existing literature reports that loss of integrin α4 expression may be associated with aggressive behavior and poor prognosis in various cancers, including GC (Ignatoski et al., 2003; Mo et al., 2022; Park et al., 2004b). Given these compelling connections, our research efforts have deliberately focused on studying the importance of interaction between EMILIN-1 and integrin α4 in our model.

The experiments employed a variety of distinct cell lines (see also Table 2 in Material and Methods section). The GES-1 cell line, derived from normal human gastric epithelial cells, represented the baseline for normal cellular behavior. In contrast, different tumor cells were used: AGS, a gastric adenocarcinoma cell line with an intestinal histotype; Hs746.T, representing metastatic gastric carcinoma with a diffuse histotype; and NCI-N87, another metastatic gastric carcinoma cell line.

Our first focus was to characterize the integrin expression profile of normal and tumor gastric cells. Significantly, our observations revealed loss of integrin α4 in GC cells (**Figure 24A**), a finding that was subsequently confirmed by functional analyses. Normal epithelial cells showed the ability to bind to EMILIN-1 in adhesion assays and were sensitive to homeostatic control by the gC1q domain in proliferation experiments (**Figure 24B** and **24C**). The binding is specific, because the cells did not adhere when an anti–α4 integrin function-blocking antibody was added or when a gC1q mutant (gC1q E933A) was used as a substrate. Accordingly, this mutant failed to influence the proliferation rate, indicating that the engagement of α4 integrin is responsible for the regulatory effects of EMILIN-1. In contrast, cancer cells did not bind EMILIN-1 or gC1q. Moreover, GES-1 adhered tightly to fibronectin (FN), used as positive control, but not to Collagen IV, which is known to promote invasion and metastasis in the gastric TME (Cui et al., 2022). In contrast, AGS bound to Collagen IV, but only to a lesser extent to FN.
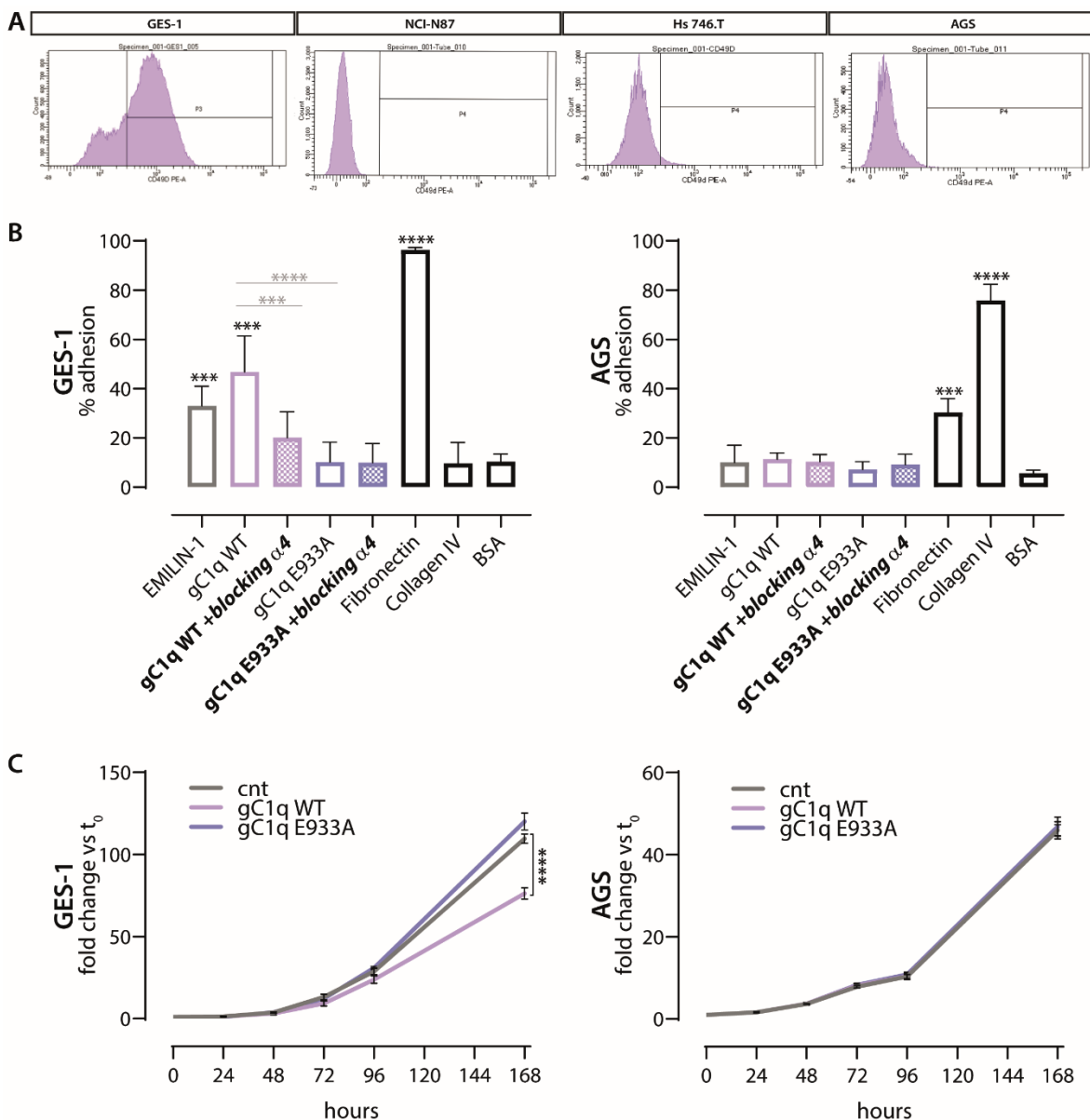
FIGURE 24. **Integrin α4 in GC cell lines.** *A) FACS analysis shows loss of integrin α4 in GC cells, which prevents their interaction with EMILIN-1. On the contrary, GES-1 normal cells express integrin α4. B) CAFCA functional assay demonstrated that integrin α4 in normal epithelium can bind EMILIN-1/gC1q whereas GC cells are not. The binding is specific as they do not bind to mutated gC1q (E933A) C) GES-1 are sensitive to gC1q antiproliferative control, whereas cancer cells (AGS) are not. The modulation is gC1q dependent since the mutant does not work. The results represent the mean ± SD of 3 independent experiments. P values were calculated using two-tailed Student's t-test versus BSA. ***P<0,001, ****P<0,0001.*

To investigate the downstream effects of this interaction, we developed new tools. Specifically, we transfected AGS GC cells with integrin α4 and carefully selected clones with increased expression (**Figure 25A**).

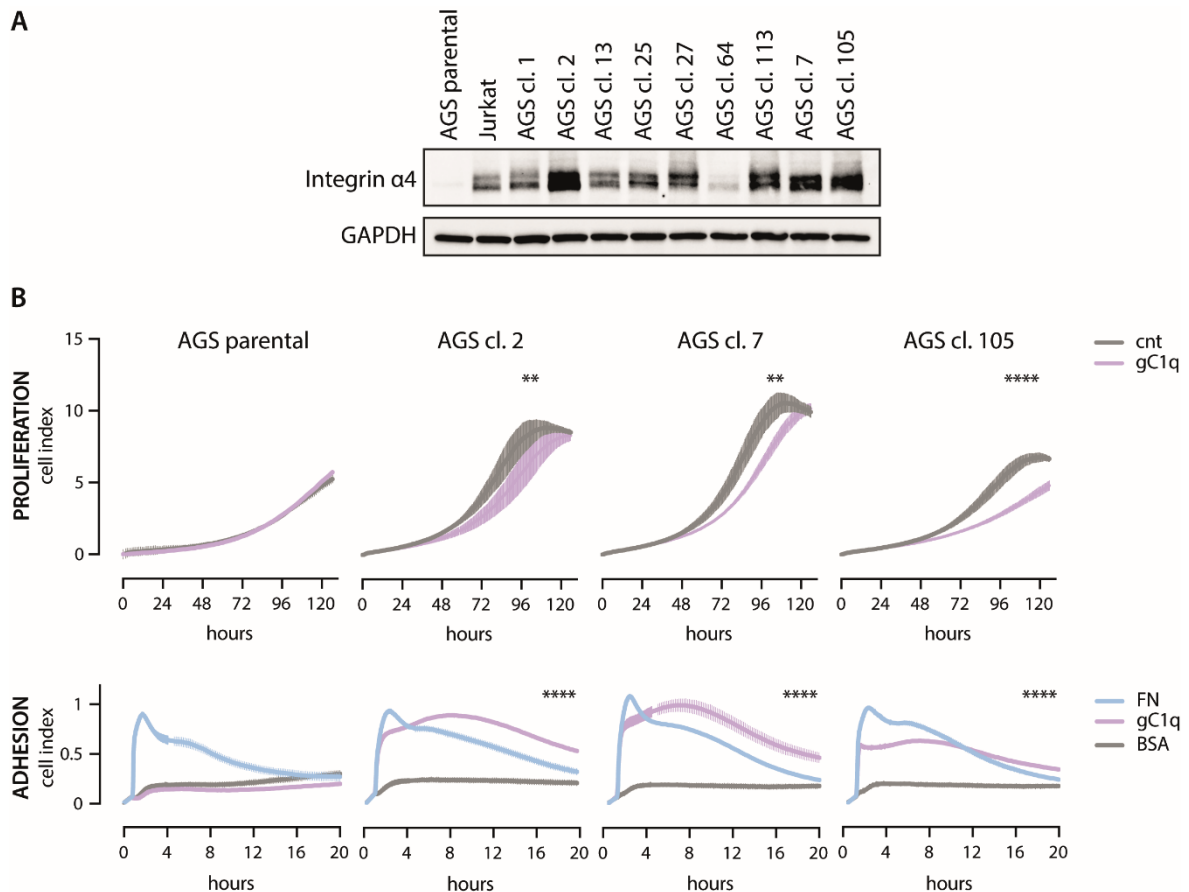FIGURE 25. **Restoration of integrin α4 expression in GC cells.** *A) Stable transfectants were selected. Jurkat cells served as positive control. B) AGS- α4 clones are sensitive to homeostatic controls by gC1q and allows renewed binding to EMILIN-1. The best clones were selected and tested in functional assays for proliferation and adhesion. The results represent the mean ± SD of 3 independent experiments. P values were calculated using two-tailed Student's t-test. **P<0,01, ****P<0,000.1.*

The production of these engineered cells is a critical step in our research, as it allows us to demonstrate that cancer cells not only escape proliferation-inhibitory mechanisms by dismantling EMILIN-1 but also disrupt their interaction with the cellular receptor integrin α4. This manipulation opens a gateway to assessing the behavior of these cells by functional assays and provides insight into how restoration of integrin α4 expression renders cancer cells sensitive to homeostatic controls by gC1q and restores their interaction with EMILIN-1 (**Figure 25B**).

We first evaluated adhesion using xCELLigence® technology, which provides both quantitative and qualitative insights into real-time cell adhesion and spreading by tracking "cell index", a measure of the number of cells bound to ECM substrates and the quality of their attachment. The cell index responds to impedance changes induced by cell attachment, allowing continuous monitoring. Our study revealed differential adhesion kinetics of all AGS-α4 clones to the EMILIN-1 gC1q domain. These kinetics were characterized by specific, strong, and long-lasting binding, with remarkable attachment persisting up to 8 hours after cell seeding. Of note, the duration of integrin binding was very different from binding to FN, which served as an adhesive positive

59

control. In this context, all cells remained adherent to the gC1q domain for a much longer period than when bound to FN. This observation underscores the specific and durable nature of cellular interaction with the EMILIN-1 gC1q domain.

We mentioned that the direct connection of EMILIN-1 gC1q domain with α4 integrin is the main mechanism underlying homeostatic role of EMILIN-1. We further investigated whether the expression of integrin α4 in AGS clones would restore sensitivity to EMILIN-1 antiproliferative effect. Indeed, α4-stable clones showed decreased proliferation after treatment with the recombinant EMILIN-1 gC1q domain, as evidenced by lower cell index values.

The transition from a functional relationship between EMILIN-1 and integrin α4 in normal gastric epithelium to the loss of this interaction in tumors provided the basis for analysis of downstream effects associated with GC progression, as we sought to understand how disruption of this ECM-protein interaction may promote gastric tumor aggressiveness.

EMILIN-1 expression is downregulated in fibroblasts treated with CM from GC cell lines.

To unravel the mechanisms underlying the reduction of EMILIN-1 in GC, we developed an experimental *in vitro* strategy aimed at mimicking the gastric microenvironment (**Figure 26A**). Our primary goal was to investigate whether GC cells can affect EMILIN-1 production in stromal fibroblasts and LECs, which are the main sources of EMILIN-1 (**Figure 26B**). To investigate this aspect, we exposed stromal cell cultures to conditioned media (CM) derived from GC epithelial cell lines, specifically NCI-N87 (a metastatic cell line), HS746.T (representing the diffuse histotype), and AGS (representing the intestinal histotype). We used normal gastric epithelial cells (GES-1) as controls.
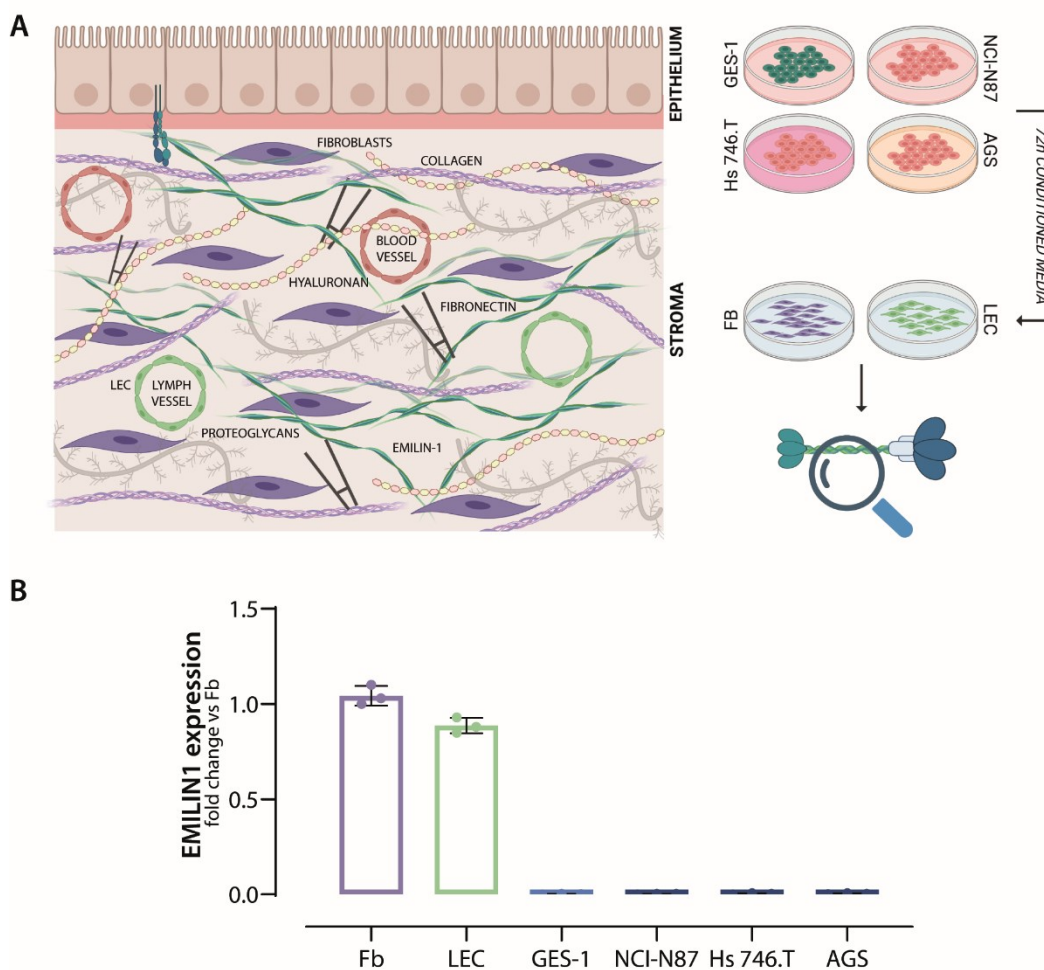
FIGURE 26. **GC Cell Lines and EMILIN-1 Production.** *A) Schematic representation of the experimental set up: stromal cells were treated with conditioned media (CM) of gastric cells for 72h. as control, growth medium of each GC cell line was used. ECM extracts, slides and RNA were then collected to determine EMILIN-1 expression. Different cell lines were used: GES-1 (normal cells), NCI-N87 (metastatic), HS746.T (diffuse histotype), and AGS (intestinal histotype) B) EMILIN1 expression in the different cell models. Gastric epithelial cells do not express EMILIN1, as expected. Results represent the mean ± SD of 3 independent experiments.*

After treatment with CM derived from gastric cells, fibroblasts were tested for EMILIN-1 expression. The results shown in **Figure 27A** indicate a clear downregulation mediated by GC cells but not by normal gastric cells. ECM extracts of treated fibroblasts, rather than cell lysates, were used for this study.

FIGURE 27. **Modulation of EMILIN-1 expression in response to CM from GC cells.** A) Western Blot analysis: EMILIN-1 is downregulated after treatment with CM from tumor cells, whereas no such modulation is observed with CM from normal cells (GES-1). The ECM ex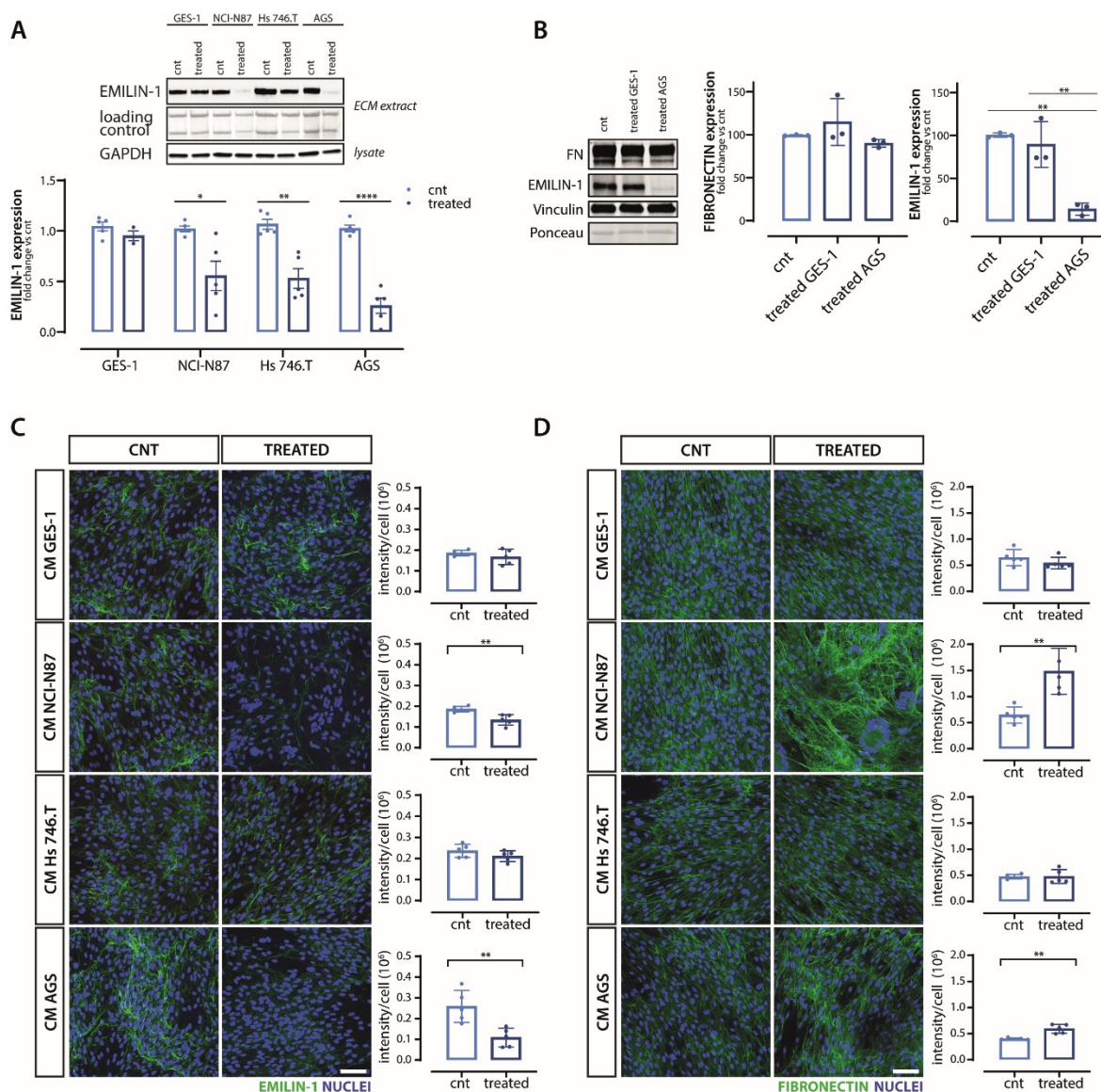tracts of treated fibroblasts were used for this analysis, considering EMILIN-1's rapid release and deposition by the cells. The results represent the mean ± SD of 5 independent experiments with different fibroblast populations. B) To ensure the specificity of our findings, we also evaluated the expression of other matrix proteins, such as fibronectin, which remained unchanged. Results represent the mean ± SD of 3 independent experiments with different fibroblast populations. C) Immunofluorescence analysis of treated fibroblasts highlights the decrease in EMILIN-1 deposition (green, left panel), D) whereas fibronectin deposition remains unchanged (green, right panel). The corresponding graphs show the quantification of EMILIN-1 and Fibronectin positive volume in the whole section field (20X). At least five fields were analyzed for each sample. P values were calculated using two-tailed Student's t-test. *P<0.05, **P<0,01, ****P<0,000.1.

This choice was based on the rapid release and deposition of EMILIN-1 by the cells, suggesting that it is predominantly found in the ECM rather than in the cytoplasm. To determine the specificity of this downregulation, we performed parallel investigations, evaluating the expression of other ECM proteins such as fibronectin. Interestingly, these studies revealed that the modulation observed for EMILIN-1 does not extend to fibronectin (**Figure 27B**).

Evaluation of protein accumulation in treated fibroblasts, performed by immunofluorescence , provided further compelling evidence for this analysis. We showed the decrease in EMILIN-1 deposition which is significant after treatment with CM of AGS and NCI-N87, whereas fibronectin deposition remained unaffected (**Figure 27C** and **27D**). The mechanisms underlying this downregulation are of particular interest. The phenomenon could be due to degradative enzymes released by cancer cells, that remodel the ECM for their advantage. Alternatively, it could be related to a decrease in gene expression. Thus, we assessed the expression of MMPs but did not detect changes in their expression in fibroblasts after treatment with CM, nor did we detect a greater amount in CM from GC cells respect to normal cells (data not shown). Therefore, we proceeded with gene expression analysis in this *in vitro* setting, where NE cannot interfere because it is secreted by neutrophils. They play an important role *in vivo* but are not obviously present in our *in vitro* experimental conditions.

We examined the expression of EMILIN1 mRNA by real-time PCR analysis on RNAs of treated fibroblasts (**Figure 28A**).
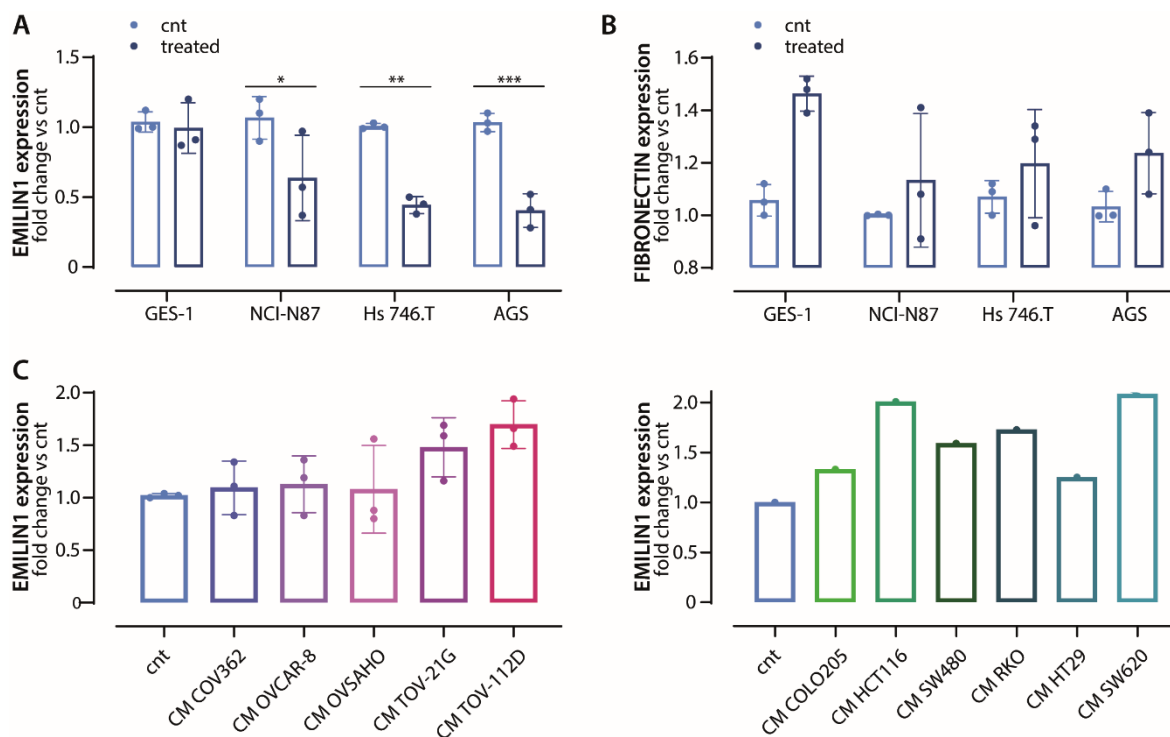
FIGURE 28. **Regulation of EMILIN1 mRNA expression.** *A) qRT-PCR analysis: downregulation of EMILIN1 mRNA in fibroblasts treated with CM from GC cells but not from normal cells. B) In contrast, fibronectin mRNA expression remained unaltered, underscoring the specificity of this effect. Results represent the mean ± SD of 3 independent experiments with different fibroblast populations. C) The response of fibroblasts to conditioned media from ovarian cancer cells followed an opposite trend, namely higher EMILIN1 expression. Results represent the mean ± SD of 3 independent experiments with different fibroblast populations. P values were calculated using two-tailed Student's t-test. *P<0.05, **P<0,01, ***P<0,001. D) The same opposite trend was observed when using CM from colon cancer cells.*

Our results showed that downregulation of EMILIN-1 occurs at the mRNA level, indicating the involvement of regulatory mechanisms that modulate gene expression. Cancer cells, but not normal epithelial cells, are able to downregulate EMILIN1 expression in fibroblasts. We extended our study to fibronectin mRNA expression and found that it does not decrease in a similar manner, highlighting the specificity of the effect on EMILIN1 (**Figure 28B**).

Furthermore, we investigated whether this regulatory phenomenon was exclusive to GC or indicative of a broader malignancy. We treated fibroblasts with different CM derived from ovarian and colon cancer cells. Surprisingly, we did not observe a decrease in mRNA levels; but rather an opposite trend (**Figure 28C**). This intriguing observation prompts us to further explore the intricate mechanisms underlying EMILIN-1 regulation and to gain valuable insights into the context-specific nature of this phenomenon.

LEC functionality is impaired when EMILIN-1 is downregulated by CM from GC cell lines.

A crucial aspect of our investigation was to determine whether LECs are also subject to a similar pattern of modulation. We used the same experimental framework to evaluate whether EMILIN1 mRNA expression in LECs was affected by the treatment with CM of GC cells.

Our observations confirmed that the mRNA for EMILIN-1 was downregulated in LECs when exposed to CM from GC cells, further highlighting the complexity of regulatory mechanisms in GC TME (**Figure 29**).
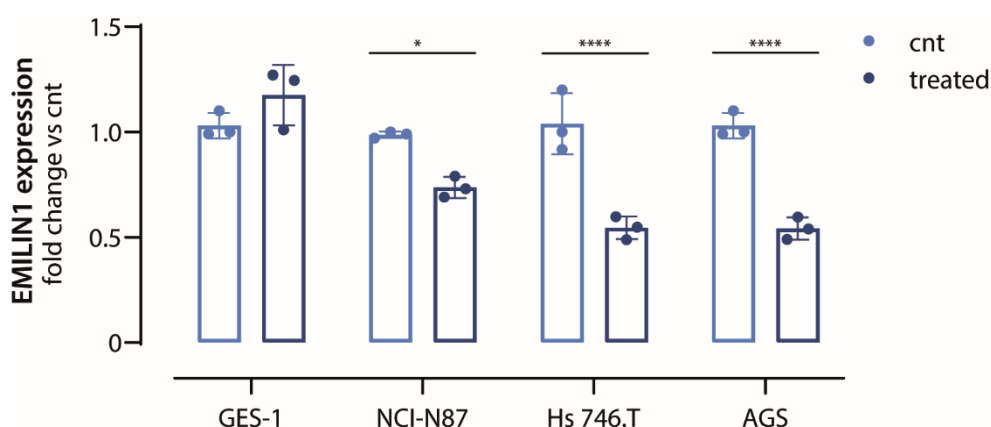

FIGURE 29. **CM from GC cell lines downregulate EMILIN1 expression in LECs.** qRT-PCR shows a decrease in EMILIN1 mRNA expression when LEC are treated with GC-derived but not normal gastric cells CM. Results represent the mean ± SD of 3 independent experiments on different fibroblast populations. P values were calculated using two-tailed Student's t-test. *P<0.05, ****P<0,0001.

Moreover, we employed the same experimental framework to evaluate whether the functionality of LECs was affected when exposed to CM from GC cells. Indeed, our findings revealed a marked impairment in the ability of endothelial cells to form tubules when treated with CM from tumor cells, whereas CM from normal cells had no such effect (**Figure 30A**). In particular, the tube length, the number of branching point and loops and the total amount of tubes was significantly diminished (**Figure 30B**).
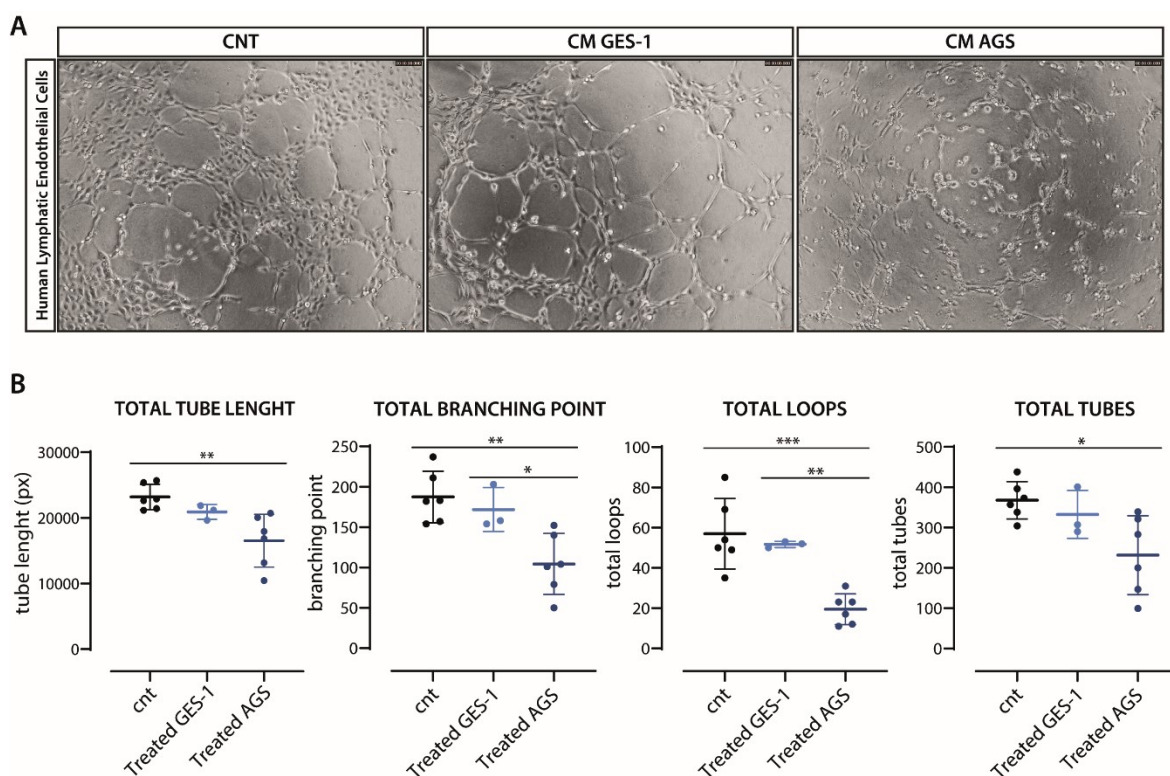
FIGURE 30. **LECs cannot form tubes when treated with CM from GC cell lines.** A) We observed a significant impairment in the ability of LECs to form tubules. B) Images were analyzed using Wimasis™ tool. Treatment with CM of GC cells, but not normal cells, impairs LEC ability to form tubules that are shorter, have fewer loops and branching points. P values were calculated using two-tailed Student's t-test. *P<0.05, **P<0,01, ***P<0,001.

This dual observation hints at the reciprocal relationship between EMILIN1 mRNA downregulation and functional effects on endothelial cells and underscores the interplay within the microenvironment.

EMILIN1 expression is regulated in the cytoplasm.

Our collective findings strongly suggest that factors secreted specifically by GC cells play a key role in regulating EMILIN1 gene expression, either at the transcriptional or post-transcriptional level. To pinpoint the precise stage of the mRNA journey at which this regulation occurs, we

performed subcellular fractionation experiments on fibroblasts exposed to the AGS CM that served as our reference model.

Our main goal was to enrich the nuclear fraction and determine whether the modulation affected the pre- or post-spliced mRNA by real-time PCR with different primers. This approach, combining subcellular fractionation with the design of oligos targeting different transcriptional regions, promises a more comprehensive understanding of EMILIN1 mRNA expression in different cellular compartments.
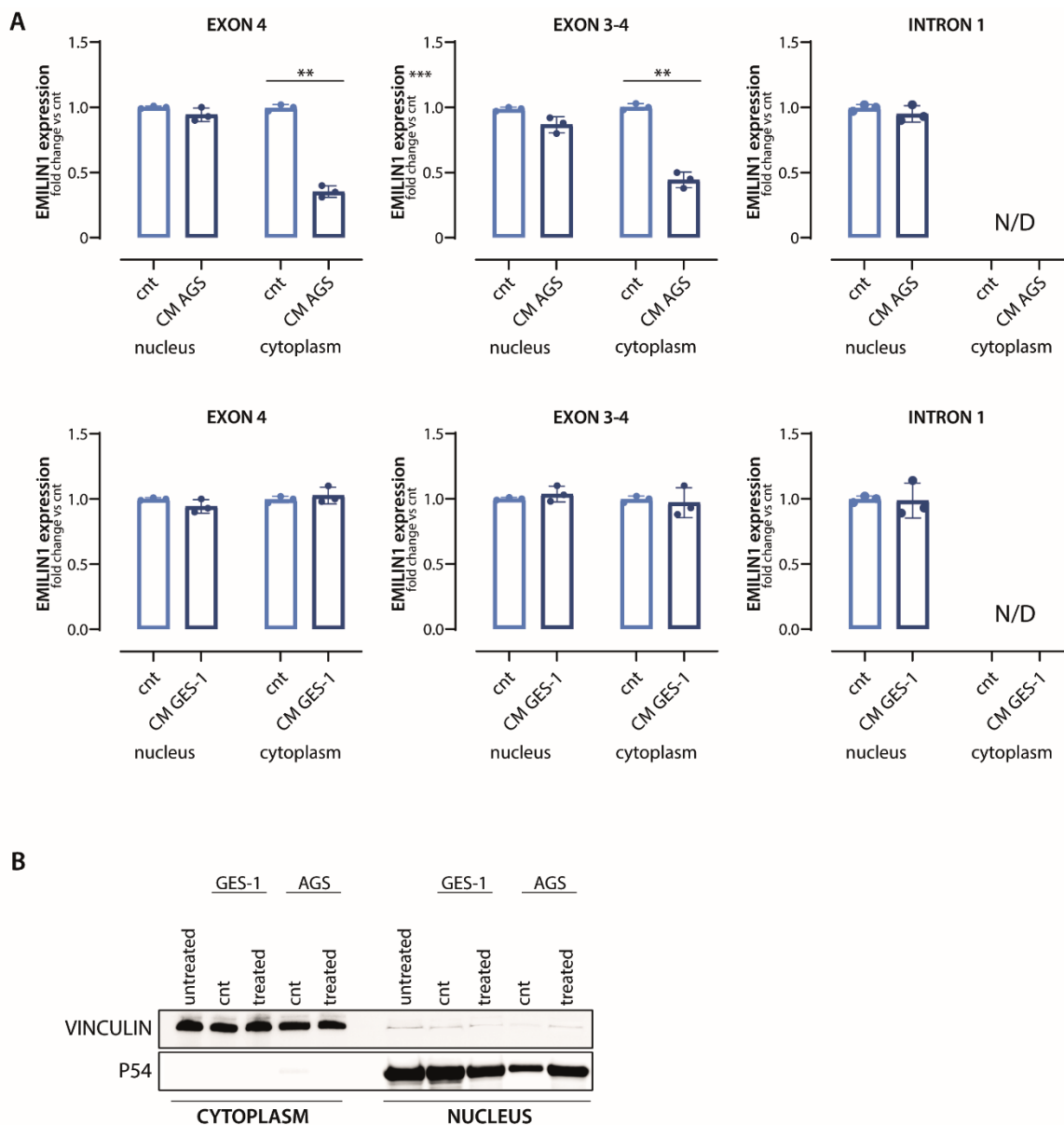
FIGURE 31. **EMILIN1 mRNA expression is hampered in the cytoplasm.** *A) Subcellular fractionation and real-time PCR were used to determine at which point in the mRNA journey the regulation occurs. Primers were designed to specifically target sequences in intron 1, exon 4 and at an exon-exon junction. The specific intron and exon were selected for optimization purposes and are not specific for the observed regulation. Results represent the mean ± SD of 3 independent experiments on different fibroblast populations. P values were calculated using two-tailed Student's t-test **P<0,01. B) Western Blot to validate the effectiveness and reliability of subcellular fractionation Vinculin and p54 were used as markers for cytoplasm and nucleus, respectively.*

We wanted to determine whether the observed modulation occurred in introns, exons, or exon-exon junctions, and thus distinguish between nuclear mRNA and cytoplasmic mRNA. Our results indicated downregulation of mature mRNA, highlighting the post-transcriptional nature of the regulatory effect (**Figure 31A**). This modulation was localized in the cytoplasm, as evidenced by the decrease in expression levels detected exclusively in this fraction with primers designed on exon 4. Of course, primers spanning an exon-exon junction were also effective in confirming downregulation in cytoplasmic mRNA. The purity of each fraction was determined, ruling out cross-reactivity (**Figure 31B**). Given the importance of post-transcriptional regulation of gene expression, we wanted to evaluate the presence of small RNAs in the cytoplasm of GC cells which can have a role in modulating EMILIN1 expression.

EMILIN1 mRNA can be targeted by multiple microRNA.

To explore the post-transcriptional regulation of EMILIN1 expression, we entered the realm of microRNAs (miRNAs), which have been extensively studied in the context of GC. Using a targeted approach, we selected eight miRNA candidates with potential interactions with EMILIN1, using a combination of existing literature and bioinformatics tools (**Figure 32A**).

To investigate the expression of these miRNA candidates, we extracted miRNAs from supernatants of cancer cells and quantified miRNA expression levels in our samples. Notably, most miRNAs exhibited low expression levels, except for miR125a-5p, which was strikingly abundant in cancer cells whereas it was barely detectable in their normal counterparts (**Figure 32B**). This observation was confirmed by a previous study by a French research group, in which miR125a-5p was ranked as one of the fifteen most highly expressed miRNAs in AGS cells, as determined by miRNome analysis (Belair et al., 2011).

Our subsequent real-time PCR analysis unveiled that miR125a-5p was consistently present in the CM of AGS and other GC cells, whereas its expression remained extremely low in normal cells. Furthermore, when we treated fibroblasts with CM derived from cancer cells, we detected increased levels of miR125a-5p in the cells, although statistical significance was not achieved (**Figure 32C**). These findings collectively underscored that miR125a-5p could be a candidate for post-transcriptional regulation of EMILIN1.

FIGURE 32. **MicroRNA profiling identifies miR125a-5p as a potential regulator of EMILIN1.** *A) A targeted approach to investigate the role of microRNAs in EMILIN1 regulation identified few prominent candidates. B) miR125a-5p exhibited higher expression levels in GC CM compared to normal counterpart. C) Higher levels of miR125a-5p were detected in all GC cell lines compared to normal GES-1. Moreover, in treated fibroblasts it seems more abundant compared to control (cnt), although not significant. Results represent the mean ± SD of 3 independent experiments on different fibroblast populations. P values were calculated using two-tailed Student's t-test. *P<0.05, **P<0,01, ****P<0,000.1.*

To determine whether miR125a-5p is responsible for downregulation of EMILIN-1, we turned to mirVANA mimics and inhibitors designed for this miRNA. Fibroblasts were transfected with the miR125a-5p mimic, and then assessed for any effect on EMILIN1 mRNA expression. However, the graph shows that the mimic did not reflect the responses observed in fibroblasts exposed to CM; instead, it resembled the behavior of a negative control (**Figure 33A**). Simultaneously, we transfected GC cells with miR125a-5p inhibitor, collected the resulting CM, and then applied it to fibroblasts. To our disappointment, the inhibitor failed to prevent the CM from downregulating EMILIN1 gene expression (**Figure 33B**). In summary, neither the mimic nor the inhibitor provided conclusive evidence for a direct role of miR125a-5p in the regulation of EMILIN1.
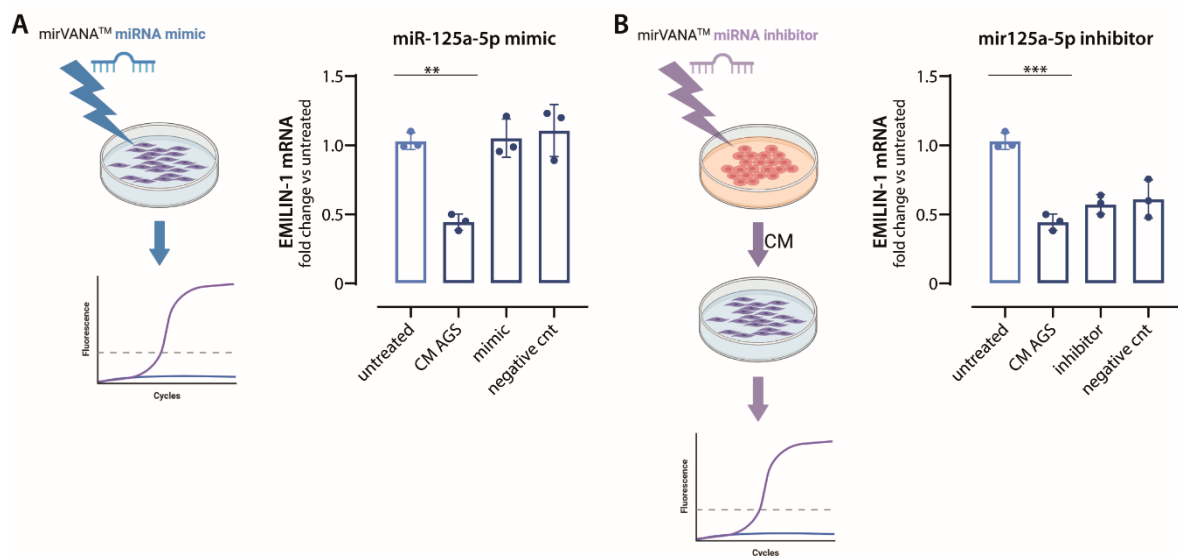

FIGURE 33. ***The use of miR125a-5p mimic and inhibitor did not clearly confirm the role of miR125a-5p in EMILIN1 regulation.*** *A) Transfection of fibroblasts with mirVANA™ miRNA mimic of miR125a-5p does not resemble that with AGS GC cells because EMILIN1 expression does not vary. B) The CM derived from AGS cells transfected with mirVANA™ miRNA mimic of miR125a-5p is still able to downregulate gene expression, so microRNA was not effectively blocked. Results represent the mean ± SD of 3 independent experiments on different fibroblast populations. P values were calculated using two-tailed Student's t-test. **P<0,01, ***P<0,001.*

In light of these results, we decided to take an entirely unbiased approach, performing comprehensive small RNA sequencing (smallRNAseq) on supernatants of GC cells. SmallRNA sequencing analysis of cell supernatants derived from both healthy gastric cells (GES-1) and GC cells (AGS) provided valuable insights into the different profile of these cell groups. At first, the relative amount of the different smallRNA populations was determined. This revealed a great abundance of miRbase RNAs with respect to other populations, especially in GC cells (**Figure 34A**). The comparison shows clear differences between the healthy and cancerous cell lines, suggesting a potentially significant regulatory role of these small RNA species. The heatmap visualizing the most differentially expressed small RNAs species between GES-1 and AGS cells highlighted those candidates that may mark the difference between healthy and GC cells and

play a role in shaping EMILIN1 expression (**Figure 34B**). However, these results are preliminary, and further validation under our experimental conditions is an essential part of our plans. The next step will be the validation of these small RNA candidates. This experimental process will be a key component of our research in the hope of identifying the exact mediators responsible for the observed differences in EMILIN-1 expression after treatment.
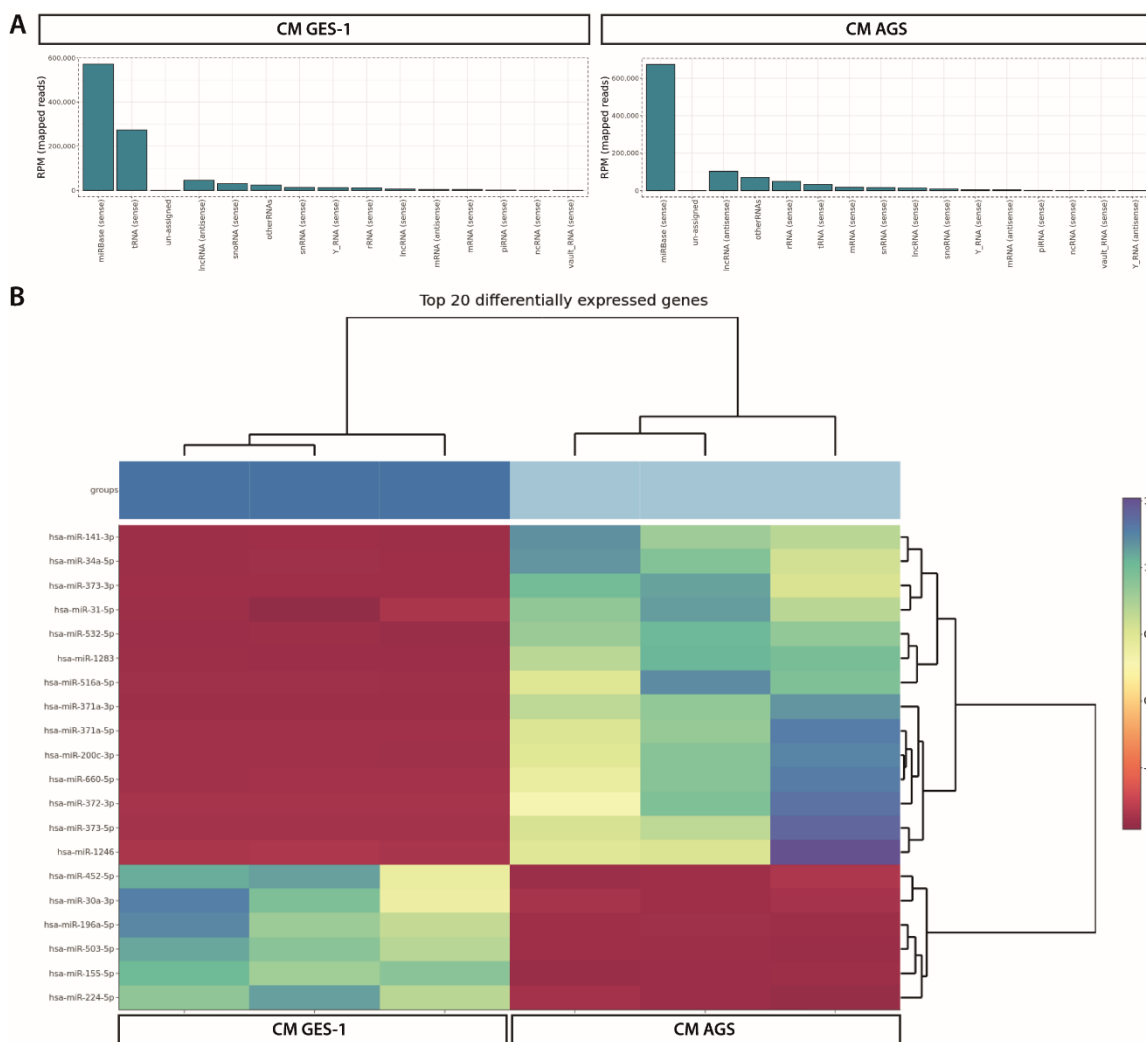
FIGURE 34. *SmallRNA Sequencing analysis of cell supernatants from healthy gastric cells (GES-1) and GC cells (AGS). A) Relative abundance of different small RNA populations in these two groups of cells. B) Heatmap highlighting the differentially expressed small RNA species between GES-1 and AGS cells. This comprehensive analysis was performed by IGAtech (Udine) on a biological triplicate of each group, to ensure robust and replicable results.*

Generation of EMILIN-1 KO fibroblasts.

Given our observations of reduced EMILIN-1 levels in treated fibroblasts, establishing a stable KO cell line was necessary to investigate the functional consequences and the potential phenotypic changes associated with EMILIN-1 depletion. This cell line could provide a consistent and controlled experimental model for dissecting EMILIN-1 impact on cellular behavior, ECM interactions, and downstream signaling pathways. To do so we created a valuable tool starting from an immortalized fibroblast cell line (Bj-5ta).

To generate EMILIN-1 KO cells, we used the CRISPR-Cas9 genome editing system. By means of guide specifically targeted to EMILIN1 gene, we generated a deletion that resulted in an effective knockout within the fibroblast population.

Validation was carried out through a combination of techniques. First, we confirmed the absence of EMILIN-1 protein in the KO cells (**Figure 35A**). This step was crucial to the success of our genetic manipulation because it directly assessed protein levels in the cells.

We also performed real-time PCR using oligos that were specifically designed to target the knocked-out sequence of the EMILIN1 gene (**Figure 35B**).
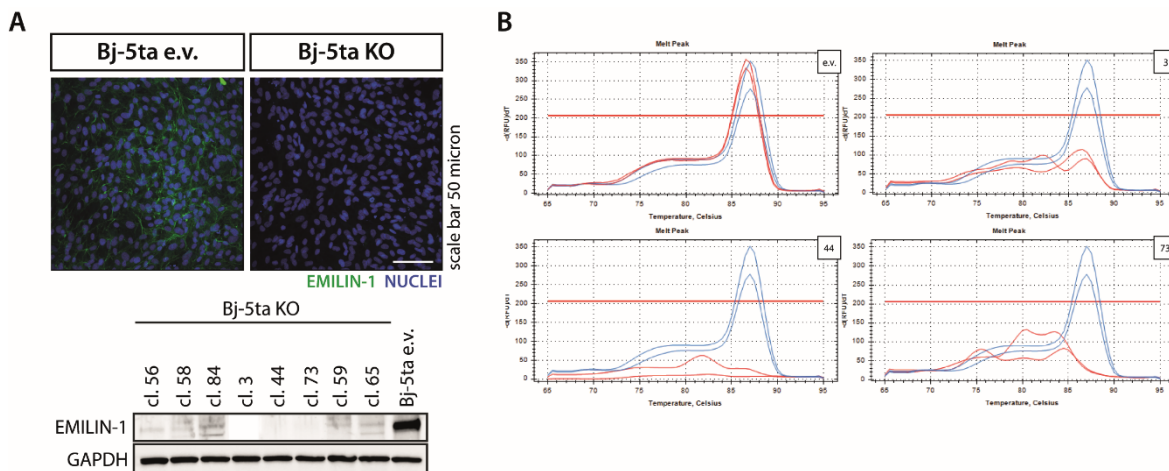
FIGURE 35. **Validation of EMILIN-1 KO tools.** *A) Immunofluorescence analysis of pool of Bj-5ta empty vector (e.v.) and KO (EMILIN-1, green; nuclei, blue). Western Blot analysis of different clones, compared to empty vector (e.v.) cells. B) qRT-PCR of selected clones, demonstrating the effective absence of gene expression.*

These rigorous validation techniques ensured the reliability of our EMILIN-1 KO fibroblast model, enabling us to proceed with our investigations into the role of EMILIN-1 in the context of GC microenvironment.

EMILIN-1 downregulation promotes a CAF phenotype.

To determine whether downmodulation of EMILIN-1 might be associated with phenotypic alteration of fibroblasts, we evaluated the expression of α-smooth muscle actin (α-SMA), which is a well-known marker for identifying cancer-associated fibroblasts (CAFs). Indeed, we detected a significant conversion to a myofibroblast phenotype. This change was closely related to the previously observed decrease in EMILIN-1 levels, suggesting a prominent role of this ECM protein in orchestrating the fibroblast response (**Figure 36A**). The trans-differentiation of fibroblasts is known to be associated with cancer progression and promotion of tumor aggressiveness (Wei et al., 2023).

To further validate this phenotypic transformation, we used EMILIN-1 KO fibroblasts. Strikingly, these genetically engineered fibroblasts exhibited a phenotype similar to the one observed in response to EMILIN-1 reduction (**Figure 36B**). This parallel phenotypic shift in the KO fibroblasts provided compelling evidence for the central role that EMILIN-1 dynamics plays in controlling fibroblast behavior.

The consequences of this change were diverse, as fibroblasts displayed different expression patterns of important markers. Indeed, to gain a deeper understanding of the regulatory mechanisms underlying this shift, we performed RT-PCR analyses. The results confirmed not only the increased α-SMA expression but also the upregulation of another gene critical for this phenotypic transition (**Figure 36C**). Indeed, Collagen 1 α-chain, a fundamental component of the ECM, exhibited heightened expression, indicating the profound ECM remodeling associated with the transition to a CAF status.

Our findings highlight a profound phenotypic transformation of fibroblasts towards the CAF status, which is closely associated with decreased EMILIN-1 levels and is important in the context of GC progression. Moreover, the parallel phenotypic changes observed in KO fibroblasts reinforce the role of EMILIN-1 dynamics in shaping the fibroblast response.
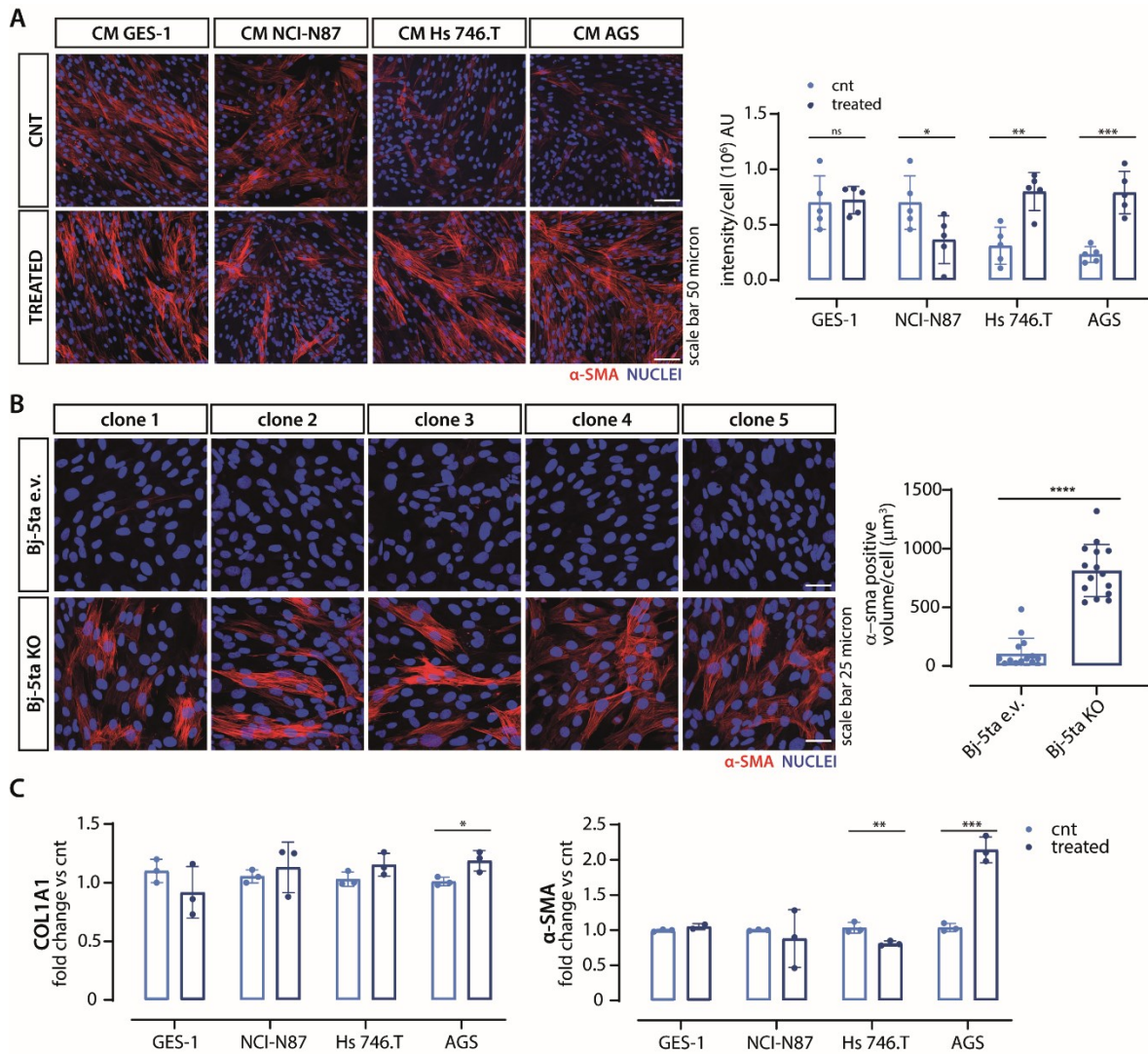
FIGURE 36. **Modified fibroblasts show a phenotypic shift towards a Cancer-Associated Fibroblast (CAF).** *A) A marked increase of alpha-smooth muscle actin (α-SMA) expression (red) in fibroblast treated with CM from GC cell lines (20X). CNTs are treated with fresh growth medium of each gastric cell line, GES-1 and NCI-N87 had the same. B) Genetically engineered KO fibroblasts clones resemble this phenotype. Associated graphs show quantification of α-SMA positive volume in the entire section field examined. For each clone, at least five fields were analyzed, and each dot represents the mean value of different clones. The results represent the mean ± SD of several independent stainings. P values were calculated using two-tailed Student's t-test. *P<0.05, **P<0,01, ***P<0,001, ****P<0,0001. C) qRT-PCR analysis shows significant upregulation of α-SMA and Collagen 1 α-chain (COL1A1), indicating a myofibroblast phenotype, whereas fibroblast activation protein (FAP) shows a marked decrease.*

DISCUSSION

GC is a severe malignancy characterized by marked aggressiveness and complex pathobiology. Emerging evidence suggests that the TME has a strong impact on cancer progression, affecting patient outcome and prognosis. The aim of our study was to investigate the role of the ECM protein EMILIN-1 in the context of GC.

Remodeling of ECM components is a common hallmark of cancer, accompanied by escape from homeostatic control, ultimately leading to abnormal proliferation, a cornerstone of cancer development and progression (Fares et al., 2020). For these reasons, our study focused on the function of the ECM protein EMILIN-1 within the context of GC.

The findings from our research have unveiled important insights into the role of EMILIN-1 in GC, contributing significantly to our understanding of this malignancy. Here a brief summary of our achievements:

- EMILIN-1 expression in GC: EMILIN-1 exhibits reduced expression not only in malignant gastric tissue but interestingly also in premalignant gastric samples. This finding is closely associated with an increase in the density of lymphatic vessels and a greater amount of NE in the neoplastic context. This correlation implies potential mechanisms involving the degradation or downregulation of EMILIN-1.
- Establishment of different mouse models to study the role of EMILIN-1 in GC: mice with an EMILIN-1 KO or KI background are more prone to tumor onset and show an increased propensity to tumor spread. Furthermore, these genotypes exhibit enhanced de novo lymphangiogenesis. These results highlight the importance of EMILIN-1 in the regulation of TME and its impact on disease progression.
- Mechanisms of EMILIN-1 downregulation: we investigated the mechanisms behind the observed downregulation of EMILIN-1 and found that this reduction mainly at the mRNA level.
- EMILIN-1 and α4 integrin: their interaction is necessary to control GC cell proliferation.
- EMILIN-1 and CAF phenotype switch: the decrease in EMILIN-1 expression is concomitant with an increased expression of markers characterizing CAFs. This observation underscores the important role of EMILIN-1 in orchestrating changes in the complex network of cellular crosstalk in the GC-TME.

Further dissection of the mechanisms underlying EMILIN-1 degradation is needed to gain a comprehensive understanding of this phenomenon. Although our *in vitro* findings suggest that EMILIN-1 downregulation occurs primarily at the mRNA level, since we did not observe any MMP modulation in our experimental setting, it is necessary to explore *in vivo* the involvement of these enzymes. Furthermore, the role of NE in EMILIN-1 degradation, which has been supposed to occur

in vivo, should be confirmed *in vitro* by replicating the TME conditions with peculiar co-culture systems, in which neutrophils or their products could exert their activity. These efforts will contribute to a more thorough understanding of the processes governing EMILIN-1 modulation.

The presence of degradative enzymes goes along with a decline in EMILIN-1 transcription, which in turn might contribute to a reduction in the levels of EMILIN-1. This interconnected process seems to pave the way for an increased presence of TGFβ, which could stem from the confluence of factors: the diminished EMILIN-1 levels and the possible release of this cytokine from the ECM triggered by elastase activity (Dallas et al., 2002). Furthermore, elastase exhibits the capability to stimulate the production of TGFβ from epithelial cells (Lee et al., 2006). This prompts the intriguing question: could TGFβ transmembrane signaling, known for its role in orchestrating the transcription of multiple targets, serve as the connecting link? This signaling mechanism might potentially bridge NE activity with the suppression of EMILIN-1 production, possibly through interactions with specific receptors on fibroblasts or gastric cells. This hypothesis presents an avenue for further investigation to better understand this intricate interplay between NE, TGFβ, and EMILIN-1 regulation.

Loss of EMILIN-1 has previously been linked to neoplastic progression in skin and colorectal cancer models (Amor López et al., 2021; Capuano et al., 2019b; Danussi et al., 2012). A striking finding of our study is the relationship between reduced EMILIN-1 levels and malignant or pre-neoplastic gastric tissue. Loss of EMILIN-1 appears to be closely associated with the presence of aberrant LVs in these tissues. This leads us to believe that EMILIN-1 may act as a sentinel in the gastric microenvironment, both exerting anti-proliferative and oncosuppressive functions and protecting the functional integrity of LVs.

Spontaneous GC models established using either chemical carcinogens, Helicobacter pylori infection, or transgenic technology have time limitations (approximately 10–12 months). Therefore, before setting this kind of models, we wanted to test whether EMILIN-1 played a role in gastric tumor growth and progression by using our transgenic mice.

In our in vivo experiments, we employed the syngeneic YTN16 cell line, to generate a solid model to gain insight into these complex dynamics. Using genetically modified EMILIN-1 mice, we found that both KO and KI animals were more prone to develop larger tumors. This observation strongly suggests that EMILIN-1 plays an important role in exerting an anti-proliferative effect in GC. Importantly, this effect is strongly attributable to the gC1q domain, as KO and KI displayed similar behavior. Further insights emerged from the histological analysis of tumor sections. We observed a significant increase in intratumoral lymphangiogenesis in EMILIN-1 mutant animals compared with their WT counterparts. Since lymphatic spread is a crucial event in tumor progression and

metastasis, the marked aberrant lymphangiogenesis observed in these tumors points to the importance of EMILIN-1 this context.

While our initial studies employed a syngeneic GC cell line, known for its aggressive behavior (Fujimori et al., 2020), the limitations of this model for studying early tumor onset prompted us to explore alternative approaches. Because we had observed a similar pattern of tumor growth and spread in KO and KI animals, implying that the effect is based on the engagement between EMILIN-1 and integrins, we decided to focus specifically on the KI model, that preserves interactions within the TGF-β pathway. We treated mice with MNU, a potent carcinogen, to potentially study the early stages of GC initiation. The efficiency of tumor induction by MNU is approximately 60% according to literature (K. Li et al., 2021). In our hands, the MNU carcinogenesis protocol resulted in the development of gastrointestinal intraepithelial neoplasia (GIN) and adenomas, which pathologists classified as fully developed malignant lesions, with marked distinctions observed between different genetic backgrounds. While WT mice had a limited percentage of lesions (confirming the low rate of incidence as described in literature), both heterozygous and homozygous KI mice developed numerous GINs and adenomas. These observations provide important insights into the impact of EMILIN-1 on early-stage neoplastic changes.

Comprehensive histological analysis of mouse stomach tissues was also informative. Initial staining with Alcian/PAS showed that the architecture of KI tumors was more impaired than that of WT tumors. In KI mice, we observed a marked increase in positivity for the proliferation marker Ki67, as well as for H2AX staining. WT mice had only a few strongly H2AX-positive cells distributed throughout the adenoma area, whereas the KI group had numerous positive cells across the entire GIN area, implying an increased level of DNA damage.

MNU-induced tumors develop mainly in the gastric antrum and are pathologically uniformly well or moderately differentiated adenocarcinomas. The tumors are rich in stromal cells and occasionally invade the submucosa (Hayakawa et al., 2013; Tomita et al., 2007). Although this model has been used in particular to study diffuse-type GC, considering its important stromal involvement (Humar et al., 2009; Monster et al., 2022), we believe that MNU protocol could be used in general to investigate the role of ECM, as we have shown for EMILIN-1, to study the critical interactions that take place between the epithelial and stromal components of the gastric mucosa and to clarify the early steps of cancer initiation. Even if the MNU model is not thought to undergo a classic atrophy-metaplasia-dysplasia sequence, we have observed some degree of intestinal metaplasia, corroborated by previous studies (Binato et al., 2017; Moreira et al., 2022). Moreover, the results obtained with this model support the hypothesis that intestinal metaplasia

is important as a para-cancerous condition rather than as a precancerous lesion, and that "intestinalization" of GC progresses with chronic inflammation (Tsukamoto et al., 2007).

The resulting analysis obtained by using different models has offered critical insights into GC progression. These findings are consistent with our previous research dealing with skin and colorectal cancer models, emphasizing the anti-proliferative effect of EMILIN-1 and how its absence, as seen in EMILIN-1-deficient mice, contributes to enhanced tumor growth.

In our ongoing research, we plan to reinforce this evidence by expanding our cohort of mice subjected to chemical carcinogenesis and explore the role of EMILIN-1 in gastric cancer further. This expansion will help us gain more insights into impact of EMILIN-1 on tumor progression. In addition, we intend to perform orthotopic injections of syngeneic cancer cells that express luciferase, which will allow us to study tumor behavior and metastasis in real-time within the mouse stomach.

Our study has also provided valuable insights into the potential mechanisms underlying the EMILIN-1-mediated changes in the tumor microenvironment. As demonstrated in previous studies, the regulation played by EMILIN-1 in proliferation is due to its interaction with integrin α4. The shift from a functional relationship between EMILIN-1 and integrin α4 in normal gastric epithelium to the loss of this interaction in tumors opens new perspectives in this field. The impact of this loss on the downstream signaling effects has needed further investigations on the complex functional dynamics of gastric TME.

For this reason, we established an *in vitro* model using stromal fibroblasts and LECs, which are major producers of EMILIN-1 in the gastric microenvironment. The exposure to CM from GC cells led to the downregulation of EMILIN-1 in stromal cells.

Our studies at the molecular level revealed that this downregulation occurs primarily at the mRNA level. A transcriptional or post-transcriptional regulatory mechanism may be involved in this process, as EMILIN1 gene expression appears to be modulated by factors secreted by GC cells. Interestingly, the investigation on miR125a-5p, a microRNA predicted to target EMILIN1, yielded disappointing results. This miRNA emerges as a fundamental player in GC (R. Li et al., 2021), and showed significantly higher expression in cancer cells compared to their normal counterparts. However, neither the miR125a-5p mimic nor the inhibitor could effectively recapitulate the impact of CM on EMILIN1 expression in fibroblasts. This suggests the involvement of other regulatory agents in EMILIN1 downregulation. SmallRNAseq performed on GC cell supernatants, which includes microRNAs and other non-coding RNAs will help to identify not only known players but also previously unrecognized factors. Deciphering the unknown regulators and

effectors that influence EMILIN1 expression is particularly important because loss of EMILIN-1 has also been associated with a shift in fibroblast phenotype towards a malignant and pro-tumorigenic one.

It is well known that the emergence of a CAF phenotype within the TME is a hallmark of cancer progression and contributes significantly to various aspects of malignant behavior. CAFs contribute to ECM remodeling, leading to tissue stiffness, pro-inflammatory signaling, and fostering a microenvironment conducive to cancer progression (Sun et al., 2022; Wei et al., 2023).

The transition to a CAF-like phenotype is characterized by a shift towards increased expression of α-SMA, a well-known marker of activated fibroblasts that participate in cancer progression. α-SMA-expressing CAFs can enhance the colony formation, proliferation, and invasiveness of pancreatic cancer cells (Fujita et al., 2010). They also promote tumor growth in cholangiocarcinoma and breast cancer (Chuaysri et al., 2009; Muchlińska et al., 2022). Moreover, CAFs play critical roles in oral squamous cell carcinoma progression as an inducer of tumor invasion, angiogenesis, and lymphangiogenesis (Lin et al., 2017). In addition, a significant positive correlation has been found between expression of α-SMA and LV density in ovarian cancer (Zhang et al., 2011). A meta-analysis study highlighted that high persistence of CAFs was closely associated with pathological indicators related to advanced GC (e.g., stage, lymph node metastasis, and vascular metastasis), suggesting that CAFs play a key role in GC invasion and metastasis (Wei et al., 2023). Moreover, increased expression of α-SMA was demonstrated to be associated with poor prognosis in patients with gastric cancer (Cong et al., 2020, p. 20; Wei et al., 2023; Zhan et al., 2020; Zhang et al., 2020; Zhi et al., 2010).

In our study, switch to a CAF phenotype is closely associated with the reduction of EMILIN-1 in the TME. Downregulation of EMILIN-1 after treatment with CM from GC cell lines was associated with increased expression of CAF markers. Interestingly, EMILIN-1 KO fibroblasts resemble this phenotype. The observed heightened α-SMA expression may signify a more pro-fibrotic and tumor-promoting fibroblast population when the protein is lacking, capable of stimulating ECM remodeling and tissue stiffness, favoring cancer progression and metastasis. In addition, we observed an increased expression of COL1A1, which has been identified as gene with high potential to be predictive tool for poor prognosis in GC patients (Ucaryilmaz Metin and Ozcan, 2022). COL1A1 is significantly upregulated in hepatocellular carcinoma tumor tissues and confers survival advantage and enhanced oncogenicity to tumoral cells (Ma et al., 2019). Similar evidence for the promotion of a preparatory environment for tumor development was previously studied in a psoriasis mouse model, in which the KO e KI mouse background was characterized by the

79

induction of a myofibroblast phenotype that in turn drove macrophages towards the M1 phenotype (Pivetta et al., 2022).

These observations highlight the importance of EMILIN-1 in maintaining tissue homeostasis and controlling fibroblast behavior in the TME. Nevertheless, despite existing literature favoring the tumor-promoting role of α-SMA-positive CAFs in GC, we aim to substantiate our discoveries by exploring different experimental settings. Indeed, α-SMA positive CAFs exhibit the potential for both tumor-promoting and tumor-restricting properties, in different tumor contexts (Becker et al., 2020; McAndrews et al., 2022; Özdemir et al., 2014). As future plan, we intend to establish additional in vivo models in nude mice. These models will involve the injection of co-cultures of GC cells with either WT or EMILIN-1 KO fibroblasts.

The dual effect of EMILIN-1 reduction on both fibroblasts and LECs underscores the role this ECM protein plays in shaping the tumor stroma. Understanding these intricate interactions is essential to gain insights into the dynamics of the TME and, consequently, to develop novel strategies to target cancer progression.

In summary, our study provides new insights into the potential role of EMILIN-1 in regulating GC growth and dissemination and highlights the consequences of its loss in the microenvironment (**Figure 37**). The regulatory mechanisms need to be further investigated, keeping in mind that molecules other than the originally hypothesized microRNA may be involved.
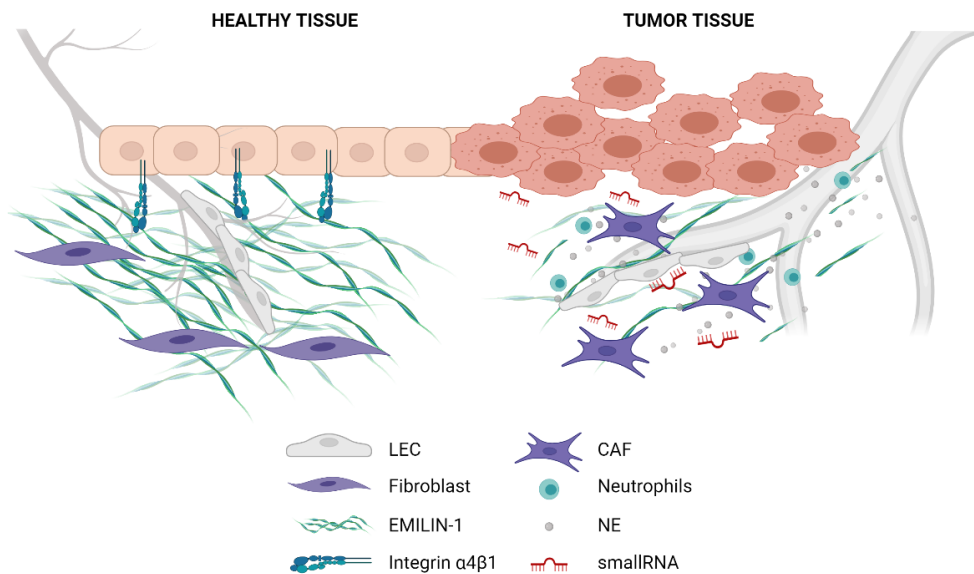
FIGURE 37. **Summary of results.** *EMILIN-1 binds integrin α4 in normal gastric epithelium and exerts an anti-proliferative control. It also maintains a proper structure and function of the lymphatic vasculature. The protective role of EMILIN-1 is lost in tumors, where EMILIN-1 is downregulated and integrin α4 is absent. The consequences are loss of the homeostatic effect on proliferation and the presence of aberrant LVs that allow the persistence of inflammatory cells, such as neutrophils, and the release of proteolytic enzymes able to degrade EMILIN-1. Created with BioRender.com.*

Our discoveries carry profound implications, shedding light on promising therapeutic targets within the EMILIN-1 pathway and paving the way for novel approaches to the early diagnosis of GC. We are confident that discovery of the intricate network of regulatory elements controlling EMILIN-1 expression may provide the basis for future advances in this field and, ultimately, for more effective strategies to address GC.

REFERENCES

Abouelkheir, G.R., Upchurch, B.D., Rutkowski, J.M., 2017. Lymphangiogenesis: fuel, smoke, or extinguisher of inflammation's fire? Exp. Biol. Med. 242, 884–895. https://doi.org/10.1177/1535370217697385

Adamo, C.S., Beyens, A., Schiavinato, A., Keene, D.R., Tufa, S.F., Mörgelin, M., Brinckmann, J., Sasaki, T., Niehoff, A., Dreiner, M., Pottie, L., Muiño-Mosquera, L., Gulec, E.Y., Gezdirici, A., Braghetta, P., Bonaldo, P., Wagener, R., Paulsson, M., Bornaun, H., De Rycke, R., De Bruyne, M., Baeke, F., Devine, W.P., Gangaram, B., Tam, A., Balasubramanian, M., Ellard, S., Moore, S., Symoens, S., Shen, J., Cole, S., Schwarze, U., Holmes, K.W., Hayflick, S.J., Wiszniewski, W., Nampoothiri, S., Davis, E.C., Sakai, L.Y., Sengle, G., Callewaert, B., 2022. EMILIN1 deficiency causes arterial tortuosity with osteopenia and connects impaired elastogenesis with defective collagen fibrillogenesis. Am. J. Hum. Genet. 109, 2230–2252. https://doi.org/10.1016/j.ajhg.2022.10.010

Akagi, T., Shiraishi, N., Kitano, S., 2011. Lymph Node Metastasis of Gastric Cancer. Cancers 3, 2141–2159. https://doi.org/10.3390/cancers3022141

Alexander, J.S., Ganta, V.C., Jordan, P.A., Witte, M.H., 2010. Gastrointestinal lymphatics in health and disease. Pathophysiology, Lymphatic Vessel Functions in Health and Disease 17, 315–335. https://doi.org/10.1016/j.pathophys.2009.09.003

Amin, M.B., Greene, F.L., Edge, S.B., Compton, C.C., Gershenwald, J.E., Brookland, R.K., Meyer, L., Gress, D.M., Byrd, D.R., Winchester, D.P., 2017. The Eighth Edition AJCC Cancer Staging Manual: Continuing to build a bridge from a population-based to a more "personalized" approach to cancer staging. CA. Cancer J. Clin. 67, 93–99. https://doi.org/10.3322/caac.21388

Amor López, A., Mazariegos, M.S., Capuano, A., Ximénez-Embún, P., Hergueta-Redondo, M., Recio, J.Á., Muñoz, E., Al-Shahrour, F., Muñoz, J., Megías, D., Doliana, R., Spessotto, P., Peinado, H., 2021. Inactivation of EMILIN-1 by Proteolysis and Secretion in Small Extracellular Vesicles Favors Melanoma Progression and Metastasis. Int. J. Mol. Sci. 22, 7406. https://doi.org/10.3390/ijms22147406

Angel, P.M., Narmoneva, D.A., Sewell-Loftin, M.K., Munjal, C., Dupuis, L., Landis, B.J., Jegga, A., Kern, C.B., Merryman, W.D., Baldwin, H.S., Bressan, G.M., Hinton, R.B., 2017. Proteomic Alterations Associated with Biomechanical Dysfunction are Early Processes in the Emilin1 Deficient Mouse Model of Aortic Valve Disease. Ann. Biomed. Eng. 45, 2548–2562. https://doi.org/10.1007/s10439-017-1899-0

Arnold, M., Park, J.Y., Camargo, M.C., Lunet, N., Forman, D., Soerjomataram, I., 2020. Is gastric cancer becoming a rare disease? A global assessment of predicted incidence trends to 2035. Gut 69, 823–829. https://doi.org/10.1136/gutjnl-2019-320234

Bass, A.J., Thorsson, V., Shmulevich, I., Reynolds, S.M., Miller, M., Bernard, B., Hinoue, T., Laird, P.W., Curtis, C., Shen, H., Weisenberger, D.J., Schultz, N., Shen, R., Weinhold, N., Kelsen, D.P., Bowlby, R., Chu, A., Kasaian, K., Mungall, A.J., Robertson, A.G., Sipahimalani, P., Cherniack, A., Getz, G., Liu, Y., Noble, M.S., Pedamallu, C., Sougnez, C., Taylor-Weiner, A., Akbani, R., Lee, J.-S., Liu, W., Mills, G.B., Yang, D., Zhang, W., Pantazi, A., Parfenov, M., Gulley, M., Piazuelo, M.B., Kim, J., Sheth, M., Rabkin, C.S., Ng, S., Sougnez, C., Dhalla, N., Moore, R.A., Schein, J.E., Beroukhim, R., Gehlenborg, N., Sun, Y., Raphael, B.J., Benz, C., Ibbs, M., Duke University, University of California, S.C., University of California San Francisco, International Genomics Consortium, Chonnam National University Medical School, Cureline, 2014. Comprehensive molecular characterization of gastric adenocarcinoma. Nature 513, 202–209. https://doi.org/10.1038/nature13480

Battista, S., Ambrosio, M.R., Limarzi, F., Gallo, G., Saragoni, L., 2021. Molecular Alterations in Gastric Preneoplastic Lesions and Early Gastric Cancer. Int. J. Mol. Sci. 22, 6652. https://doi.org/10.3390/ijms22136652

Bausys, R., Bausys, A., Vysniauskaite, I., Maneikis, K., Klimas, D., Luksta, M., Strupas, K., Stratilatovas, E., 2017. Risk factors for lymph node metastasis in early gastric cancer patients: Report from Eastern Europe country– Lithuania. BMC Surg. 17, 108. https://doi.org/10.1186/s12893-017-0304-0

Bazigou, E., Xie, S., Chen, C., Weston, A., Miura, N., Sorokin, L., Adams, R., Muro, A.F., Sheppard, D., Makinen, T., 2009. Integrin-α9 Is Required for Fibronectin Matrix Assembly during Lymphatic Valve Morphogenesis. Dev. Cell 17, 175–186. https://doi.org/10.1016/j.devcel.2009.06.017

Becker, L.M., O'Connell, J.T., Vo, A.P., Cain, M.P., Tampe, D., Bizarro, L., Sugimoto, H., McGow, A.K., Asara, J.M., Lovisa, S., McAndrews, K.M., Zielinski, R., Lorenzi, P.L., Zeisberg, M., Raza, S., LeBleu, V.S., Kalluri, R., 2020. Epigenetic Reprogramming of Cancer-Associated Fibroblasts Deregulates Glucose Metabolism and Facilitates Progression of Breast Cancer. Cell Rep. 31, 107701. https://doi.org/10.1016/j.celrep.2020.107701

Belair, C., Baud, J., Chabas, S., Sharma, C.M., Vogel, J., Staedel, C., Darfeuille, F., 2011. Helicobacter pylori interferes with an embryonic stem cell micro RNA cluster to block cell cycle progression. Silence 2, 7. https://doi.org/10.1186/1758-907X-2-7

Binato, R., Santos, E.C., Boroni, M., Demachki, S., Assumpção, P., Abdelhay, E., 2017. A common molecular signature of intestinal-type gastric carcinoma indicates processes related to gastric carcinogenesis. Oncotarget 9, 7359–7371. https://doi.org/10.18632/oncotarget.23670

Bockerstett, K.A., DiPaolo, R.J., 2017. Regulation of Gastric Carcinogenesis by Inflammatory Cytokines. Cell. Mol. Gastroenterol. Hepatol. 4, 47–53. https://doi.org/10.1016/j.jcmgh.2017.03.005

Bonnans, C., Chou, J., Werb, Z., 2014. Remodelling the extracellular matrix in development and disease. Nat. Rev. Mol. Cell Biol. 15, 786–801. https://doi.org/10.1038/nrm3904

Brown, M., Assen, F.P., Leithner, A., Abe, J., Schachner, H., Asfour, G., Bago-Horvath, Z., Stein, J.V., Uhrin, P., Sixt, M., Kerjaschki, D., 2018. Lymph node blood vessels provide exit routes for metastatic tumor cell dissemination in mice. Science 359, 1408–1411. https://doi.org/10.1126/science.aal3662

Calvo, F., Ege, N., Grande-Garcia, A., Hooper, S., Jenkins, R.P., Chaudhry, S.I., Harrington, K., Williamson, P., Moeendarbary, E., Charras, G., Sahai, E., 2013. Mechanotransduction and YAP-dependent matrix remodelling is required for the generation and maintenance of cancer-associated fibroblasts. Nat. Cell Biol. 15, 637–646. https://doi.org/10.1038/ncb2756

Capuano, A., Fogolari, F., Bucciotti, F., Spessotto, P., Nicolosi, P.A., Mucignat, M.T., Cervi, M., Esposito, G., Colombatti, A., Doliana, R., 2018. The α4β1/EMILIN1 interaction discloses a novel and unique integrin-ligand type of engagement. Matrix Biol. 66, 50–66. https://doi.org/10.1016/j.matbio.2017.10.001

Capuano, A., Pivetta, E., Baldissera, F., Bosisio, G., Wassermann, B., Bucciotti, F., Colombatti, A., Sabatelli, P., Doliana, R., Spessotto, P., 2019a. Integrin binding site within the gC1q domain orchestrates EMILIN-1-induced lymphangiogenesis. Matrix Biol. 81, 34–49. https://doi.org/10.1016/j.matbio.2018.10.006

Capuano, A., Pivetta, E., Sartori, G., Bosisio, G., Favero, A., Cover, E., Andreuzzi, E., Colombatti, A., Cannizzaro, R., Scanziani, E., Minoli, L., Bucciotti, F., Amor Lopez, A.I., Gaspardo, K., Doliana, R., Mongiat, M., Spessotto, P., 2019b. Abrogation of EMILIN1-β1 integrin interaction promotes experimental colitis and colon carcinogenesis. Matrix Biol. 83, 97–115. https://doi.org/10.1016/j.matbio.2019.08.006

Chang, C., Werb, Z., 2001. The many faces of metalloproteases: cell growth, invasion, angiogenesis and metastasis. Trends Cell Biol. 11, S37–S43. https://doi.org/10.1016/S0962-8924(01)02122-5

Chen, Hongxia, Guan, R., Lei, Y., Chen, J., Ge, Q., Zhang, X., Dou, R., Chen, Hongyuan, Liu, H., Qi, X., Zhou, X., Chen, C., 2015. Lymphangiogenesis in Gastric Cancer regulated through Akt/mTOR-VEGF-C/VEGF-D axis. BMC Cancer 15, 103. https://doi.org/10.1186/s12885-015-1109-0

Chen, J., Zhao, G., Wang, Y., 2020. Analysis of lymph node metastasis in early gastric cancer: a single institutional experience from China. World J. Surg. Oncol. 18, 57. https://doi.org/10.1186/s12957-020-01834-7

Chen, X., Song, E., 2019. Turning foes to friends: targeting cancer-associated fibroblasts. Nat. Rev. Drug Discov. 18, 99–115. https://doi.org/10.1038/s41573-018-0004-1

Chen, Y., Zhou, Q., Wang, H., Zhuo, W., Ding, Y., Lu, J., Wu, G., Xu, N., Teng, L., 2020. Predicting Peritoneal Dissemination of Gastric Cancer in the Era of Precision Medicine: Molecular Characterization and Biomarkers. Cancers 12, 2236. https://doi.org/10.3390/cancers12082236

Chen, Y.-C., Fang, W.-L., Wang, R.-F., Liu, C.-A., Yang, M.-H., Lo, S.-S., Wu, C.-W., Li, A.F.-Y., Shyr, Y.-M., Huang, K.-H., 2016. Clinicopathological Variation of Lauren Classification in Gastric Cancer. Pathol. Oncol. Res. 22, 197–202. https://doi.org/10.1007/s12253-015-9996-6

Chen, Z., Zhang, P., Xi, H., Wei, B., Chen, L., Tang, Y., 2021. Recent Advances in the Diagnosis, Staging, Treatment, and Prognosis of Advanced Gastric Cancer: A Literature Review. Front. Med. 8.

Chiarello, M.M., Fico, V., Pepe, G., Tropeano, G., Adams, N.J., Altieri, G., Brisinda, G., 2022. Early gastric cancer: A challenge in Western countries. World J. Gastroenterol. 28, 693–703. https://doi.org/10.3748/wjg.v28.i7.693

Cho, Y., Na, K., Jun, Y., Won, J., Yang, J.H., Chung, S., 2021. Three-Dimensional In Vitro Lymphangiogenesis Model in Tumor Microenvironment. Front. Bioeng. Biotechnol. 9.

Chuaysri, C., Thuwajit, P., Paupairoj, A., Chau-In, S., Suthiphongchai, T., Thuwajit, C., 2009. Alpha-smooth muscle actin-positive fibroblasts promote biliary cell proliferation and correlate with poor survival in cholangiocarcinoma. Oncol. Rep. 21, 957–969. https://doi.org/10.3892/or_00000309

Colombatti, A., Doliana, R., Bot, S., Canton, A., Mongiat, M., Mungiguerra, G., Paron-Cilli, S., Spessotto, P., 2000. The EMILIN protein family. Matrix Biol., On the occasion of the XVII Meeting of the FECTS 19, 289–301. https://doi.org/10.1016/S0945-053X(00)00074-3

Colombatti, A., Spessotto, P., Doliana, R., Mongiat, M., Bressan, G., Esposito, G., 2012. The EMILIN/Multimerin Family. Front. Immunol. 2.

Cong, X., Zhang, Yongle, Zhu, Z., Li, S., Yin, X., Zhai, Z., Zhang, Yu, Xue, Y., 2020. CD66b+ neutrophils and α-SMA+ fibroblasts predict clinical outcomes and benefits from postoperative chemotherapy in gastric adenocarcinoma. Cancer Med. 9, 2761–2773. https://doi.org/10.1002/cam4.2939

Correa, P., 2013. Gastric Cancer. Gastroenterol. Clin. North Am. 42, 211–217. https://doi.org/10.1016/j.gtc.2013.01.002

Cox, D., Brennan, M., Moran, N., 2010. Integrins as therapeutic targets: lessons and opportunities. Nat. Rev. Drug Discov. 9, 804–820. https://doi.org/10.1038/nrd3266

Cui, X., Shan, T., Qiao, L., 2022. Collagen type IV alpha 1 (COL4A1) silence hampers the invasion, migration and epithelial–mesenchymal transition (EMT) of gastric cancer cells through blocking Hedgehog signaling pathway. Bioengineered 13, 8972–8981. https://doi.org/10.1080/21655979.2022.2053799

Dallas, S.L., Rosser, J.L., Mundy, G.R., Bonewald, L.F., 2002. Proteolysis of latent transforming growth factor-beta (TGF-beta)-binding protein-1 by osteoclasts. A cellular mechanism for release of TGF-beta from bone matrix. J. Biol. Chem. 277, 21352–21360. https://doi.org/10.1074/jbc.M111663200

Danussi, C., Del Bel Belluz, L., Pivetta, E., Modica, T.M.E., Muro, A., Wassermann, B., Doliana, R., Sabatelli, P., Colombatti, A., Spessotto, P., 2013. EMILIN1/α9β1 Integrin Interaction Is Crucial in Lymphatic Valve Formation and Maintenance. Mol. Cell. Biol. 33, 4381–4394. https://doi.org/10.1128/MCB.00872-13

Danussi, C., Petrucco, A., Wassermann, B., Modica, T.M.E., Pivetta, E., Del Bel Belluz, L., Colombatti, A., Spessotto, P., 2012. An EMILIN1-negative microenvironment promotes tumor cell proliferation and lymph node invasion. Cancer Prev. Res. Phila. Pa 5, 1131–1143. https://doi.org/10.1158/1940-6207.CAPR-12-0076-T

Danussi, C., Petrucco, A., Wassermann, B., Pivetta, E., Modica, T.M.E., Belluz, L.D.B., Colombatti, A., Spessotto, P., 2011. EMILIN1–α4/α9 integrin interaction inhibits dermal fibroblast and keratinocyte proliferation. J. Cell Biol. 195, 131–145. https://doi.org/10.1083/jcb.201008013

Danussi, C., Spessotto, P., Petrucco, A., Wassermann, B., Sabatelli, P., Montesi, M., Doliana, R., Bressan, G.M., Colombatti, A., 2008. Emilin1 Deficiency Causes Structural and Functional Defects of Lymphatic Vasculature. Mol. Cell. Biol. 28, 4026–4039. https://doi.org/10.1128/MCB.02062-07

Deng, J.-Y., Liang, H., 2014. Clinical significance of lymph node metastasis in gastric cancer. World J. Gastroenterol. 20, 3967–3975. https://doi.org/10.3748/wjg.v20.i14.3967

Doliana, R., Bot, S., Bonaldo, P., Colombatti, A., 2000. EMI, a novel cysteine-rich domain of EMILINs and other extracellular proteins, interacts with the gC1q domains and participates in multimerization. FEBS Lett. 484, 164–168. https://doi.org/10.1016/s0014-5793(00)02140-2

Doliana, R., Mongiat, M., Bucciotti, F., Giacomello, E., Deutzmann, R., Volpin, D., Bressan, G.M., Colombatti, A., 1999. EMILIN, a Component of the Elastic Fiber and a New Member of the

C1q/Tumor Necrosis Factor Superfamily of Proteins*. J. Biol. Chem. 274, 16773–16781. https://doi.org/10.1074/jbc.274.24.16773

Edlund, K., Lindskog, C., Saito, A., Berglund, A., Pontén, F., Göransson-Kultima, H., Isaksson, A., Jirström, K., Planck, M., Johansson, L., Lambe, M., Holmberg, L., Nyberg, F., Ekman, S., Bergqvist, M., Landelius, P., Lamberg, K., Botling, J., Ostman, A., Micke, P., 2012. CD99 is a novel prognostic stromal marker in non-small cell lung cancer. Int. J. Cancer 131, 2264–2273. https://doi.org/10.1002/ijc.27518

Fares, J., Fares, M.Y., Khachfe, H.H., Salhab, H.A., Fares, Y., 2020. Molecular principles of metastasis: a hallmark of cancer revisited. Signal Transduct. Target. Ther. 5, 1–17. https://doi.org/10.1038/s41392-020-0134-x

Fridlender, Z.G., Sun, J., Kim, S., Kapoor, V., Cheng, G., Ling, L., Worthen, G.S., Albelda, S.M., 2009. Polarization of Tumor-Associated Neutrophil Phenotype by TGF-β: "N1" versus "N2" TAN. Cancer Cell 16, 183–194. https://doi.org/10.1016/j.ccr.2009.06.017

Fu, H., Ma, Y., Yang, M., Zhang, C., Huang, H., Xia, Y., Lu, L., Jin, W., Cui, D., 2016. Persisting and Increasing Neutrophil Infiltration Associates with Gastric Carcinogenesis and E-cadherin Downregulation. Sci. Rep. 6, 1–14. https://doi.org/10.1038/srep29762

Fujimori, D., Kinoshita, J., Yamaguchi, T., Nakamura, Y., Gunjigake, K., Ohama, T., Sato, K., Yamamoto, M., Tsukamoto, T., Nomura, S., Ohta, T., Fushida, S., 2020. Established fibrous peritoneal metastasis in an immunocompetent mouse model similar to clinical immune microenvironment of gastric cancer. BMC Cancer 20, 1014. https://doi.org/10.1186/s12885-020-07477-x

Fujita, H., Ohuchida, K., Mizumoto, K., Nakata, K., Yu, J., Kayashima, T., Cui, L., Manabe, T., Ohtsuka, T., Tanaka, M., 2010. alpha-Smooth Muscle Actin Expressing Stroma Promotes an Aggressive Tumor Biology in Pancreatic Ductal Adenocarcinoma. Pancreas 39, 1254–1262. https://doi.org/10.1097/MPA.0b013e3181dbf647

Gao, P., Zhou, G.-Y., Zhang, Q.-H., Su, Z.-X., Zhang, T.-G., Xiang, L., Wang, Y., Zhang, S.-L., Mu, K., 2009. Lymphangiogenesis in gastric carcinoma correlates with prognosis. J. Pathol. 218, 192–200. https://doi.org/10.1002/path.2523

Ghebrehiwet, B., Hosszu, K., Valentino, A., Peerschke, E., 2012. The C1q Family of Proteins: Insights into the Emerging Non-Traditional Functions. Front. Immunol. 3.

Gifford, A.M., Chalmers, J.D., 2014. The role of neutrophils in cystic fibrosis. Curr. Opin. Hematol. 21, 16. https://doi.org/10.1097/MOH.0000000000000009

Gillot, L., Baudin, L., Rouaud, L., Kridelka, F., Noël, A., 2021. The pre-metastatic niche in lymph nodes: formation and characteristics. Cell. Mol. Life Sci. 78, 5987–6002. https://doi.org/10.1007/s00018-021-03873-z

Giraldo, N.A., Sanchez-Salas, R., Peske, J.D., Vano, Y., Becht, E., Petitprez, F., Validire, P., Ingels, A., Cathelineau, X., Fridman, W.H., Sautès-Fridman, C., 2019. The clinical role of the TME in solid cancer. Br. J. Cancer 120, 45–53. https://doi.org/10.1038/s41416-018-0327-z

Gu, L., Ding, D., Wei, C., Zhou, D., 2023. Cancer-associated fibroblasts refine the classifications of gastric cancer with distinct prognosis and tumor microenvironment characteristics. Front. Oncol. 13.

Gupta, S.K., Oommen, S., Aubry, M.-C., Williams, B.P., Vlahakis, N.E., 2013. Integrin α9β1 promotes malignant tumor growth and metastasis by potentiating epithelial-mesenchymal transition. Oncogene 32, 141–150. https://doi.org/10.1038/onc.2012.41

Gupta, S.K., Vlahakis, N.E., 2010. Integrin α9β1. Cell Adhes. Migr. 4, 194–198. https://doi.org/10.4161/cam.4.2.10900

Hanahan, D., Weinberg, R.A., 2011. Hallmarks of Cancer: The Next Generation. Cell 144, 646–674. https://doi.org/10.1016/j.cell.2011.02.013

Hayakawa, Y., Fox, J.G., Gonda, T., Worthley, D.L., Muthupalani, S., Wang, T.C., 2013. Mouse Models of Gastric Cancer. Cancers 5, 92–130. https://doi.org/10.3390/cancers5010092

Hu, B., Hajj, N.E., Sittler, S., Lammert, N., Barnes, R., Meloni-Ehrig, A., 2012. Gastric cancer: Classification, histology and application of molecular pathology. J. Gastrointest. Oncol. 3. https://doi.org/10.3978/j.issn.2078-6891.2012.021

Huang, H.-L., Leung, C.Y., Saito, E., Katanoda, K., Hur, C., Kong, C.Y., Nomura, S., Shibuya, K., 2020. Effect and cost-effectiveness of national gastric cancer screening in Japan: a microsimulation modeling study. BMC Med. 18, 257. https://doi.org/10.1186/s12916-020-01729-0

Humar, B., Blair, V., Charlton, A., More, H., Martin, I., Guilford, P., 2009. E-Cadherin Deficiency Initiates Gastric Signet-Ring Cell Carcinoma in Mice and Man. Cancer Res. 69, 2050–2056. https://doi.org/10.1158/0008-5472.CAN-08-2457

Hynes, R.O., 2009. The Extracellular Matrix: Not Just Pretty Fibrils. Science 326, 1216–1219. https://doi.org/10.1126/science.1176009

Ignatoski, K.M.W., Grewal, N.K., Markwart, S., Livant, D.L., Ethier, S.P., 2003. p38MAPK Induces Cell Surface α4 Integrin Downregulation to Facilitate erbB-2-Mediated Invasion. Neoplasia 5, 128–134. https://doi.org/10.1016/S1476-5586(03)80004-0

Imai, Y., Shimaoka, M., Kurokawa, M., 2010. Essential roles of VLA-4 in the hematopoietic system. Int. J. Hematol. 91, 569–575. https://doi.org/10.1007/s12185-010-0555-3

Jang, M., Koh, I., Lee, J.E., Lim, J.Y., Cheong, J.-H., Kim, P., 2018. Increased extracellular matrix density disrupts E-cadherin/β-catenin complex in gastric cancer cells. Biomater. Sci. 6, 2704–2713. https://doi.org/10.1039/C8BM00843D

Jaroenlapnopparat, A., Bhatia, K., Coban, S., 2022. Inflammation and Gastric Cancer. Diseases 10, 35. https://doi.org/10.3390/diseases10030035

Jia, W., Luo, Q., Wu, J., Shi, Y., Guan, Q., 2023. Neutrophil elastase as a potential biomarker related to the prognosis of gastric cancer and immune cell infiltration in the tumor immune microenvironment. Sci. Rep. 13, 1–15. https://doi.org/10.1038/s41598-023-39404-y

Jiang, X., Wang, J., Deng, X., Xiong, F., Zhang, S., Gong, Z., Li, Xiayu, Cao, K., Deng, H., He, Y., Liao, Q., Xiang, B., Zhou, M., Guo, C., Zeng, Z., Li, G., Li, Xiaoling, Xiong, W., 2020. The role of microenvironment in tumor angiogenesis. J. Exp. Clin. Cancer Res. 39, 204. https://doi.org/10.1186/s13046-020-01709-5

Jun, J.K., Choi, K.S., Lee, H.-Y., Suh, M., Park, B., Song, S.H., Jung, K.W., Lee, C.W., Choi, I.J., Park, E.-C., Lee, D., 2017. Effectiveness of the Korean National Cancer Screening Program in Reducing Gastric Cancer Mortality. Gastroenterology 152, 1319-1328.e7. https://doi.org/10.1053/j.gastro.2017.01.029

Kanda, M., Kodera, Y., 2016. Molecular mechanisms of peritoneal dissemination in gastric cancer. World J. Gastroenterol. 22, 6829–6840. https://doi.org/10.3748/wjg.v22.i30.6829

Kemi, N., Eskuri, M., Herva, A., Leppänen, J., Huhta, H., Helminen, O., Saarnio, J., Karttunen, T.J., Kauppila, J.H., 2018. Tumour-stroma ratio and prognosis in gastric adenocarcinoma. Br. J. Cancer 119, 435–439. https://doi.org/10.1038/s41416-018-0202-y

Khanderia, E., Markar, S.R., Acharya, A., Kim, Y., Kim, Y.-W., Hanna, G.B., 2016. The Influence of Gastric Cancer Screening on the Stage at Diagnosis and Survival: A Meta-Analysis of Comparative Studies in the Far East. J. Clin. Gastroenterol. 50, 190–197. https://doi.org/10.1097/MCG.0000000000000466

Kim, B., Cho, S.-J., 2021. Endoscopic Screening and Surveillance for Gastric Cancer. Gastrointest. Endosc. Clin. N. Am. 31, 489–501. https://doi.org/10.1016/j.giec.2021.03.004

Kim, H., Kataru, R.P., Koh, G.Y., 2014. Inflammation-associated lymphangiogenesis: a double-edged sword? J. Clin. Invest. 124, 936–942. https://doi.org/10.1172/JCI71607

Kinami, S., Saito, H., Takamura, H., 2022. Significance of Lymph Node Metastasis in the Treatment of Gastric Cancer and Current Challenges in Determining the Extent of Metastasis. Front. Oncol. 11.

Klein, T., Bischoff, R., 2011. Physiology and pathophysiology of matrix metalloproteases. Amino Acids 41, 271–290. https://doi.org/10.1007/s00726-010-0689-x

Koike Folgueira, M.A.A., Carraro, D.M., Brentani, H., da Costa Patrão, D.F., Barbosa, E.M., Netto, M.M., Caldeira, J.R.F., Katayama, M.L.H., Soares, F.A., Oliveira, C.T., Reis, L.F.L., Kaiano, J.H.L., Camargo, L.P., Vêncio, R.Z.N., Snitcovsky, I.M.L., Makdissi, F.B.A., da Silva e Silva, P.J., Góes, J.C.G.S., Brentani, M.M., 2005. Gene Expression Profile Associated with Response to

Doxorubicin-Based Therapy in Breast Cancer. Clin. Cancer Res. 11, 7434–7443. https://doi.org/10.1158/1078-0432.CCR-04-0548

Kon, S., Uede, T., 2018. The role of α9β1 integrin and its ligands in the development of autoimmune diseases. J. Cell Commun. Signal. 12, 333–342. https://doi.org/10.1007/s12079-017-0413-7

Korivi, B.R., Faria, S., Aly, A., Sun, J., Patnana, M., Jensen, C.T., Wagner-Bartak, N., Bhosale, P.R., 2019. Intestinal and diffuse gastric cancer: a retrospective study comparing primary sites. Clin. Imaging 56, 33–40. https://doi.org/10.1016/j.clinimag.2019.03.002

Krishnaswamy, V.R., Benbenishty, A., Blinder, P., Sagi, I., 2019. Demystifying the extracellular matrix and its proteolytic remodeling in the brain: structural and functional insights. Cell. Mol. Life Sci. 76, 3229–3248. https://doi.org/10.1007/s00018-019-03182-6

Krotova, K., Khodayari, N., Oshins, R., Aslanidi, G., Brantly, M.L., 2020. Neutrophil elastase promotes macrophage cell adhesion and cytokine production through the integrin-Src kinases pathway. Sci. Rep. 10, 1–10. https://doi.org/10.1038/s41598-020-72667-3

Laurén, P., 1965. The Two Histological Main Types of Gastric Carcinoma: Diffuse and so-Called Intestinal-Type Carcinoma. Acta Pathol. Microbiol. Scand. 64, 31–49. https://doi.org/10.1111/apm.1965.64.1.31

Lee, J.E., Kim, K.T., Shin, S.-J., Cheong, J.-H., Choi, Y.Y., 2023. Genomic and evolutionary characteristics of metastatic gastric cancer by routes. Br. J. Cancer 129, 672–682. https://doi.org/10.1038/s41416-023-02338-3

Lee, J.Y., Gong, E.J., Chung, E.J., Park, H.W., Bae, S.E., Kim, E.H., Kim, J., Do, Y.S., Kim, T.H., Chang, H.-S., Song, H.J., Choe, J., Jung, H.-Y., 2017. The Characteristics and Prognosis of Diffuse-Type Early Gastric Cancer Diagnosed during Health Check-Ups. Gut Liver 11, 807–812. https://doi.org/10.5009/gnl17033

Lee, K.-Y., Ho, S.-C., Lin, H.-C., Lin, S.-M., Liu, C.-Y., Huang, C.-D., Wang, C.-H., Chung, K.F., Kuo, H.-P., 2006. Neutrophil-Derived Elastase Induces TGF-β1 Secretion in Human Airway Smooth Muscle via NF-κB Pathway. Am. J. Respir. Cell Mol. Biol. 35, 407–414. https://doi.org/10.1165/rcmb.2006-0012OC

Li, H., Fan, X., Houghton, J., 2007. Tumor microenvironment: The role of the tumor stroma in cancer. J. Cell. Biochem. 101, 805–815. https://doi.org/10.1002/jcb.21159

Li, K., Wang, A., Liu, H., Li, B., 2021. Protocol for chemically induced murine gastric tumor model. STAR Protoc. 2, 100814. https://doi.org/10.1016/j.xpro.2021.100814

Li, R., Hu, Z., Wang, Z., Zhu, T., Wang, G., Gao, B., Wang, J., Deng, X., 2021. miR-125a-5p promotes gastric cancer growth and invasion by regulating the Hippo pathway. J. Clin. Lab. Anal. 35, e24078. https://doi.org/10.1002/jcla.24078

Li, Y., Xie, D., Chen, X., Hu, T., Lu, S., Han, Y., 2020. Prognostic Value of the Site of Distant Metastasis and Surgical Interventions in Metastatic Gastric Cancer: A Population-Based Study. Technol. Cancer Res. Treat. 19, 1533033820964131. https://doi.org/10.1177/1533033820964131

Li, Z., Wu, X., Gao, X., Shan, F., Ying, X., Zhang, Y., Ji, J., 2021. Development and validation of a novel staging system integrating the number and location of lymph nodes for gastric adenocarcinoma. Br. J. Cancer 124, 942–950. https://doi.org/10.1038/s41416-020-01190-z

Lin, N.-N., Wang, P., Zhao, D., Zhang, F.-J., Yang, K., Chen, R., 2017. Significance of oral cancer-associated fibroblasts in angiogenesis, lymphangiogenesis, and tumor invasion in oral squamous cell carcinoma. J. Oral Pathol. Med. 46, 21–30. https://doi.org/10.1111/jop.12452

Lirosi, M.C., Biondi, A., Ricci, R., 2017. Surgical anatomy of gastric lymphatic drainage. Transl. Gastroenterol. Hepatol. 2. https://doi.org/10.21037/tgh.2016.12.06

Liu, F., Wu, Q., Dong, Z., Liu, K., 2023. Integrins in cancer: Emerging mechanisms and therapeutic opportunities. Pharmacol. Ther. 247, 108458. https://doi.org/10.1016/j.pharmthera.2023.108458

Liu, L., Wang, Z.W., Ji, J., Zhang, J.N., Yan, M., Zhang, J., Liu, B.Y., Zhu, Z.G., Yu, Y.Y., 2013. A cohort study and meta-analysis between histopathological classification and prognosis of gastric carcinoma. Anticancer Agents Med. Chem. 13, 227–234. https://doi.org/10.2174/1871520611313020007

Liu, Y., Li, C., Lu, Y., Liu, C., Yang, W., 2022. Tumor microenvironment-mediated immune tolerance in development and treatment of gastric cancer. Front. Immunol. 13.

Lordick, F., Allum, W., Carneiro, F., Mitry, E., Tabernero, J., Tan, P., Van Cutsem, E., van de Velde, C., Cervantes, A., 2014. Unmet needs and challenges in gastric cancer: The way forward. Cancer Treat. Rev. 40, 692–700. https://doi.org/10.1016/j.ctrv.2014.03.002

Lordick, F., Carneiro, F., Cascinu, S., Fleitas, T., Haustermans, K., Piessen, G., Vogel, A., Smyth, E.C., 2022. Gastric cancer: ESMO Clinical Practice Guideline for diagnosis, treatment and follow-up☆. Ann. Oncol. 33, 1005–1020. https://doi.org/10.1016/j.annonc.2022.07.004

Lu, P., Takai, K., Weaver, V.M., Werb, Z., 2011. Extracellular Matrix Degradation and Remodeling in Development and Disease. Cold Spring Harb. Perspect. Biol. 3, a005058. https://doi.org/10.1101/cshperspect.a005058

Lugano, R., Ramachandran, M., Dimberg, A., 2020. Tumor angiogenesis: causes, consequences, challenges and opportunities. Cell. Mol. Life Sci. 77, 1745–1770. https://doi.org/10.1007/s00018-019-03351-7

Ma, H.-P., Chang, H.-L., Bamodu, O.A., Yadav, V.K., Huang, T.-Y., Wu, A.T.H., Yeh, C.-T., Tsai, S.-H., Lee, W.-H., 2019. Collagen 1A1 (COL1A1) Is a Reliable Biomarker and Putative Therapeutic Target for Hepatocellular Carcinogenesis and Metastasis. Cancers 11, 786. https://doi.org/10.3390/cancers11060786

Machlowska, J., Baj, J., Sitarz, M., Maciejewski, R., Sitarz, R., 2020. Gastric Cancer: Epidemiology, Risk Factors, Classification, Genomic Characteristics and Treatment Strategies. Int. J. Mol. Sci. 21, 4012. https://doi.org/10.3390/ijms21114012

Maiorani, O., Pivetta, E., Capuano, A., Modica, T.M.E., Wassermann, B., Bucciotti, F., Colombatti, A., Doliana, R., Spessotto, P., 2017. Neutrophil elastase cleavage of the gC1q domain impairs the EMILIN1-α4β1 integrin interaction, cell adhesion and anti-proliferative activity. Sci. Rep. 7, 1–13. https://doi.org/10.1038/srep39974

Mak, T.K., Li, X., Huang, H., Wu, K., Huang, Z., He, Y., Zhang, C., 2022. The cancer-associated fibroblast-related signature predicts prognosis and indicates immune microenvironment infiltration in gastric cancer. Front. Immunol. 13.

Manzanedo, I., Pereira, F., Pérez-Viejo, E., Serrano, Á., 2023. Gastric Cancer with Peritoneal Metastases: Current Status and Prospects for Treatment. Cancers 15, 1777. https://doi.org/10.3390/cancers15061777

Mao, X., Xu, J., Wang, W., Liang, C., Hua, J., Liu, J., Zhang, B., Meng, Q., Yu, X., Shi, S., 2021. Crosstalk between cancer-associated fibroblasts and immune cells in the tumor microenvironment: new findings and future perspectives. Mol. Cancer 20, 131. https://doi.org/10.1186/s12943-021-01428-1

McAndrews, K.M., Chen, Y., Darpolor, J.K., Zheng, X., Yang, S., Carstens, J.L., Li, B., Wang, H., Miyake, T., Correa de Sampaio, P., Kirtley, M.L., Natale, M., Wu, C.-C., Sugimoto, H., LeBleu, V.S., Kalluri, R., 2022. Identification of Functional Heterogeneity of Carcinoma-Associated Fibroblasts with Distinct IL6-Mediated Therapy Resistance in Pancreatic Cancer. Cancer Discov. 12, 1580–1597. https://doi.org/10.1158/2159-8290.CD-20-1484

McMahon, M., Ye, S., Pedrina, J., Dlugolenski, D., Stambas, J., 2021. Extracellular Matrix Enzymes and Immune Cell Biology. Front. Mol. Biosci. 8.

Meyer, A.R., Goldenring, J.R., 2018. Injury, repair, inflammation and metaplasia in the stomach. J. Physiol. 596, 3861–3867. https://doi.org/10.1113/JP275512

Mo, J., Zhang, J., Huang, H., Liu, C., Cheng, Y., Mo, Y., Wu, S., Zhong, Y., Zhong, C., Zhang, B., 2022. The early predictive effect of low expression of the ITGA4 in colorectal cancer. J. Gastrointest. Oncol. 13. https://doi.org/10.21037/jgo-22-92

Modica, T.M.E., Maiorani, O., Sartori, G., Pivetta, E., Doliana, R., Capuano, A., Colombatti, A., Spessotto, P., 2017. The extracellular matrix protein EMILIN1 silences the RAS-ERK

pathway via α4β1 integrin and decreases tumor cell growth. Oncotarget 8, 27034–27046. https://doi.org/10.18632/oncotarget.15067

Mohan, V., Das, A., Sagi, I., 2020. Emerging roles of ECM remodeling processes in cancer. Semin. Cancer Biol., Translating Extracellular Matrix 62, 192–200. https://doi.org/10.1016/j.semcancer.2019.09.004

Monster, J.L., Kemp, L.J.S., Gloerich, M., van der Post, R.S., 2022. Diffuse gastric cancer: Emerging mechanisms of tumor initiation and progression. Biochim. Biophys. Acta BBA - Rev. Cancer 1877, 188719. https://doi.org/10.1016/j.bbcan.2022.188719

Moreira, A.M., Ferreira, R.M., Carneiro, P., Figueiredo, J., Osório, H., Barbosa, J., Preto, J., Pinto-do-Ó, P., Carneiro, F., Seruca, R., 2022. Proteomic Identification of a Gastric Tumor ECM Signature Associated With Cancer Progression. Front. Mol. Biosci. 9.

Moreira, A.M., Pereira, J., Melo, S., Fernandes, M.S., Carneiro, P., Seruca, R., Figueiredo, J., 2020. The Extracellular Matrix: An Accomplice in Gastric Cancer Development and Progression. Cells 9, 394. https://doi.org/10.3390/cells9020394

Morgan, E., Arnold, M., Camargo, M.C., Gini, A., Kunzmann, A.T., Matsuda, T., Meheus, F., Verhoeven, R.H.A., Vignat, J., Laversanne, M., Ferlay, J., Soerjomataram, I., 2022. The current and future incidence and mortality of gastric cancer in 185 countries, 2020–40: A population-based modelling study. eClinicalMedicine 47. https://doi.org/10.1016/j.eclinm.2022.101404

Morooka, N., Futaki, S., Sato-Nishiuchi, R., Nishino, M., Totani, Y., Shimono, C., Nakano, I., Nakajima, H., Mochizuki, N., Sekiguchi, K., 2017. Polydom Is an Extracellular Matrix Protein Involved in Lymphatic Vessel Remodeling. Circ. Res. 120, 1276–1288. https://doi.org/10.1161/CIRCRESAHA.116.308825

Muchlińska, A., Nagel, A., Popęda, M., Szade, J., Niemira, M., Zieliński, J., Skokowski, J., Bednarz-Knoll, N., Żaczek, A.J., 2022. Alpha-smooth muscle actin-positive cancer-associated fibroblasts secreting osteopontin promote growth of luminal breast cancer. Cell. Mol. Biol. Lett. 27, 45. https://doi.org/10.1186/s11658-022-00351-7

Munjal, C., Opoka, A.M., Osinska, H., James, J.F., Bressan, G.M., Hinton, R.B., 2014. TGF-β mediates early angiogenesis and latent fibrosis in an Emilin1-deficient mouse model of aortic valve disease. Dis. Model. Mech. 7, 987–996. https://doi.org/10.1242/dmm.015255

Nagtegaal, I.D., Odze, R.D., Klimstra, D., Paradis, V., Rugge, M., Schirmacher, P., Washington, K.M., Carneiro, F., Cree, I.A., Board, the W.C. of T.E., 2020. The 2019 WHO classification of tumours of the digestive system. Histopathology 76, 182–188. https://doi.org/10.1111/his.13975

Nawaz, M., Shah, N., Zanetti, B.R., Maugeri, M., Silvestre, R.N., Fatima, F., Neder, L., Valadi, H., 2018. Extracellular Vesicles and Matrix Remodeling Enzymes: The Emerging Roles in Extracellular Matrix Remodeling, Progression of Diseases and Tissue Repair. Cells 7, 167. https://doi.org/10.3390/cells7100167

Ni, Y., Zhou, X., Yang, J., Shi, H., Li, H., Zhao, X., Ma, X., 2021. The Role of Tumor-Stroma Interactions in Drug Resistance Within Tumor Microenvironment. Front. Cell Dev. Biol. 9.

Ou, J.-J., Wu, F., Liang, H.-J., 2010. Colorectal tumor derived fibronectin alternatively spliced EDA domain exserts lymphangiogenic effect on human lymphatic endothelial cells. Cancer Biol. Ther. 9, 186–191. https://doi.org/10.4161/cbt.9.3.10651

Oya, Y., Hayakawa, Y., Koike, K., 2020. Tumor microenvironment in gastric cancers. Cancer Sci. 111, 2696–2707. https://doi.org/10.1111/cas.14521

Özdemir, B.C., Pentcheva-Hoang, T., Carstens, J.L., Zheng, X., Wu, C.-C., Simpson, T.R., Laklai, H., Sugimoto, H., Kahlert, C., Novitskiy, S.V., De Jesus-Acosta, A., Sharma, P., Heidari, P., Mahmood, U., Chin, L., Moses, H.L., Weaver, V.M., Maitra, A., Allison, J.P., LeBleu, V.S., Kalluri, R., 2014. Depletion of Carcinoma-Associated Fibroblasts and Fibrosis Induces Immunosuppression and Accelerates Pancreas Cancer with Reduced Survival. Cancer Cell 25, 719–734. https://doi.org/10.1016/j.ccr.2014.04.005

Paduch, R., 2016. The role of lymphangiogenesis and angiogenesis in tumor metastasis. Cell. Oncol. 39, 397–410. https://doi.org/10.1007/s13402-016-0281-9

Park, J., Song, S.-H., Kim, T.Y., Choi, M.-C., Jong, H.-S., Kim, T.-Y., Lee, J.W., Kim, N.K., Kim, W.-H., Bang, Y.-J., 2004a. Aberrant methylation of integrin α4 gene in human gastric cancer cells. Oncogene 23, 3474–3480. https://doi.org/10.1038/sj.onc.1207470

Park, J., Song, S.-H., Kim, T.Y., Choi, M.-C., Jong, H.-S., Kim, T.-Y., Lee, J.W., Kim, N.K., Kim, W.-H., Bang, Y.-J., 2004b. Aberrant methylation of integrin α4 gene in human gastric cancer cells. Oncogene 23, 3474–3480. https://doi.org/10.1038/sj.onc.1207470

Park, K.C., Dharmasivam, M., Richardson, D.R., 2020. The Role of Extracellular Proteases in Tumor Progression and the Development of Innovative Metal Ion Chelators That Inhibit Their Activity. Int. J. Mol. Sci. 21, 6805. https://doi.org/10.3390/ijms21186805

Paupert, J., Van De Velde, M., Kridelka, F., Noël, A., 2014. Tumor Angiogenesis and Lymphangiogenesis: Microenvironmental Soil for Tumor Progression and Metastatic Dissemination, in: Feige, J.-J., Pagès, G., Soncin, F. (Eds.), Molecular Mechanisms of Angiogenesis: From Ontogenesis to Oncogenesis. Springer, Paris, pp. 283–306. https://doi.org/10.1007/978-2-8178-0466-8_13

Pellino, A., Riello, E., Nappo, F., Brignola, S., Murgioni, S., Djaballah, S.A., Lonardi, S., Zagonel, V., Rugge, M., Loupakis, F., Fassan, M., 2019. Targeted therapies in metastatic gastric cancer:

Current knowledge and future perspectives. World J. Gastroenterol. 25, 5773–5788. https://doi.org/10.3748/wjg.v25.i38.5773

Pereira, E.R., Kedrin, D., Seano, G., Gautier, O., Meijer, E.F.J., Jones, D., Chin, S.-M., Kitahara, S., Bouta, E.M., Chang, J., Beech, E., Jeong, H.-S., Carroll, M.C., Taghian, A.G., Padera, T.P., 2018. Lymph node metastases can invade local blood vessels, exit the node, and colonize distant organs in mice. Science 359, 1403–1407. https://doi.org/10.1126/science.aal3622

Petrelli, F., Berenato, R., Turati, L., Mennitto, A., Steccanella, F., Caporale, M., Dallera, P., Braud, F. de, Pezzica, E., Bartolomeo, M.D., Sgroi, G., Mazzaferro, V., Pietrantonio, F., Barni, S., 2017. Prognostic value of diffuse versus intestinal histotype in patients with gastric cancer: a systematic review and meta-analysis. J. Gastrointest. Oncol. 8. https://doi.org/10.21037/jgo.2017.01.10

Pimentel-Nunes, P., Libânio, D., Marcos-Pinto, R., Areia, M., Leja, M., Esposito, G., Garrido, M., Kikuste, I., Megraud, F., Matysiak-Budnik, T., Annibale, B., Dumonceau, J.-M., Barros, R., Fléjou, J.-F., Carneiro, F., van Hooft, J.E., Kuipers, E.J., Dinis-Ribeiro, M., 2019. Management of epithelial precancerous conditions and lesions in the stomach (MAPS II): European Society of Gastrointestinal Endoscopy (ESGE), European Helicobacter and Microbiota Study Group (EHMSG), European Society of Pathology (ESP), and Sociedade Portuguesa de Endoscopia Digestiva (SPED) guideline update 2019. Endoscopy 51, 365–388. https://doi.org/10.1055/a-0859-1883

Pivetta, E., Capuano, A., Vescovo, M., Scanziani, E., Cappelleri, A., Rampioni Vinciguerra, G.L., Vecchione, A., Doliana, R., Mongiat, M., Spessotto, P., 2022. EMILIN-1 deficiency promotes chronic inflammatory disease through TGFβ signaling alteration and impairment of the gC1q/α4β1 integrin interaction. Matrix Biol. 111, 133–152. https://doi.org/10.1016/j.matbio.2022.06.005

Podgrabinska, S., Braun, P., Velasco, P., Kloos, B., Pepper, M.S., Jackson, D.G., Skobe, M., 2002. Molecular characterization of lymphatic endothelial cells. Proc. Natl. Acad. Sci. 99, 16069–16074. https://doi.org/10.1073/pnas.242401399

Ressl, S., Vu, B.K., Vivona, S., Martinelli, D.C., Südhof, T.C., Brunger, A.T., 2015. Structures of C1q-like Proteins Reveal Unique Features among the C1q/TNF Superfamily. Structure 23, 688–699. https://doi.org/10.1016/j.str.2015.01.019

Rha, S.Y., Lee, H.J., Lee, J., 2020. Unmet needs in the physical and daily living domain mediates the influence of symptom experience on the quality of life of gastric cancer patients. Support. Care Cancer Off. J. Multinatl. Assoc. Support. Care Cancer 28, 1419–1431. https://doi.org/10.1007/s00520-019-04954-3

Rihawi, K., Ricci, A.D., Rizzo, A., Brocchi, S., Marasco, G., Pastore, L.V., Llimpe, F.L.R., Golfieri, R., Renzulli, M., 2021. Tumor-Associated Macrophages and Inflammatory Microenvironment in Gastric Cancer: Novel Translational Implications. Int. J. Mol. Sci. 22, 3805. https://doi.org/10.3390/ijms22083805

Riihimäki, M., Hemminki, A., Sundquist, K., Sundquist, J., Hemminki, K., 2016. Metastatic spread in patients with gastric cancer. Oncotarget 7, 52307–52316. https://doi.org/10.18632/oncotarget.10740

Rojas, A., Araya, P., Gonzalez, I., Morales, E., 2020. Gastric Tumor Microenvironment, in: Birbrair, A. (Ed.), Tumor Microenvironments in Organs: From the Brain to the Skin – Part A, Advances in Experimental Medicine and Biology. Springer International Publishing, Cham, pp. 23–35. https://doi.org/10.1007/978-3-030-36214-0_2

Schiavinato, A., Keene, D.R., Wohl, A.P., Corallo, D., Colombatti, A., Wagener, R., Paulsson, M., Bonaldo, P., Sengle, G., 2016. Targeting of EMILIN-1 and EMILIN-2 to Fibrillin Microfibrils Facilitates their Incorporation into the Extracellular Matrix. J. Invest. Dermatol. 136, 1150–1160. https://doi.org/10.1016/j.jid.2016.02.021

Smith, M.G., Hold, G.L., Tahara, E., El-Omar, E.M., 2006. Cellular and molecular aspects of gastric cancer. World J. Gastroenterol. 12, 2979–2990. https://doi.org/10.3748/wjg.v12.i19.2979

Smyth, E.C., Nilsson, M., Grabsch, H.I., Van Grieken, N.C., Lordick, F., 2020. Gastric cancer. The Lancet 396, 635–648. https://doi.org/10.1016/S0140-6736(20)31288-5

Spessotto, P., Cervi, M., Mucignat, M.T., Mungiguerra, G., Sartoretto, I., Doliana, R., Colombatti, A., 2003. β1 Integrin-dependent Cell Adhesion to EMILIN-1 Is Mediated by the gC1q Domain*. J. Biol. Chem. 278, 6160–6167. https://doi.org/10.1074/jbc.M208322200

Spessotto, P., Giacomello, E., Perris, R., 2000. Fluorescence Assays to Study Cell Adhesion and Migration In Vitro, in: Streuli, C.H., Grant, M.E. (Eds.), Extracellular Matrix Protocols, Methods in Molecular Biology™. Humana Press, Totowa, NJ, pp. 321–343. https://doi.org/10.1385/1-59259-063-2:321

Stachura, J., Wachowska, M., Kilarski, W.W., Güç, E., Golab, J., Muchowicz, A., 2016. The dual role of tumor lymphatic vessels in dissemination of metastases and immune response development. OncoImmunology 5, e1182278. https://doi.org/10.1080/2162402X.2016.1182278

Steele, M.M., Schieler, A.M., Kelley, P.M., Tempero, R.M., 2011. β1 integrin regulates MMP-10 dependant tubulogenesis in human lymphatic endothelial cells. Matrix Biol. 30, 218–224. https://doi.org/10.1016/j.matbio.2011.03.001

Stegemann, C., Didangelos, A., Barallobre-Barreiro, J., Langley, S.R., Mandal, K., Jahangiri, M., Mayr, M., 2013. Proteomic identification of matrix metalloproteinase substrates in the human

vasculature. Circ. Cardiovasc. Genet. 6, 106–117. https://doi.org/10.1161/CIRCGENETICS.112.964452

Suh, Y.-S., Lee, J., Woo, H., Shin, D., Kong, S.-H., Lee, H.-J., Shin, A., Yang, H.-K., 2020. National cancer screening program for gastric cancer in Korea: Nationwide treatment benefit and cost. Cancer 126, 1929–1939. https://doi.org/10.1002/cncr.32753

Sun, H., Wang, Xu, Wang, Xin, Xu, M., Sheng, W., 2022. The role of cancer-associated fibroblasts in tumorigenesis of gastric cancer. Cell Death Dis. 13, 1–9. https://doi.org/10.1038/s41419-022-05320-8

Sung, H., Ferlay, J., Siegel, R.L., Laversanne, M., Soerjomataram, I., Jemal, A., Bray, F., 2021. Global Cancer Statistics 2020: GLOBOCAN Estimates of Incidence and Mortality Worldwide for 36 Cancers in 185 Countries. CA. Cancer J. Clin. 71, 209–249. https://doi.org/10.3322/caac.21660

Tagirasa, R., Yoo, E., 2022. Role of Serine Proteases at the Tumor-Stroma Interface. Front. Immunol. 13.

Tanabe, S., Ishido, K., Matsumoto, T., Kosaka, T., Oda, I., Suzuki, H., Fujisaki, J., Ono, H., Kawata, N., Oyama, T., Takahashi, A., Doyama, H., Kobayashi, M., Uedo, N., Hamada, K., Toyonaga, T., Kawara, F., Tanaka, S., Yoshifuku, Y., 2017. Long-term outcomes of endoscopic submucosal dissection for early gastric cancer: a multicenter collaborative study. Gastric Cancer 20, 45–52. https://doi.org/10.1007/s10120-016-0664-7

Thrift, A.P., El-Serag, H.B., 2020. Burden of Gastric Cancer. Clin. Gastroenterol. Hepatol. 18, 534–542. https://doi.org/10.1016/j.cgh.2019.07.045

Tian, Y., Pang, Y., Yang, P.-G., Guo, H.-H., Liu, Yang, Zhang, Z., Ding, P.-A., Zheng, T., Li, Y., Fan, L.-Q., Zhang, Z.-D., Wang, D., Zhao, X.-F., Tan, B.-B., Liu, Yu, Zhao, Q., 2023. Clinical implications of micro lymph node metastasis for patients with gastric cancer. BMC Cancer 23, 536. https://doi.org/10.1186/s12885-023-11023-w

Tomita, H., Yamada, Y., Oyama, T., Hata, K., Hirose, Y., Hara, A., Kunisada, T., Sugiyama, Y., Adachi, Y., Linhart, H., Mori, H., 2007. Development of gastric tumors in Apc(Min/+) mice by the activation of the beta-catenin/Tcf signaling pathway. Cancer Res. 67, 4079–4087. https://doi.org/10.1158/0008-5472.CAN-06-4025

Truffi, M., Sorrentino, L., Corsi, F., 2020. Fibroblasts in the Tumor Microenvironment, in: Birbrair, A. (Ed.), Tumor Microenvironment: Non-Hematopoietic Cells, Advances in Experimental Medicine and Biology. Springer International Publishing, Cham, pp. 15–29. https://doi.org/10.1007/978-3-030-37184-5_2

Tsukamoto, T., Mizoshita, T., Tatematsu, M., 2007. Animal Models of Stomach Carcinogenesis. Toxicol. Pathol. 35, 636–648. https://doi.org/10.1080/01926230701420632

Ucaryilmaz Metin, C., Ozcan, G., 2022. Comprehensive bioinformatic analysis reveals a cancer-associated fibroblast gene signature as a poor prognostic factor and potential therapeutic target in gastric cancer. BMC Cancer 22, 692. https://doi.org/10.1186/s12885-022-09736-5

Velikova, G., Banks, R.E., Gearing, A., Hemingway, I., Forbes, M.A., Preston, S.R., Jones, M., Wyatt, J., Miller, K., Ward, U., Al-Maskatti, J., Singh, S.M., Ambrose, N.S., Primrose, J.N., Selby, P.J., 1997. Circulating soluble adhesion molecules E-cadherin, E-selectin, intercellular adhesion molecule-1 (ICAM-1) and vascular cell adhesion molecule-1 (VCAM-1) in patients with gastric cancer. Br. J. Cancer 76, 1398–1404. https://doi.org/10.1038/bjc.1997.569

Verdone, G., Corazza, A., Colebrooke, S.A., Cicero, D., Eliseo, T., Boyd, J., Doliana, R., Fogolari, F., Viglino, P., Colombatti, A., Campbell, I.D., Esposito, G., 2009. NMR-based homology model for the solution structure of the C-terminal globular domain of EMILIN1. J. Biomol. NMR 43, 79–96. https://doi.org/10.1007/s10858-008-9290-y

Verdone, G., Doliana, R., Corazza, A., Colebrooke, S.A., Spessotto, P., Bot, S., Bucciotti, F., Capuano, A., Silvestri, A., Viglino, P., Campbell, I.D., Colombatti, A., Esposito, G., 2008. The Solution Structure of EMILIN1 Globular C1q Domain Reveals a Disordered Insertion Necessary for Interaction with the α4β1 Integrin*. J. Biol. Chem. 283, 18947–18956. https://doi.org/10.1074/jbc.M801085200

Vizovisek, M., Ristanovic, D., Menghini, S., Christiansen, M.G., Schuerle, S., 2021. The Tumor Proteolytic Landscape: A Challenging Frontier in Cancer Diagnosis and Therapy. Int. J. Mol. Sci. 22, 2514. https://doi.org/10.3390/ijms22052514

Waldum, H.L., Fossmark, R., 2018. Types of Gastric Carcinomas. Int. J. Mol. Sci. 19, 4109. https://doi.org/10.3390/ijms19124109

Wang, C., Chu, M., 2022. Advances in Drugs Targeting Lymphangiogenesis for Preventing Tumor Progression and Metastasis. Front. Oncol. 11.

Wang, Y., Zhai, J., Zhang, T., Han, S., Zhang, Y., Yao, X., Shen, L., 2020. Tumor-Associated Neutrophils Can Predict Lymph Node Metastasis in Early Gastric Cancer. Front. Oncol. 10.

Wei, J., Wang, M., Li, G., 2023. Cancer-associated fibroblasts, and clinicopathological characteristics and prognosis of gastric cancer: A systematic review and meta-analysis. Front. Oncol. 13.

Wessler, S., Krisch, L.M., Elmer, D.P., Aberger, F., 2017. From inflammation to gastric cancer – the importance of Hedgehog/GLI signaling in Helicobacter pylori-induced chronic inflammatory and neoplastic diseases. Cell Commun. Signal. 15, 15. https://doi.org/10.1186/s12964-017-0171-4

Wiig, H., Keskin, D., Kalluri, R., 2010. Interaction between the extracellular matrix and lymphatics: Consequences for lymphangiogenesis and lymphatic function. Matrix Biol. 29, 645–656. https://doi.org/10.1016/j.matbio.2010.08.001

Winkler, J., Abisoye-Ogunniyan, A., Metcalf, K.J., Werb, Z., 2020. Concepts of extracellular matrix remodelling in tumour progression and metastasis. Nat. Commun. 11, 1–19. https://doi.org/10.1038/s41467-020-18794-x

Yada, T., Yokoi, C., Uemura, N., 2013. The Current State of Diagnosis and Treatment for Early Gastric Cancer. Diagn. Ther. Endosc. 2013, 241320. https://doi.org/10.1155/2013/241320

Yakirevich, E., Resnick, M.B., 2013. Pathology of Gastric Cancer and Its Precursor Lesions. Gastroenterol. Clin. North Am., Gastric Cancer 42, 261–284. https://doi.org/10.1016/j.gtc.2013.01.004

Yamamoto, M., Nomura, S., Hosoi, A., Nagaoka, K., Iino, T., Yasuda, T., Saito, T., Matsushita, H., Uchida, E., Seto, Y., Goldenring, J.R., Kakimi, K., Tatematsu, M., Tsukamoto, T., 2018. Established gastric cancer cell lines transplantable into C57BL/6 mice show fibroblast growth factor receptor 4 promotion of tumor growth. Cancer Sci. 109, 1480–1492. https://doi.org/10.1111/cas.13569

Yang, Z., Xue, F., Li, M., Zhu, X., Lu, X., Wang, C., Xu, E., Wang, X., Zhang, L., Yu, H., Ren, C., Wang, H., Wang, Y., Chen, J., Guan, W., Xia, X., 2021. Extracellular Matrix Characterization in Gastric Cancer Helps to Predict Prognosis and Chemotherapy Response. Front. Oncol. 11.

Zacchigna, L., Vecchione, C., Notte, A., Cordenonsi, M., Dupont, S., Maretto, S., Cifelli, G., Ferrari, A., Maffei, A., Fabbro, C., Braghetta, P., Marino, G., Selvetella, G., Aretini, A., Colonnese, C., Bettarini, U., Russo, G., Soligo, S., Adorno, M., Bonaldo, P., Volpin, D., Piccolo, S., Lembo, G., Bressan, G.M., 2006. Emilin1 Links TGF-β Maturation to Blood Pressure Homeostasis. Cell 124, 929–942. https://doi.org/10.1016/j.cell.2005.12.035

Zanetti, M., Braghetta, P., Sabatelli, P., Mura, I., Doliana, R., Colombatti, A., Volpin, D., Bonaldo, P., Bressan, G.M., 2004. EMILIN-1 Deficiency Induces Elastogenesis and Vascular Cell Defects. Mol. Cell. Biol. 24, 638–650. https://doi.org/10.1128/MCB.24.2.638-650.2004

Zeng, D., Li, M., Zhou, R., Zhang, J., Sun, H., Shi, M., Bin, J., Liao, Y., Rao, J., Liao, W., 2019. Tumor Microenvironment Characterization in Gastric Cancer Identifies Prognostic and Immunotherapeutically Relevant Gene Signatures. Cancer Immunol. Res. 7, 737–750. https://doi.org/10.1158/2326-6066.CIR-18-0436

Zhan, S., Liu, Z., Zhang, M., Guo, T., Quan, Q., Huang, L., Guo, L., Cao, L., Zhang, X., 2020. Overexpression of B7-H3 in α-SMA-Positive Fibroblasts Is Associated With Cancer Progression and Survival in Gastric Adenocarcinomas. Front. Oncol. 9.

Zhang, J., Li, S., Zhao, Y., Ma, P., Cao, Y., Liu, C., Zhang, X., Wang, W., Chen, L., Li, Y., 2020. Cancer-associated fibroblasts promote the migration and invasion of gastric cancer cells via activating IL-17a/JAK2/STAT3 signaling. Ann. Transl. Med. 8, 877–877. https://doi.org/10.21037/atm-20-4843

Zhang, W., Huang, P., 2011. Cancer-stromal interactions. Cancer Biol. Ther. 11, 150–156. https://doi.org/10.4161/cbt.11.2.14623

Zhang, Y., Tang, H., Cai, J., Zhang, T., Guo, J., Feng, D., Wang, Z., 2011. Ovarian cancer-associated fibroblasts contribute to epithelial ovarian carcinoma metastasis by promoting angiogenesis, lymphangiogenesis and tumor cell invasion. Cancer Lett. 303, 47–55. https://doi.org/10.1016/j.canlet.2011.01.011

Zhao, X., Li, K., Chen, M., Liu, L., 2023. Metabolic codependencies in the tumor microenvironment and gastric cancer: Difficulties and opportunities. Biomed. Pharmacother. 162, 114601. https://doi.org/10.1016/j.biopha.2023.114601

Zhao, Y., Zhang, X., Yao, J., Jin, Z., Liu, C., 2020. Expression patterns and the prognostic value of the EMILIN/Multimerin family members in low-grade glioma. PeerJ 8, e8696. https://doi.org/10.7717/peerj.8696

Zheng, H., Li, X., Hara, T., Masuda, S., Yang, X., Guan, Y., Takano, Y., 2008. Mixed-type gastric carcinomas exhibit more aggressive features and indicate the histogenesis of carcinomas. Virchows Arch. 452, 525–534. https://doi.org/10.1007/s00428-007-0572-7

Zhi, K., Shen, X., Zhang, H., Bi, J., 2010. Cancer-associated fibroblasts are positively correlated with metastatic potential of human gastric cancers. J. Exp. Clin. Cancer Res. 29, 66. https://doi.org/10.1186/1756-9966-29-66

Zhu, T., Hu, X., Wei, P., Shan, G., 2018. Molecular background of the regional lymph node metastasis of gastric cancer (Review). Oncol. Lett. 15, 3409–3414. https://doi.org/10.3892/ol.2018.7813